An Energy and Cost Performance Optimization Platform for Commercial Building System Design

Weili Xu

PH.D. THESIS

May 10, 2017

School of Architecture

Carnegie Mellon University

Pittsburgh, PA 15213

Doctoral Committee:

Khee Poh Lam, Ph.D. RIBA, Professor (Chair)

School of Architecture, Carnegie Mellon University

Vivian Loftness, FAIA, LEED AP, Paul Mellon Professor

School of Architecture, Carnegie Mellon University

Chris Hendrickson, Hamerschlag University Professor Emeritus

Civil & Environmental Engineering, Carnegie Mellon University

---

A Dissertation Submitted in Partial Fulfillment of the Requirements for the Degree of Doctor of Philosophy in Building Performance and Diagnostics in the School of Architecture, Carnegie Mellon University

Copyright Declaration

I hereby declare that I am the sole author of this thesis.

I authorize Carnegie Mellon University, Pittsburgh, PA, USA to lend this thesis to other institutions or individuals for the purpose of scholarly research.

I authorize Carnegie Mellon University, Pittsburgh, PA, USA to reproduce this thesis by photocopying or by other means, in total or in part, at the request of other institutions or individuals for the purpose of scholarly research.

Dedicated to my wonderful wife, Je Sun Oh

my beloved daughter, Stella Xu

my supportive parents, AnHua Xu and LaiPing Xu

and my parents-in-law, Seung Min Oh and Eun Young Oh.

Acknowledgments

First and foremost, I express my special appreciation to Professor Khee Poh Lam, chair of my Ph.D. thesis committee. Khee Poh has been a tremendous mentor and friend for me. Genuine contribution of his time and ideas made my Ph.D. experience productive and stimulating. His passion and diligence will continue to influence me from past to future.

I am also grateful to my committee member Professor Vivian Loftness. She is such a nice person with great respect for her students. She taught me the concept of tunneling through the cost barrier that greatly inspired the topic of "system integration" in this thesis.

My special thanks go to Professor Chris Hendrickson. I learned a very important knowledge about life cycle cost from his class that was used in my research. I also want to thank him for his brilliant comments and suggestions.

I give my sincerely gratitude to Dr. Minuro Yonezawa from Toshiba America Research, Dr. Mikito Iwamasa and Aisu Hideyuki and everyone else in Toshiba Research Development Center, Japan, who have participated and helped in the development of the proposed optimization algorithm.

I also want to thank my friends for the countless discussions that inspired many research ideas. My sincere thanks go to Adrian Chong, Chao Ding, Omer T. Karaguzel, Yunjeong Mo, Haopeng Wang, Shalini Ramesh, Rohini Srivastava, Erica Cochran, Bertrand Lasternas, Jihyun Park, Zhiang Zhang and all my friends in the Intelligent Workplace and School of Architecture.

I want to give special thanks to Dr. Matt Nelson from CMU Global Communication Center, who gave me valuable comments and suggestions on the writing of my dissertation.

Last but not least, I want to thank my family. Words cannot express how grateful I am to my mother and my farther, my mother-in-law and father-in-law. Special

thanks go to Je Sun Oh, for providing me with the strength and continuous support through the ups and downs of writing a dissertation.

Abstract

Energy and cost performance optimization for commercial building system design is growing in popularity, but it is often criticized for its time consuming process. Moreover, the current process lacks integration, which not only affects time performance, but also investors' confidence in the predicted performance of the generated design. Such barriers keep building owners and design teams from embracing life cycle cost consideration. This thesis proposes a computationally efficient design optimization platform to improve the time performance and to streamline the workflow in an integrated multi-objective building system design optimization process.

First, building system cost estimation is typically completed through a building information model based quantity take-off process, which does not provide sufficient design decision support features in the design process. To remedy this issue, an automatic cost estimation framework that integrates EnergyPlus with an external database to perform building systems' capital and operation costs is proposed.

Optimization, typically used for building system design selection, requires a large amount of computational time. The optimization process evaluates building envelope, electrical and HVAC systems in an integrated system not only to explore the cost-saving potential from a single high performance system, but also the interrelated effects among different systems. An innovative optimization strategy that integrates machine learning techniques with a conventional evolutionary algorithm is proposed. This strategy can reduce run time and improve the quality of the solutions.

Lastly, developing baseline energy models typically takes days or weeks depending on the scale of the design. An automated system for generating baseline energy model according to ANSI/ASHRAE/IESNA Standard 90.1 performance rating method is thus proposed to provide a quick appraisal of optimal designs in

comparison with the baseline energy requirements.

The main contribution of this thesis is the development of a new design optimization platform to expedite the conventional decision making process. The platform integrates three systems: (1) cost estimation, (2) optimization and (3) benchmark comparison for minimizing the first cost and energy operation costs. This allows designers to confidently select an optimal design with high performance building systems by making a comparison with the minimum energy baseline set by standards in the building industry.

Two commercial buildings are selected as case studies to demonstrate the effectiveness of this platform. One building is the Center for Sustainable Landscapes in Pittsburgh, PA. This case study is used as a new construction project. With 54 million possible design solutions, the platform is able to identify optimal designs in four hours. Some of the design solutions not only save the operation costs by up to 23% compared to the ASHRAE baseline design, but also reduce the capital cost ranging from 5% to 23%. Also, compared with the ASHRAE baseline design, one design solution demonstrates that the high investment of a product, building integrative photovoltaic (BiPV) system, can be justified through the integrative design optimization approach by the lower operation costs (20%) as well as the lower capital cost (12%). The second building is the One Montgomery Plaza, a large office building in Norristown, PA. This case study focuses on using the platform for a retrofit project. The calibrated energy model requires one hour to complete the simulation. There are 4000 possible design solutions proposed and the platform is able to find the optimal design solution in around 50 hours. Similarly, the results indicate that up to 25% capital cost can be saved with $1.7 million less operation costs in 25 years, compare to the ASHRAE baseline design.

Keywords: *Design decision support, Construction cost estimation, Life cycle cost analysis, Multi-objective optimization, Building energy baseline automation*

Contents

List of Figures

List of Tables

Chapter 1

Introduction

Energy efficient buildings have demonstrated higher life cycle profits and lower market risks in a number of studies and market reports (Enkvist et al., 2007; Eichholtz et al., 2012; WGBC, 2013; National Research Council, 2013), which encourage both public sectors and private investors to pursue energy efficient buildings in their property portfolios. Building system design optimization using life cycle cost analysis (LCCA) as a performance goal is one of the many approaches to achieve energy efficient buildings. This technique is used at the schematic or detail design phase to assist with selecting building systems. Figure 1.1 depicts a typical building system design optimization workflow and its role in the conventional project delivery process. It can be observed that many processes are isolated and require manual process (e.g. cost estimation, baseline modeling). The motivation of implementing such a system is to find a good design solution that can satisfy performance goals efficiently, thus reducing the time and cost of design decision-making in the building design phase.

1.1 Problem discussion

1.1.1 Building system optimization problem

Building system design optimization typically couples an optimization algorithm with building energy simulation to maximum single or multiple performance goals (Nguyen et al., 2014).

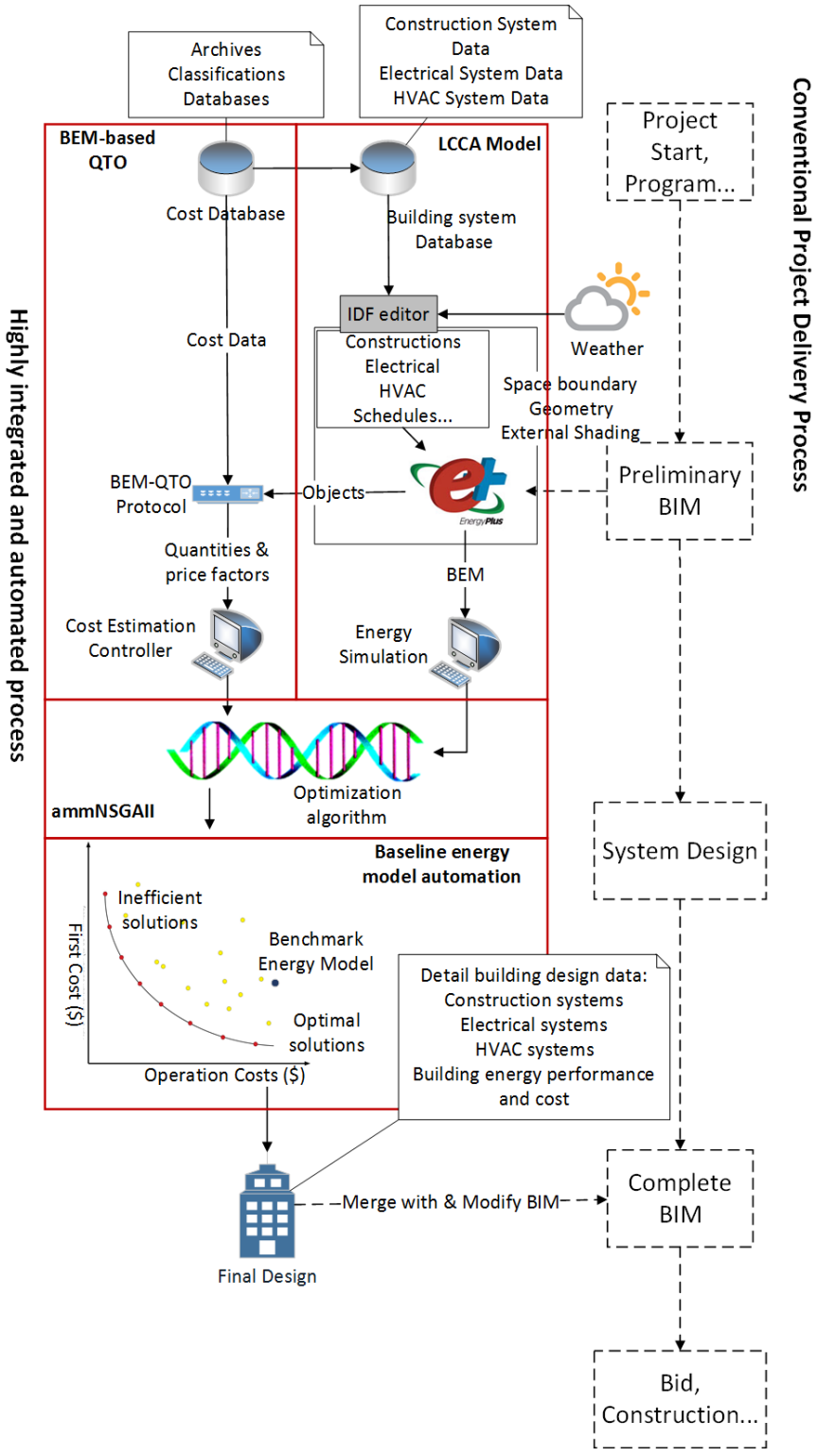

Figure 1.1: Typical building system design optimization workflow in the conventional project delivery process (Dashed line: processes that are not considered in this thesis.)

Optimization algorithms have advantages over the other optimization procedures in complex system design problems because of the challenges that the current building industry are facing (Evins, 2013):

- The design of energy efficient buildings is not straightforward. All buildings are unique and there are no such design prototypes.
- There are many physical processes that lead to conflicting objectives such as high energy performance and low capital cost.
- The design space of possible solutions is subject to combinatory explosion, which means the problem size is growing exponentially as the number of design alternatives increase.

Hence, meta-heuristic algorithms such as evolutionary algorithms are popular in solving this type of problem because they can effectively provide "good" solutions within a computing timeframe that is "small enough" (Glover and Sörensen, 2015). Flager, et al. (2012) developed a semi-automated multi-objective optimization process using the multi-objective genetic algorithm (MOGA) (Flager et al., 2012). The study objective was to find the best combination of glazing type and window-to-wall ratio that had the lowest life cycle cost and environmental impact. The results showed the optimized cases had achieved savings on both design parameters and also demonstrated the evaluation time reduction from weeks to 84 man-hours by using the advanced optimization algorithm. Karaguzel, Zhang and Lam (2014) constructed an optimization framework that integrated EnergyPlus and GenOpt for minimizing the life cycle cost of a commercial building (Karaguzel et al., 2014). The particle swarm optimization (PSO) algorithm was implemented for searching the feasible space in multiple dimensions, which were glazing types and wall and roof insulation values. This algorithm successfully found global optimal solutions within 60% of the evaluation time of the brute force approach. In the results, the optimized design solution yielded a 28.7% life cycle cost savings compared to an initial solution. The initial solution in the study was equipped with the cheapest design options. However, both of these studies focus on one or multiple independent building systems, which ignore the synergistic effects among building systems.

Some studies address the synergistic effects by evaluating building designs in an integrated view. However, due to the complexity of the building systems in energy simulation engines, work around approaches are often found in such studies. Evins, et al. (2012) carried out a multi-objective optimization study to reduce a modular hotel unit's carbon emission and construction cost in different climates (Evins et al., 2012). The design variables included building envelope systems as well as HVAC systems and renewable energy systems. An initial case was created in this study using the design options with the lowest unit price for comparison. Although building simulation was conducted in EnergyPlus, the HVAC energy consumption was calculated externally by applying system efficiencies on an ideal load system's results. Such a work around approach calculates the HVAC's energy performance and cost using the system efficiency metric only, which is not accurate for capital cost estimation and energy consumption prediction. Pountney also addressed the system integration effects on building life cycle cost by including HVAC system performance-related parameters such as boiler efficiency and AHU fan power in the design variables (Pountney, 2012). This approach focuses on optimizing an HVAC system's performance instead of testing different HVAC systems. After including the synergistic effects of the building systems, the optimization algorithm was able to identify better design solutions with less capital costs within 9000 evaluations. Due to the use of the Simplified Building Energy Model (SBEM) and parallel computing, the optimization was completed within a day. Other similar building design optimization studies are well summarized in (Evins, 2013; Nguyen et al., 2014; Shi et al., 2016).

In summary, the effectiveness and efficiency of optimization algorithms have been demonstrated in building system design optimization studies. However, such studies also require thousands of simulations in a typical optimization study. Due to the mathematical properties of the energy model, this process could take days to weeks to complete. Despite the algorithm effectiveness, the current practices focus on either optimizing one specific building system or optimizing integrated building systems. Table 1.1 summaries the approaches each literature uses. Optimizing one particular building system could potentially attain sub-optimal solutions from

Table 1.1: Building systems investigated in the building cost optimization studies

Studies	**Objectives**	**Approach**	**Possible issue**
Flager et al. (2012)	Life cycle cost, carbon emission	Envelope system	Maybe sub-optimal in an integrated system.
Karaguzel et al. (2014)	Life cycle cost	Envelope system	Maybe sub-optimal in an integrated system.
Evins et al. (2012)	Capital cost, carbon emission	Integrated system	HVAC energy is calculated using a work-around method.
Pountney (2012)	Life cycle cost	Integrated system	Optimize a boiler's efficiency and capacity can produce impractical product.

a whole building perspective. On the other hand, optimizing an integrated building system usually adopts work around approaches for HVAC system modeling, which can lead to inaccurate performance evaluations.

1.1.2 Cost estimation problem

In addition to the building systems, various performance goals are also investigated in building system design optimization studies. Currently, there are more than 20 different objectives found in the literature and among them, life cycle costs are listed as the most frequent performance goals employed in most of the building system design optimization (Evins, 2013). To perform a life cycle cost analysis, building system capital cost estimation is important. However, there is no systematic building system cost estimation method in most of these studies. One of the most common approaches is to perform a simple estimation. This estimation typically uses a fixed price for each design option. Ascione, et al. (2015) conducted a multi-objective optimization to minimize energy consumption and discomfort hours under a budget constraint. The design options included envelope, boiler and chiller types, and HVAC control. Each option was associated with a price. The project budget was calculated by summing up every design option price in a solution (Ascione et al., 2015). A similar capital cost estimation approach can also be found in (Hamdy et al., 2011) and (Evins et al., 2012). Alternatively, some studies adopted

Table 1.2: Cost estimation in building cost optimization studies

Studies	**Approach**	**Remark**	**Possible issue**
Ascione et al. (2015)	Simple estimation	Assign a cost to a design option	Overestimate or underestimate capital cost.
Barg et al. (2015)	Customized QTO	Extract unit cost with customized price factor	Difficult to replicate the study.

the customized quantity take-off (QTO) approach combined with a building energy model. The customized QTO method is manually established by the author for a specific case and it varies from study to study. Barg, Flager and Fischer applied multi-objective optimization on minimizing the life cycle cost and carbon footprint of an office building. The building element quantities were manually extracted from the building energy model and the unit price for each building element was collected from RSMeans® (Barg et al., 2015). The same approach can be found in (Karaguzel et al., 2014) and (Pountney, 2012). Although this approach has a similar concept as the building information model based quantity take-off, it is missing a structured classification standard, which prevents the case study from being replicated. This issue was found by comparing the price factors for the same building element in different studies. For instance, window price factor in (Barg et al., 2015; Karaguzel et al., 2014) include U-value and SHGC whereas in (Stocker et al., 2015), the window's price only depends on U-value. Also, none of these approaches are tightly integrated with the building energy model, so they typically involve a manual process that is very time consuming. Table 1.2 summaries these two cost estimation techniques.

1.1.3 Optimization results analysis problem

One advantage of employing multi-objective optimization is the presentation of results. Pareto optimality is commonly used in analyzing the design solutions from these studies. For a building system design problem, the pareto optimality is defined as a distribution of design solutions where there is no alternative design solution that can achieve the same performance, while making at least one of its objectives better off. This distribution of design solutions is also called

Table 1.3: Results analysis in building cost optimization studies

Studies	**Approach**	**Remark**	**Possible issue**
Evins et al. (2012)	Cheapest	Select cheapest design options	The base case may fail to meet the minimum energy requirements.
Flager et al. (2012)	Common practice	Use expert judgement	Expert judgment may vary from study to study.

pareto front or pareto set. Pareto front efficiently narrows down the design solutions into a smaller set, and it offers a view that helps clients understand the trade-offs between different optimal solutions (Deb, 2011). However, this technique does not provide cost performance improvements of optimized cases, which is the key metric for conducting optimization. The current studies often compare the optimized design case with a vaguely defined base case model. Most of the studies identify the base case as a building design that consist of the cheapest building systems or the design with the poorest performance (Karaguzel et al., 2014; Evins et al., 2012). Some other studies define this base case as an industry common practice (Flager et al., 2012). Table 1.3 lists the possible issues for these two approaches. Different definitions of the base case will certainly result in different improvements, and more importantly, none of these base cases are explicitly confirmed to meet with local or national minimum energy requirements or benchmarks. Lack of comparison with standards requirements or market benchmarks will reduce the investors confidence in the optimized design solutions.

1.1.4 Summary

The current practices indicate issues in the building system design optimization:

- Building system design optimization typically focuses on either optimizing one specific building system or optimizing integrated building systems. However, optimizing one particular building system could potentially attain sub-optimal solutions from a whole building perspective. On the other hand, optimizing integrated building systems usually adopts work around approaches, which can lead to inaccurate performance evaluations.
- The commonly used metaheuristic algorithms are not subject to combinatorial explosion.

However, the optimization process still requires days or weeks to complete because of the computational intensive building simulation process.

- The process lacks a systematic building system cost estimation method. Most of the current system cost estimation techniques are performed manually with data sources from an external database or surveyed from manufacturers or project contractors. Furthermore, the system's price factors vary from study to study. This creates difficulties in applying the same methodology to another building project.
- The improvements from optimized cases are typically calculated by comparing a vaguely defined base case. For most of the studies, the base cases are modeled with building systems that have the cheapest cost or poorest performance, which may not qualify to meet the minimum energy requirements set by standards. This could lower building owners' confidence on the optimized case.
- Several processes such as cost estimation, building system integration and benchmark comparisons are not fully integrated in the conventional building system design optimization workflow, and they are commonly addressed in a manual approach or some work around methods, which affects the time performance as well as the accuracy of the optimized solution.

1.2 Market for building system design optimization

Adopting an optimization algorithm in solving building system design problems is gradually becoming a mainstream research effort. In 2016, nearly 500 optimization papers were published in the *Journal of Energy and Building* (ScienceDirect, 2016). In industry, case studies (EcoGlobe, 2016) and design competitions (ASHRAE, 2016b) also demonstrated the advantages of integrating optimization algorithms in the building design process. Following the competition, approximately 200 people attended the webinar for the tutorial of the optimization module in DesignBuilder software.

Table 1.4: State-of-art optimization strategies in building design optimization

Studies	**Algorithm**	**Remark**
Eisenhower et al. (2012)	Meta-model	Fast, however, train a meta-model may take longer than run a conventional algorithm.
Hamdy et al. (2011)	Hybrid algorithms	Fast, however, it is subject to combinatory expansion and its speed still depends on objective functions.

1.3 Review of State-of-the-art

1.3.1 Building system design optimization techniques

Coupling optimization with energy simulation for design decision support has been actively discussed among academia for decades; however, it is still rare to find this technique being implemented in real world cases. One of the greatest barriers is the computationally expensive process due to the mathematical properties of the energy model. In such a process, the main difficulty arises in the immense computational time required in evaluating a solution using energy simulation (Eisenhower et al., 2012). Recent studies focus on proposing advanced optimization strategies such as optimizing a meta-model (Eisenhower et al., 2012; Rysanek and Choudhary, 2013) or hybrid optimization algorithms (Juan et al., 2010; Hamdy et al., 2011) to alleviate the effect. A meta-model approach optimizes design parameters on a "model of model" instead of real simulations. This method requires a fixed database that contains design variables and parameters for constructing the meta-model. Therefore, it demands hundreds of simulations upfront. Furthermore, a meta-model is commonly not general enough to adapt to different cases such as evaluating the energy consumption of a building in different climates. On the other hand, hybrid optimization algorithms typically start with an evolutionary search in a large space to advance the population to the optimal region. Once the search space is narrowed down sufficiently, the search process will switch to a fast and accurate gradient-based search algorithm to converge on the optimal region (Greiner et al., 2015). However, the time

spent by the evolutionary algorithm is still highly dependent on the number of design options and objective functions, which could make the project impossible from a practical point of view. Table 1.4 lists the features of these two algorithms. It implies the need for an innovative optimization process to be developed for building system design optimization. This new optimization process should not only improve the time performance, but also improve the search effectiveness for finding high quality design solutions.

1.3.2 Cost estimation techniques

A common method to perform automatic cost estimation is BIM-based quantity take-off (QTO). QTO is the measurement of the schematics or work results of a construction project. It is one of the key steps in the construction delivery process and the foundation of several other critical tasks (Monteiro and Martins, 2013). The BIM-based QTO method focuses on implementing a data mapping strategy to connect the cost information and the data that contains the quantity of building elements in a BIM model. A few case studies have demonstrated that the BIM-based QTO not only shortens the time, but also reduces the risk of budgeting issues (Tiwari et al., 2009; Choi et al., 2015). To achieve automated QTO, several possible BIM-based cost estimation approaches are suggested in (Wu et al., 2014; Eastman et al., 2011) , namely BIM to cost estimation, software integration, and BIM quantification tools. The BIM to cost estimation approach utilizes BIM's estimating function to export quantities into a spreadsheet or external database. Then the quantity surveyors can price each item based on the exported information. This approach is semi-automated. It does not support fast cost updates with changes on the BIM model (Hardin and McCool, 2015). The software integration approach mainly focuses on integrating cost estimating software with a BIM tool for a direct cost estimation in an integrated platform. An example could be Tocoman iLink, which offers a direct link to the Autodesk Revit® through a plug-in (Autodesk, 2007). A similar plug-in software that provides multi-level cost estimations in the early design stage can also be found in Sketchup™ platform (Cheung et al., 2012). Lastly, BIM quantification tools suggest the extraction of the a BIM model to an external platform, which is specifically developed for performing both quan-

Table 1.5: State-of-art QTO techniques

Studies	**Approach**	**Remark**
Hardin and McCool (2015)	BIM to cost estimation	Semi-automated and does not support updates and LCCA.
Cheung et al. (2012)	Software integration	Plug-in in design tools, fast and accurate, but the quality subjects to the integrity of BIM data and it does not support LCCA.
Autodesk (2007)	BIM quantification tools	Data integration through specialized tool, but the quality subjects to the integrity of BIM data and it does not support LCCA.

tification extraction and cost estimation. Such type of software include the Autodesk QTO® and the Vico Office™. Similar to the first approach, these tools still require manually take-off cost items. However, with complete access to the BIM data, these tools are capable of providing model visualization of the project as well as finding useful information for a high quality cost estimation. Table 1.5 summaries these techniques. Although BIM-based QTO is growing in popularity, this technique is facing slow adoption issue, as reported in several survey studies worldwide (Wu et al., 2014; Aibinu and Venkatesh, 2013). This is partly due to the lack of awareness of the benefits from the BIM-based QTO approach, but the challenges from the inadequate data quality issue are more critical and have arisen in every BIM-based QTO survey study. A survey conducted in 2011 shows that more than 80% of the BIM models received by general contractors do not contain the sufficient data for performing a good quality cost estimation (Sattineni and Bradford, 2011). This certainly jeopardizes the BIM-QTO automation process and force the quantity surveyors to move back to the manual process. Also, as discussed in the research, BIM-based QTO is not an ideal framework to support design decision making based on life cycle cost analysis.

1.3.3 Baseline energy model development

ASHRAE 90.1 performance rating method (PRM) requires energy modelers to develop minimum efficiency energy models for evaluating relative design improvements in comparison to

Table 1.6: State-of-art baseline energy model automation techniques

Tools	**Approach**	**Remark**
DesignBuilder (2016)	Templates	Provides abundant baseline templates. (The V5.0 just released its new baseline automation system)
Trane (2016)	Templates and guidelines	Provides envelope and lighting templates. User needs to create HVAC system following the instruction.
Roth (2016)	Fully automated	Fully automated process. It can be called via OpenStudio measure. However, it cannot be extended to EnergyPlus raw file.
CBECCCOM (2016)	Fully automated	Fully automated process. It is only available for CBECC-Com user even though its simulation engine is EnergyPlus.

the performance of the proposed energy model. PRM is an iterative process and manually performed by developing building energy models using the standard approved building energy simulation software, such as EnergyPlus. This manual process is labor intensive and error-prone. In response to this issues, tools such as DesignBuilder (DesignBuilder, 2016) and Trane Trace^{TM} 700 (Trane, 2016) can generate "baseline models" with generic templates and guidelines to facilitate this process. These approaches only offer a range of pre-defined templates as starting point to be extended by the energy modeler. However, pre-defined building and HVAC system templates have to be subjected to significant customization process to be accepted as complete and standard-compliant energy model components. Such customization approaches still inherit the problems observed in manual model development process. Recently, OpenStudio baseline model measure (Roth, 2016) and CBECC-COM (CBECCCOM, 2016) offer highly structured automated baseline model development strategies. However, the function is only available for the software tool users, which could be difficult to extend their application to design support for a variety of EnergyPlus-based design tools. Table 1.6 lists the baseline

generation feature of each design tool.

1.4 Hypothesis of the dissertation

In sum, the hypothesis of this thesis is:

- *An integrated life cycle design optimization tool, combining BEM with quantity and operational take-offs in a life cycle analysis, will efficiently search for optimal integrated system solutions among a group of interdependent building design options, to optimize capital plus operational cost performance for building owners.*

In this thesis, the definition of an "optimal integrated system solution" or "optimal design solution" is a feasible design solution that employs a group of user defined design options for a specific building design, which yields the lowest possible capital investment and highest possible operation savings. Therefore, the quality of the optimal design is limited by the accuracy of cost data and design performance data.

1.5 Proposed new approach

Figure 1.2 lists the methods and approaches concluded from literature review. The main topics cover construction cost estimation, building system design optimization and baseline generation. Under each main topics, there are one or multiple sub topics. Specific methods in each sub topic are indicated by black dots. Under each topic, several methods are reviewed and compared. The methods that were used in this dissertation are highlighted by red dots.

Considering the issues identified in the literature review, there is a demand for a novel building system design optimization approach that provides a practical and a high quality design decision support for building system selection from an integrated system perspective. This motivates the objective of this thesis to develop a quick and robust building system design optimization framework. Figure 1.3 depicts the proposed workflow of this framework. In comparison with previous studies, this framework integrates and automates different systems of the method and streamline the work processes to form a comprehensive analysis. The proposed optimiza-

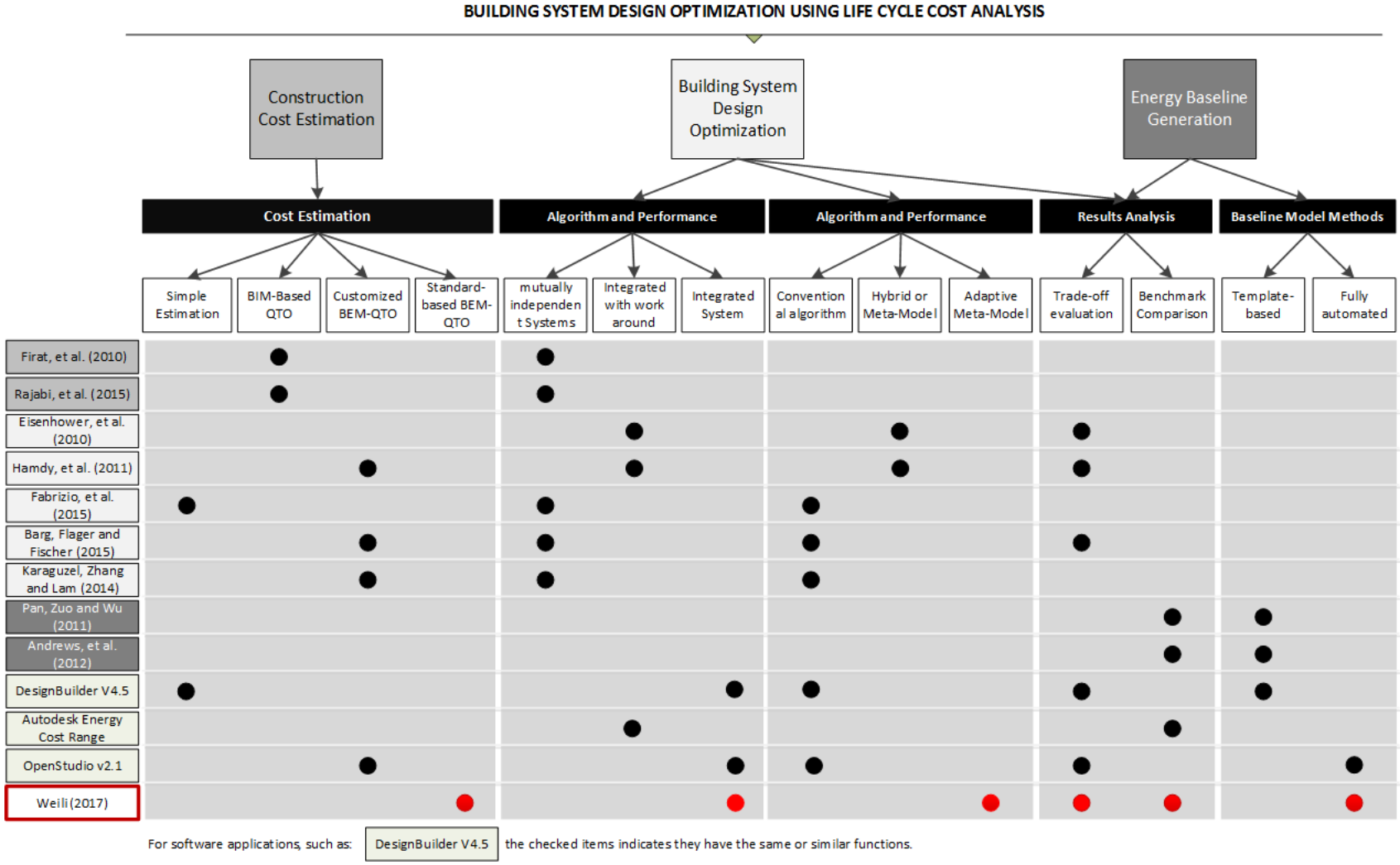

Figure 1.2: Summary of the literatures

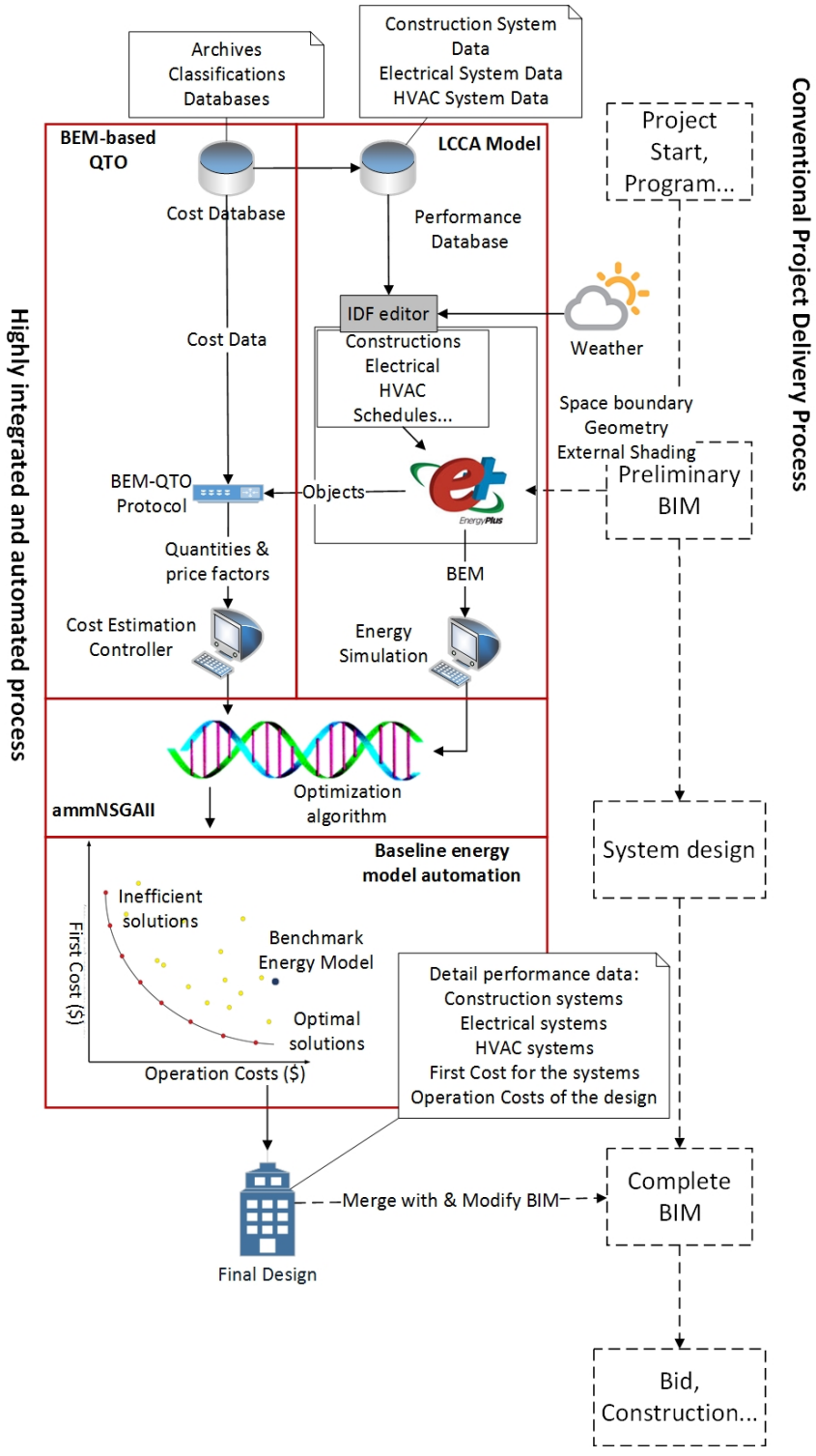

Figure 1.3: Proposed building system design optimization framework (Dashed line: processes that are not considered in this thesis.)

tion platform in this thesis aims to:

- Streamline the processes in the building system design optimization workflow.
- Performs life cycle cost analysis at the building system level to show capital cost trade-offs as well as life cycle cost trade-offs among building systems.
- Improve optimization process to achieve better time performance with high quality of results.
- Include benchmarking comparisons in the conventional optimization results analysis.

In Figure 1.3, four components of the system are identified. The development for each component will be explained in detail in the following chapters.

- Chapter 2: EnergyPlus based quantity take off system that can automatically measure the quantity of building elements based on the energy performance metrics of the elements.
- Chapter 3: LCCA model, a system, which is based on the economic module in EnergyPlus, performs long-term life cycle cost analysis with actual utility tariff.
- Chapter 4: ammNSGAII, a faster convergence meta-heuristic algorithm that implements an adaptive meta-model approach on the non-dominated sorting genetic II (NSGAII) algorithm.
- Chapter 5: Building a baseline model automaton system that automatically generates ASHRAE 90.1 compliant building energy baseline model for comparison.
- Chapter 6: Apply the method on a new construction project to demonstrate the hypothesis.
- Chapter 7: Apply the method on a retrofit project to demonstrate the hypothesis.

Chapter 2

EnergyPlus based quantity take off system

2.1 Overview

The EnergyPlus based quantity take off system is developed primarily for evaluating the capital cost of a proposed design solution. Figure 2.1 depicts the workflow and data flow of the system. In this system, the main components include a building system cost database, a building energy model (BEM) to quantity take-off (QTO) communication protocol and a cost estimation controller. Based on this system, an application, namely the EplusQTO, is developed for performing the EnergyPlus based quantity take off. Further information about this application can be found in Appendix A.

2.2 Building system cost database

As mentioned in several studies, an external cost database is critical in the cost estimation processes (Bazjanac, 2005; Wu et al., 2014). This cost database should contain building systems price factors, cost information as well as their maintenance and replacement schedule for life cycle purposes. The price factor is defined as a system's characteristics that could affect the system's price, such as boiler capacity and efficiency. The cost information of a building system consists of material cost, labor cost, equipment rental cost and overhead cost.
However, there are numerous building systems in the market. It is necessary to have a struc-

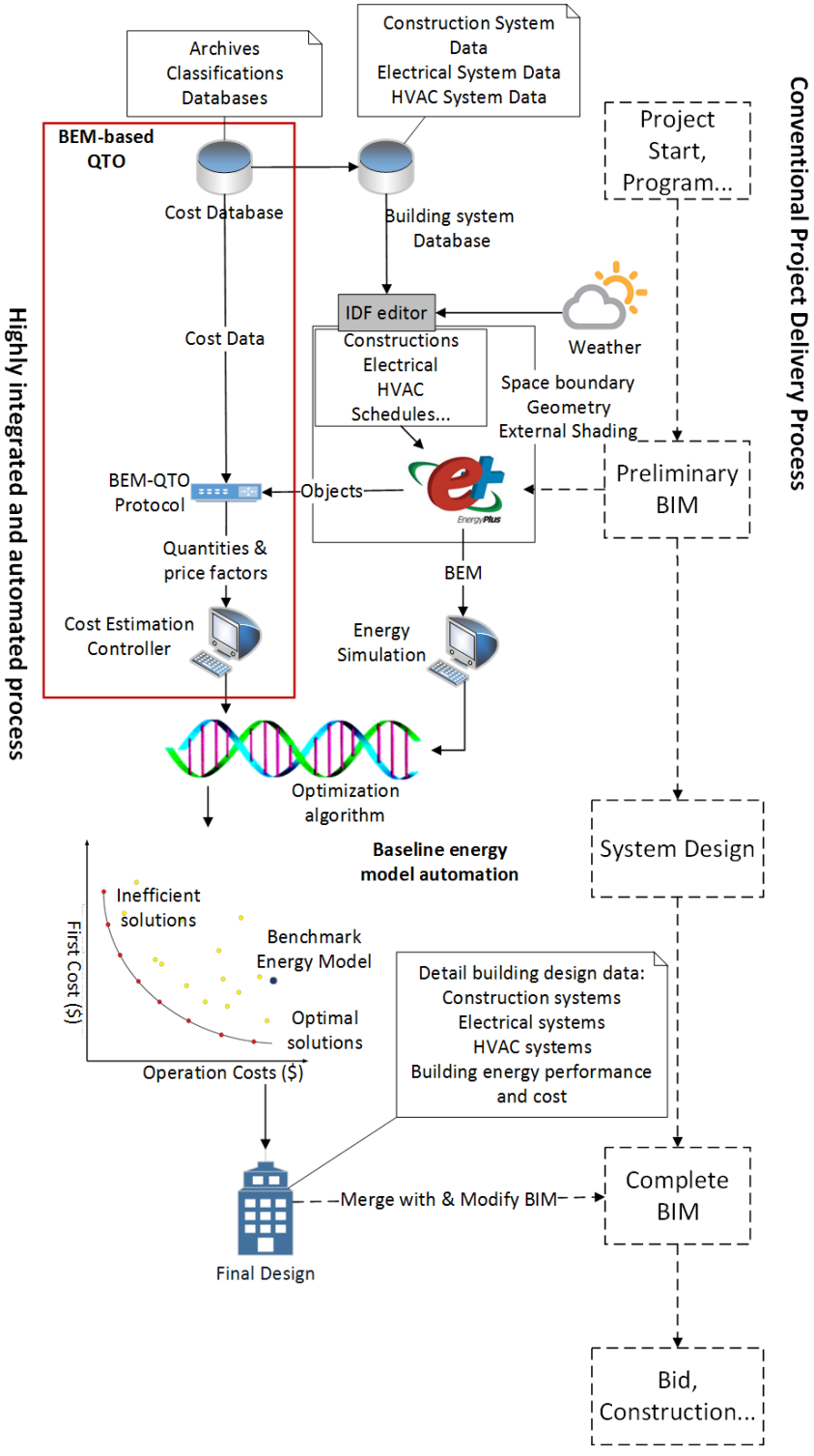

Figure 2.1: Proposed building system design optimization framework: cost estimation (Dashed line: processes that are not considered in this thesis.)

tured classification schema to classify these systems. In this proposed cost database, MasterFormat is adopted as the classification standard. It is a trade-based standard developed for organizing construction work results. This standard has been in the industry for more than 50 years, and gained recognition for organizing commercial construction specifications in the North American region (CSI, 2005). The most recent version is MasterFormat 2016, which is an updated version based on the MasterFormat 2004 release. It includes 50 divisions and each division is subdivided into a number of sections. Each type of building system and its operation, maintenance and replacement (OM&R) data are assigned with a unique number according to its 6- or 8- digits scheme (Gulledge et al., 2007). This division-subsection-numbering arrangement offers a systematic structure for managing building system data in a relational data schema. mySQL v6.0 is used as the database management system. The cost database is structured based on the MasterFormat 2016 classification standard. Cost information is mainly acquired from the RSMeans® construction cost data 2015. Additionally, literature may be used if the cost information of a system cannot be found in RSMeans® database. Figure 2.2 depicts the relational schema of the cost data. Four divisions are included to demonstrate the hierarchy of the cost data according to the MasterFormat classification standard. Each division has a primary key (PK) to connect to a lower level building system and a foreign key (FK) to connect to a higher level category. The building systems connected to divisions carry the system characteristics as well as cost vectors, which include material cost, labor cost, equipment rental cost, total cost and total cost with overhead. This allows users to adjust individual cost items based on their project information or location etc. Finally, each building system connects to a OM&R database, which contains not only the OM&R work cost, but also the typical work schedule. The OM&R data are collected from the (RSMeans, 2015; Scholand and Dillon, 2012; ASHRAE, 2015). Figure 2.3 illustrates the cost database in the mySQL v6.0 interface. The database is continuously running as a service in the operation system. It can be accessed through an application programming interface (API) for Java through the Java database connectivity (JDBC) package (Oracle, 2015).

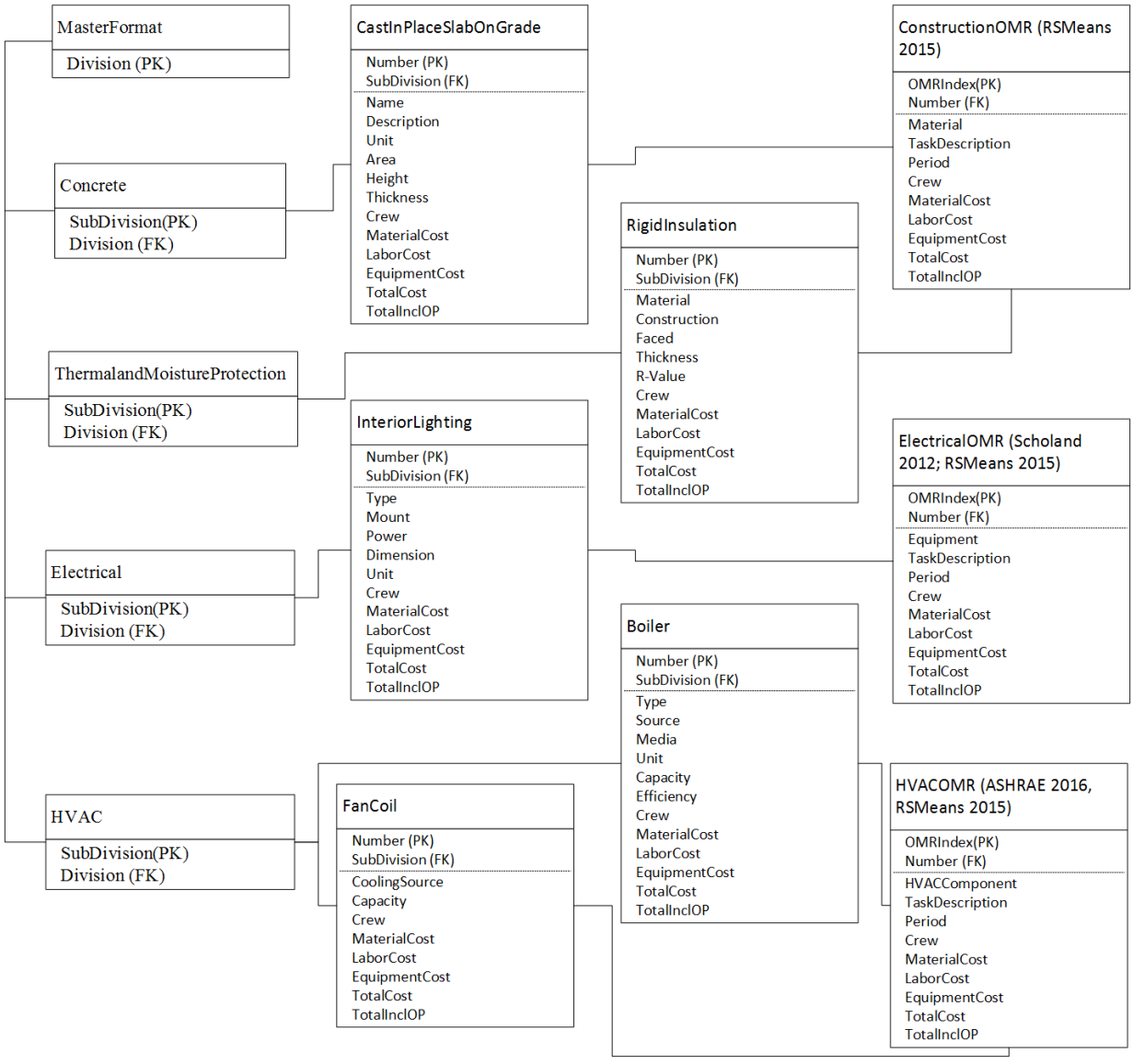

Figure 2.2: Building system cost database relational schema

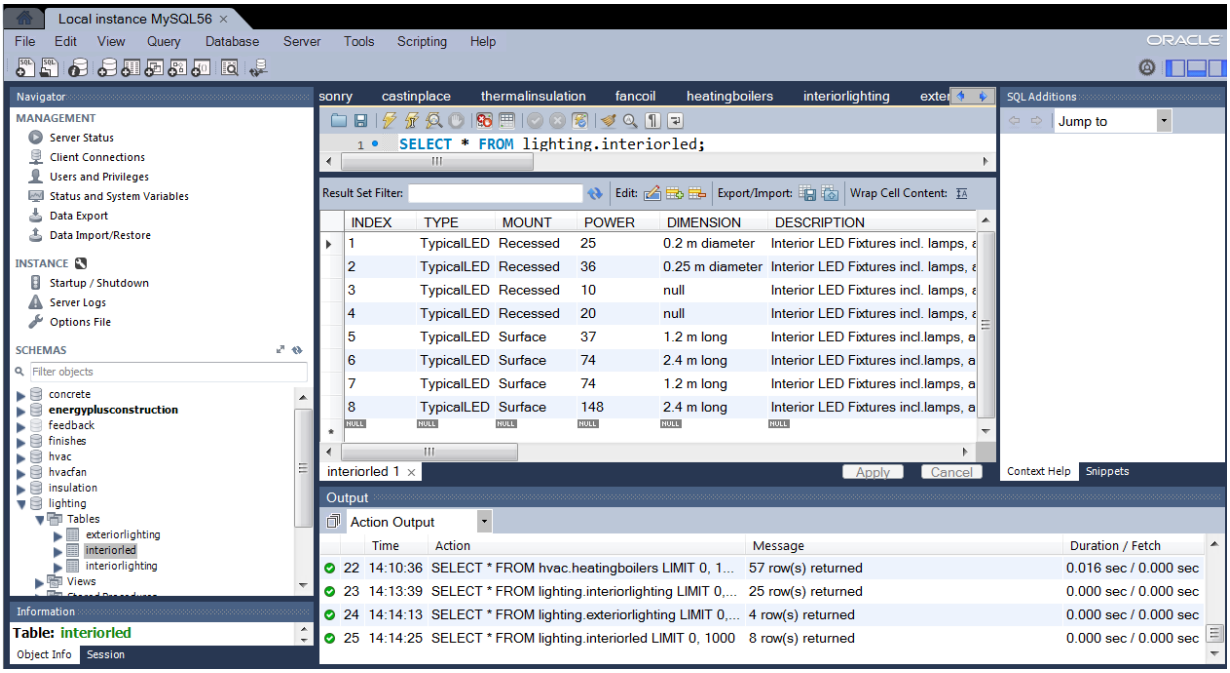

Figure 2.3: Cost database in mySQL v6.0

2.3 BEM-QTO mapping layer

2.3.1 Data communication protocol

In this BEM-QTO system, a mapping module is created to map the building system properties and characteristics with the building system design cost database. Hence, the cost estimation can be performed automatically. However, the building system in the cost database are built based on MasterFormat classification and RSMeans® database, which have very different meta-data compared to those in the EnergyPlus model. Therefore, a data communication protocol has to be implemented in order to unify these two components' semantics. The data communication protocol specify two main sections.

First, mapping the data from EnergyPlus to the cost database involves a list of building system characteristics. However, generalizing this list for all the building systems is impossible in EnergyPlus because different building systems have different properties. For instance, opaque constructions consist of layers of material objects. Each material object carries information

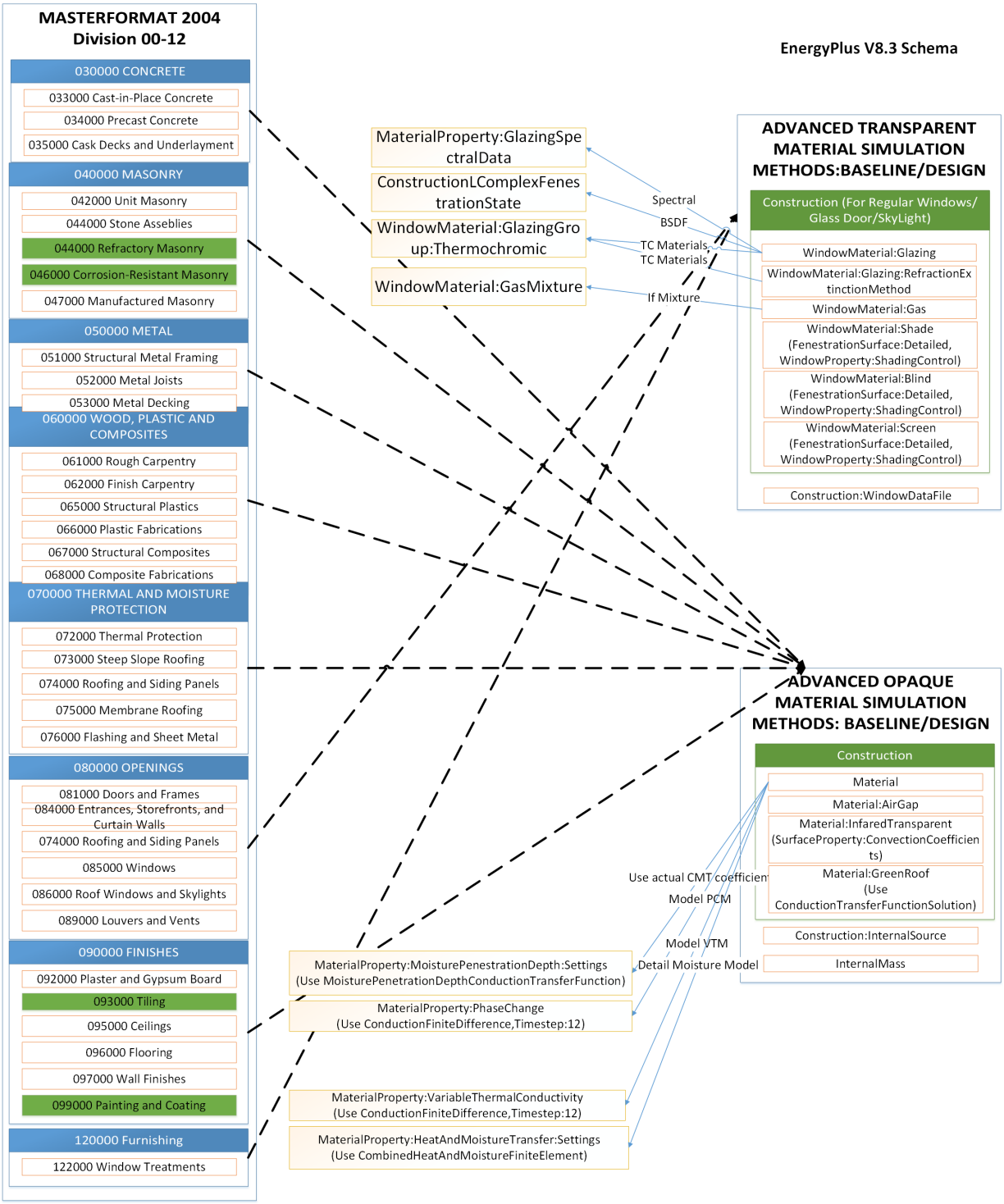

Figure 2.4: Construction data mapping between EnergyPlus and MasterFormat

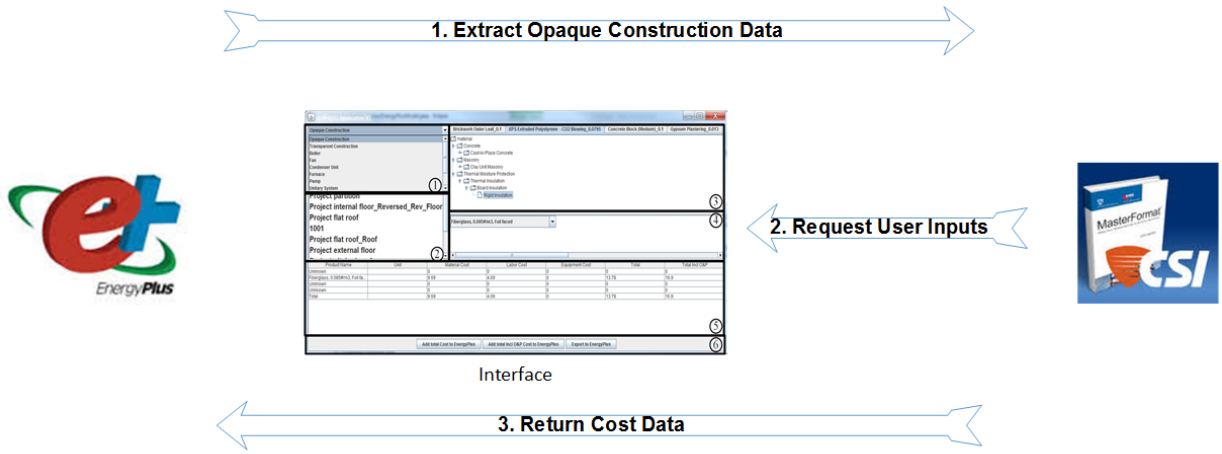

Figure 2.5: Opaque construction data communication protocol

such as material roughness, thickness, conductivity, density, specific heat, etc. This information can be grouped and mapped to various divisions in the MasterFormat directly. Compared to opaque constructions, transparent constructions have more complicated modeling methods as well as required datasets. However, only U-value, solar heat gain coefficient, visible transmittance as well as number of glazing layers are needed in cost mapping. Figure 2.4 shows the building envelope data mapping between the divisions in MasterFormats and the objects in EnergyPlus v8.3. It can be seen that most of the materials in MasterFormat can be mapped to the same or similar EnergyPlus objects such as the "*Material*" or "*WindowMaterial:Glazing*". Therefore, the development of these data lists for cost mapping depends on two factors: (1) the data inside the EnergyPlus model, and (2) the data required by the cost database. Figure 2.5 shows an example of opaque construction data protocol. For opaque materials and constructions, the data list contains floor area, surface height, surface type, thickness, conductivity, density, specific heat and thermal resistance. This information can be found in "*Material*", "*Con-*

Table 2.1: User interaction syntax

Data Type	Form	Description	Example
Input	INPUT:ELEMENT:UNIT	Request for numerical values	INPUT : boilerpower : watt
Option	OPTION:ELEMENT:ITEM	Request user to select an option	OPTION : bricktype : thinbrickveneer
Bool	BOOL:ELEMENT:ITEM	Request a yes or no selection	BOOL : fandrive : V-beltdrive

struction", "*BuildingSurface:Detailed*" and output files from an EnergyPlus model. More information about these objects can be found in (LBNL, 2016). Similarly, a transparent construction's data list carries information including glazing size, number of layers, thickness, U-value, solar heat gain coefficient and visible transmittance etc.

However, defining data lists for HVAC systems are more complicated than constructions. In EnergyPlus v8.3, there are 328 objects related to HVAC systems, and among them, 163 objects are used to describe the performance of an HVAC component. They can be organized into 12 groups namely the unitary system, heat pump system, zone HVAC, air terminals, coils, boilers, chillers, cooling tower, fan, pump, generator and solar collectors. Each group has their own data list to communicate with the cost database.

Besides the data requirements from the EnergyPlus model to the cost database, the protocol also defines a set of syntaxes to allow client and cost estimation framework communications. The necessity of client interaction is realized for cases such that additional information are required for a successful cost mapping. This information can be categorized into three data types. Table 2.1 shows these three data types and provides examples.

The last part of this data communication protocol between EnergyPlus and cost database is the cost data exported from the cost database. Once a building system is selected from the cost database, the data is sorted and arranged in a cost vector. This includes the name of the building system, quantity unit ($m^2, m, Each$, etc), and the system unit costs. The unit costs are further divided into material cost, labor cost, equipment cost, total cost and total cost including overhead and profit. This gives clients the ability to further adjust each individual cost item based

on the local rate.

In summary, the integration of the EnergyPlus model and the cost database is achieved through a well-developed data communication protocol, which is built inside a data mapping module in Figure 2.1. The mapping layer is designed to be general so that it can adapt to various BEMs for extracting building system characteristics.

2.3.2 BEM quantification extraction

The mapping protocol unifies the semantics of the data in two different components. However, to complete the system quantification extraction and cost estimation, it still requires techniques to measure and analyze the data. In EnergyPlus, "*Component:LineItem*" is the object that calculates building system costs. This object matches the unit cost to the quantity of the objects for performing the cost calculation. Table 2.2 exhaustively lists all the available objects and their cost calculation methods in the "*ComponentCost:LineItem*" object (LBNL, 2016). It can be observed that each object has different cost method. The building constructions and shading devices are typically estimated with $\$/m^2$, and the daylighting controls are often estimated with a control system set ($\$/Each$). Therefore, this object could offer sufficient estimation for these two types of building system cost estimation. However, the support for electrical and HVAC system measurements are not as sufficient as the previous two examples.

As part of the electrical system, the conventional approach for specifying a "*Lights*" object is to use an approximate lighting power density (LPD) in a thermal zone. Thus, $\$/Each$ is not an ideal cost calculation method unless the designers are certain about the total cost of lighting system for each thermal zone. Similarly, the other cost calculation method, $\$/kW$ is a good approach. However, lighting system is typically measured by the number of fixtures (n), which is not provided by EnergyPlus. Therefore, an external quantification extraction module is built to extract the quantity of building electrical systems. Unlike the constructions and shading devices, the quantity of electrical systems are converted from $\$/kW$ into the number of fixture.

Table 2.2: EnergyPlus cost line item types

Object Available	Unit Cost	Measurement Method
General	$\$/Each$	Manual
Construction	$\$/m^2$	Automatic
Coil:DX	$\$/Each$, $\$/kW$	Automatic
Coil:Cooling:DX:SingleSpeed	$\$/Each$, $\$/kW$	Automatic
Chiller:Electric	$\$/Each$, $\$/kW$	Automatic
Coil:Heating:Gas	$\$/Each$, $\$/kW$	Automatic
Daylighting:Controls	$\$/Each$	Automatic
Shading:Zone:Detailed	$\$/m^2$	Automatic
Lights	$\$/Each$, $\$/kW$	Automatic
Generator:Photovoltaic	$\$/kW$	Automatic

Equation 2.1 shows the method for converting a electrical system quantity.

$$N_e = min\left\{n \mid n \leq \frac{P}{q}\right\} \tag{2.1}$$

Where,

N_e is the number of electrical devices in a thermal zone,

P is the total power of a electric system in the thermal zone,

q is the unit power of the electrical system.

Extracting the quantity of the HVAC system is complicated because the measurement of the HVAC system is $\$/Each$ in most of the measurement standards whereas in EnergyPlus, an HVAC system object could aggregate multiple identical systems. Thus, a process is built to estimate system quantities from one EnergyPlus object. Currently, this system is able to extract the quantity of up to 10 different HVAC systems including the variable air volume system (VAV), dedicated outdoor air system with fan coil or variable refrigerant system (DOAS+FC/VRF) and heat pumps (HP). Figure 2.6 shows the process's workflow. The BEM-QTO system first analyzes the HVAC related objects in EnergyPlus. The analysis includes examining whether

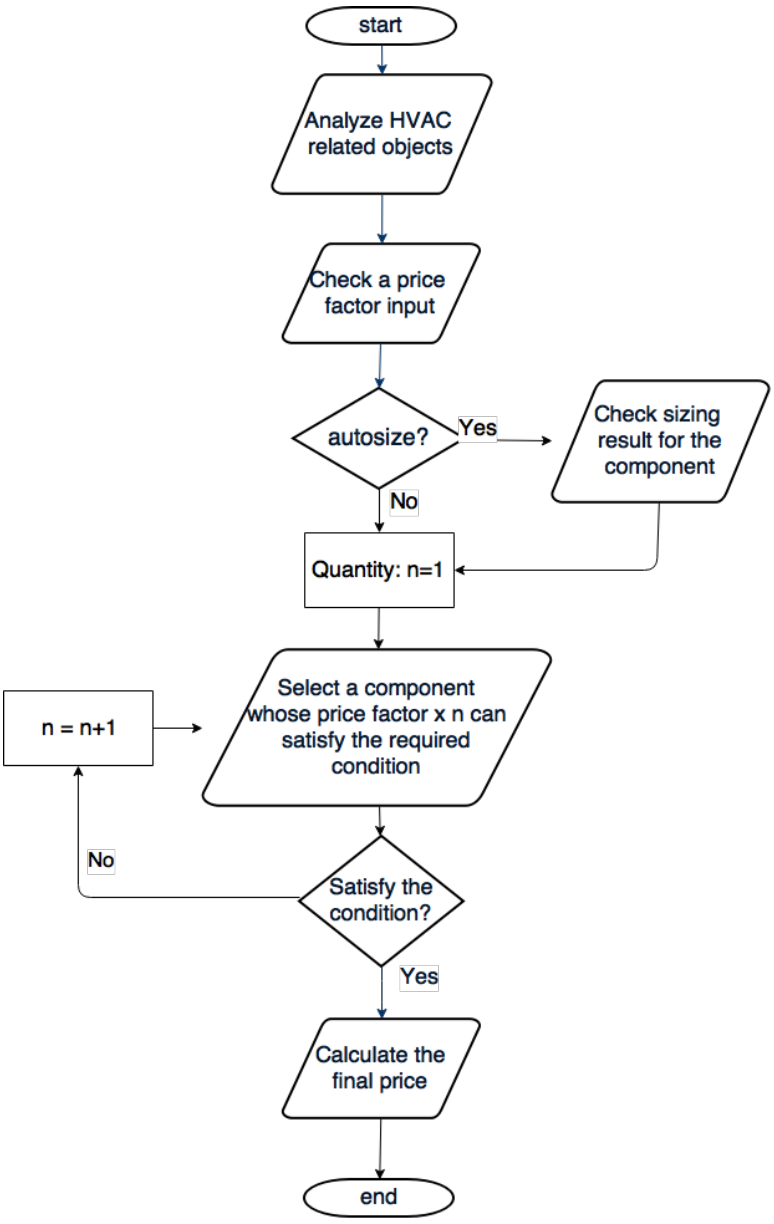

Figure 2.6: HVAC automatic quantity extraction process

this object is used, how many of them and what are the price factors. If a price factor is found to be autosized for the object, then BEM-QTO system will request the sizing results of this object from EnergyPlus output files. With the sizing results, a equipment that has equal or higher value of price factors can be selected from the cost database and the cost of the equipment will be used as the cost of the HVAC object. This workflow can also be an iterative process. It happens when none of the equipment in the cost database meet the requirements of a price factor in the HVAC object. Through several iterations, BEM-QTO system quickly identifies an equipment and the quantity of this equipment that can satisfy the price factors. Furthermore, multiple price factors can be found in some EnergyPlus objects such as a heat pump, which has cooling capacity and heating capacity. In this case, the selection of the equipment from the cost database has to satisfy all the price factors of those objects in order to carry out the final cost estimation. It is also possible for users to override the selected HVAC equipment and its quantity with the assistance of a user interface (Appendix A). Once the HVAC equipment is overridden, the final price will be calculated according to the user inputs.

2.4 Cost estimation controller

The cost estimation module is a process controller that manages or directs the flow of data between different modules. The extracted building elements cost and quantities are aggregated in this controller. Then the initial project cost is calculated. Figure 2.7 depicts a BEM-based cost estimation system domain model in the unified modeling language (UML) diagram. The controller has a “EnergyModel” module, a “MasterFormat” module and a “Mapper” module. The cost estimation is realized through a sequence of function calls from the “analyzeSystems”, which calls the “EnergyModel” to analyze the EnergyPlus model data, then to “mapCosts(String system)”.The “mapCosts” function calls the “mapper” to extract the metadata from “EnergyModel” and map it on to the “MasterFormat”. In addition, this controller also integrates an application programming interface (API) to allow specific functions or plugins to be added to this cost estimation system. The BEMQTOPlugin interfaces in Figure 2.7 shows

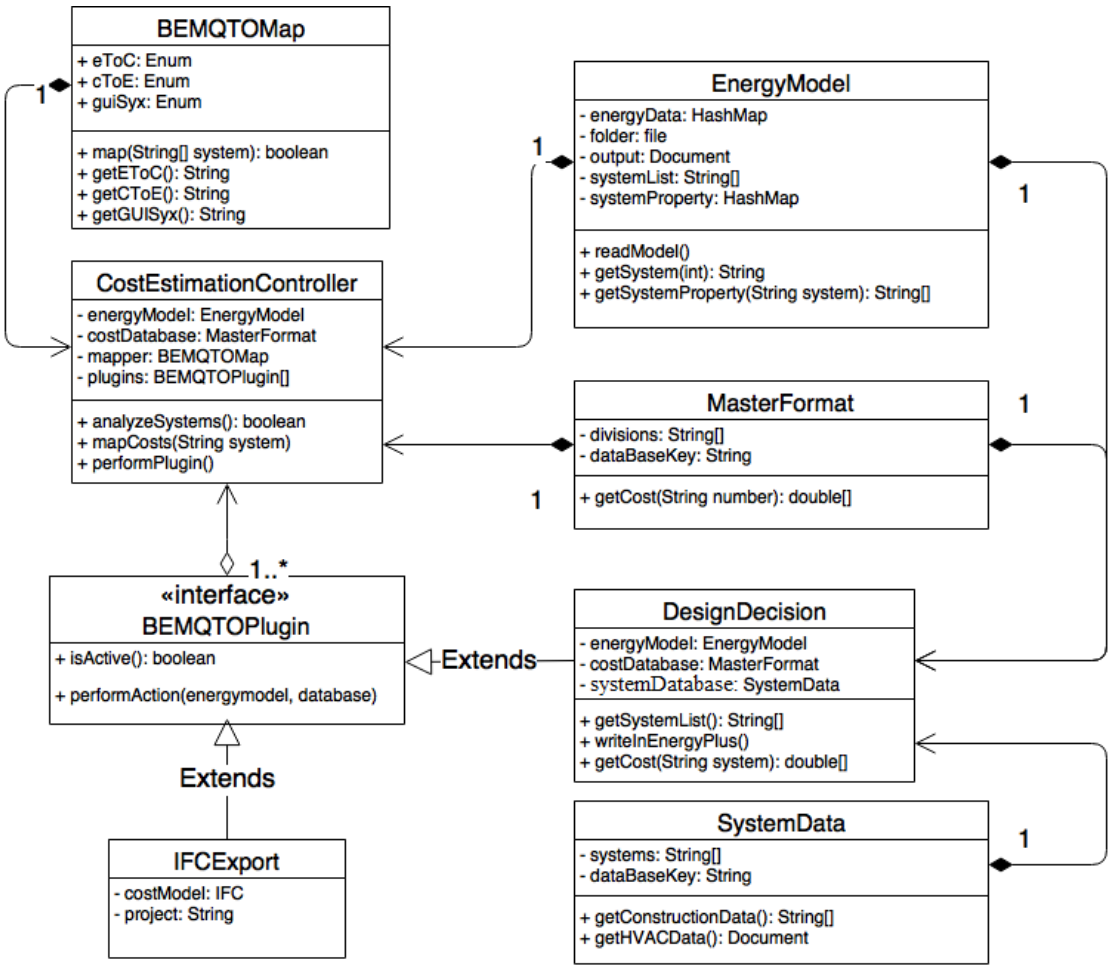

Figure 2.7: BEM based cost estimation domain process model

the details about this API as well as its relationship with the controller. Since the method in this interface allows a plugin to access both energy model and cost database, a variety of functions can be implemented in this system. In Figure 2.7, two plugins are built in this system for demonstration purposes. One is an IFC model exporter, which arranges the final cost estimation data into IFC data format. The other one shows a more complicated application that connects the system to a building system performance database for design decision support. This plugin could overwrite the systems in the EnergyPlus model, perform energy simulation and calculate the capital cost. Both plugins can be activated at the same time since their functions are mutually exclusive.

Chapter 3

The life cycle cost (LCC) model in EnergyPlus

3.1 Overview

The life cycle cost model consists of a building system database, operation cost model in EnergyPlus and building energy simulation as indicated in Figure 3.1. The primary focus of developing a life cycle cost model in EnergyPlus is to construct the fitness or the objective function for evaluating long-term operation costs for a design solution. The key feature for this model is the building system database, which contains the physical properties for design options and the data can be easily mapped to a building energy model as inputs. Moreover, the capability of the economic module in EnergyPlus is explored and tightly integrated into the whole platform in this work.

3.2 EnergyPlus building system database

The building system database is designed with two goals: (1) To manage the physical properties of building systems, (2) To connect to the cost database. There are three identified building system categories, namely the passive system, active system and energy renewable system, and their physical properties are collected from various data sources as indicated in Figure 3.2. A

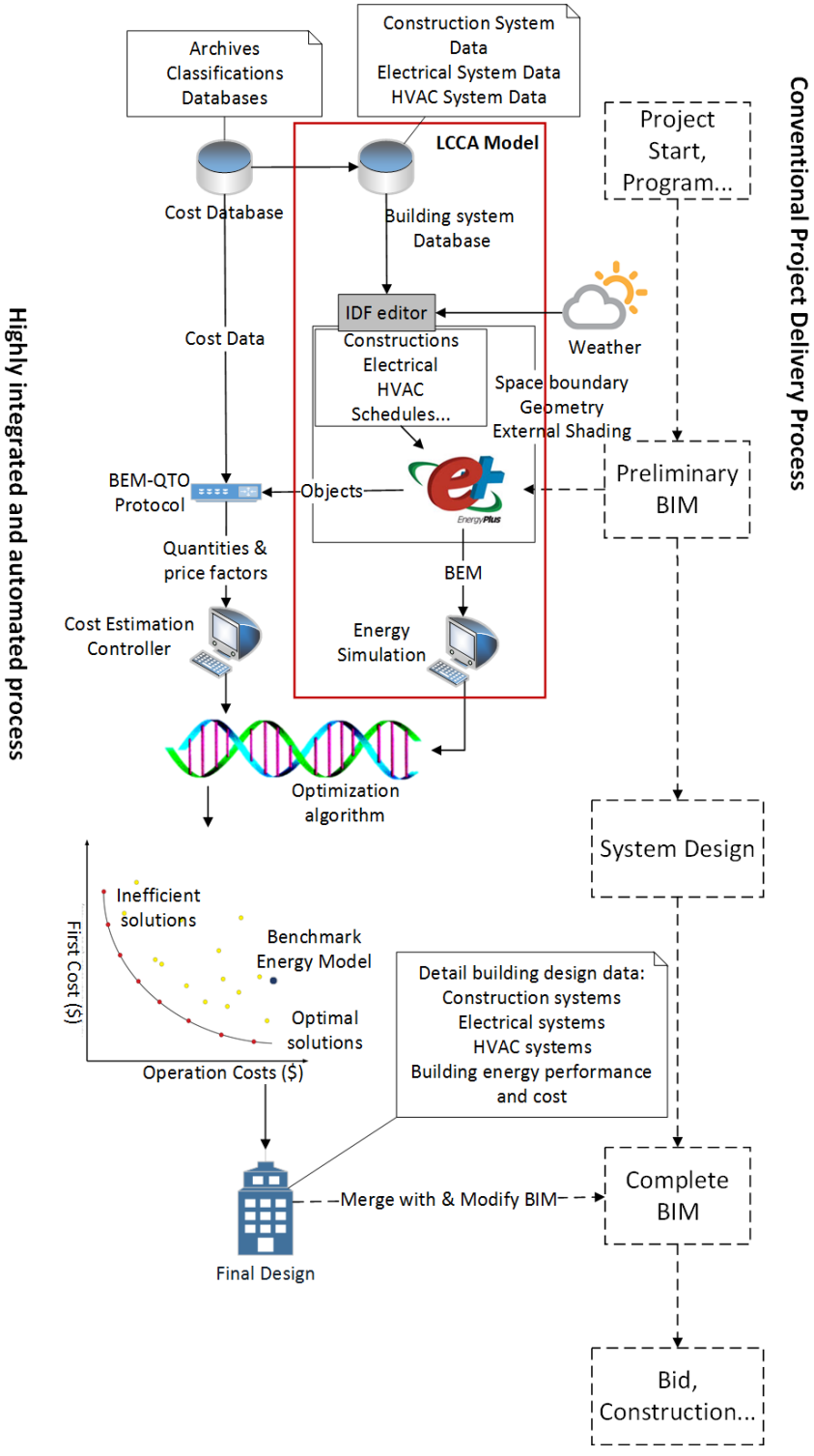

Figure 3.1: Proposed building system design optimization framework: life cycle cost model (Dashed line: processes that are not considered in this thesis)

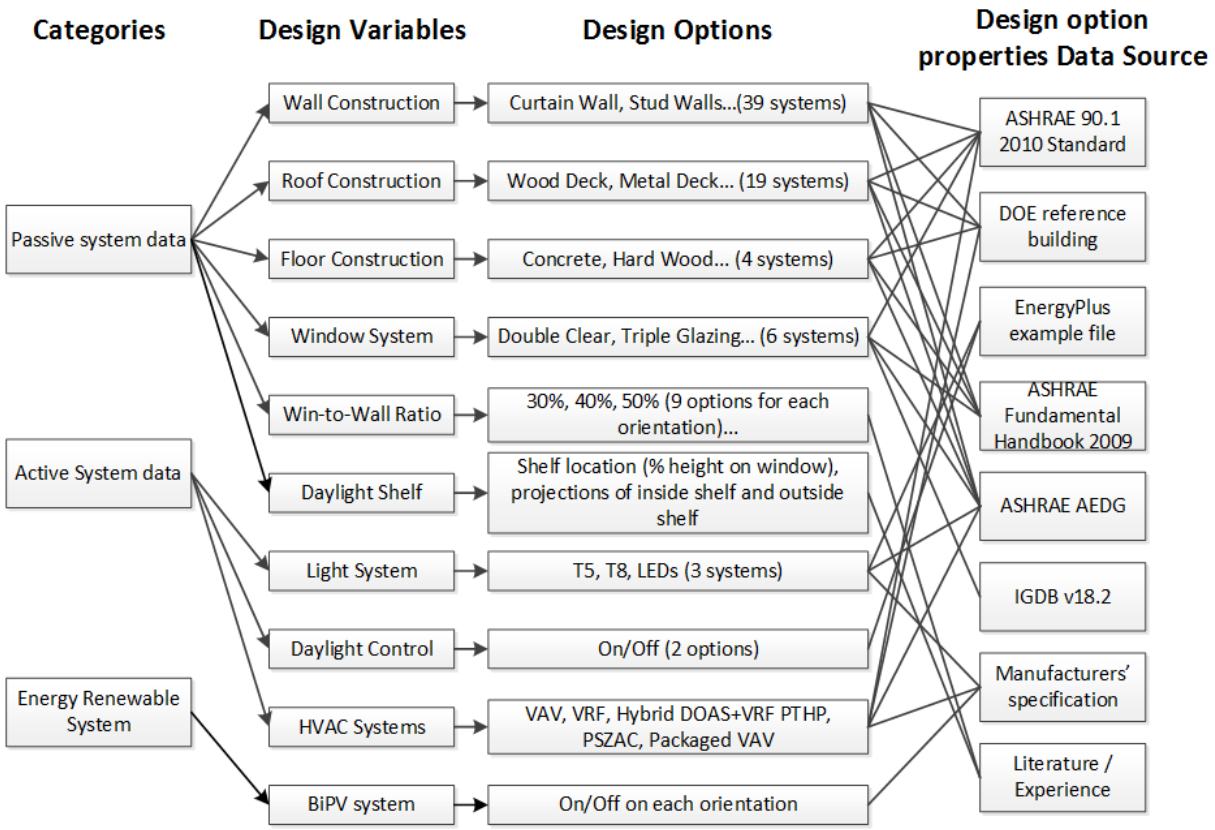

Figure 3.2: The hierarchy of building system design alternatives

detail list of the data sources is also tabulated in the Table B.1 in Appendix B. These sources include standards (ASHRAE, 2010), benchmarking and guidelines (DOE, 2017; ASHRAE, 2009) and well-established databases and manufacturers' published data. Each system type has several design parameters and each design parameter contains multiple design options. Figure 3.2 also includes the number of systems that are currently inside the building system database. The building system database is managed in a relational database schema and can be accessed through a Java application. In addition, this database is designed to connect to the cost database through two sets of keys, the "CostNumber" and "CostIndex". The "CostNumber" is the numbering system in the cost database, and it links to the "Number" key in the cost database. Similarly, the "CostIndex" shows the index of the cost information in the cost database. For instance the material cost index or the labor cost index. It links to the "Index" in the cost database. Fur-

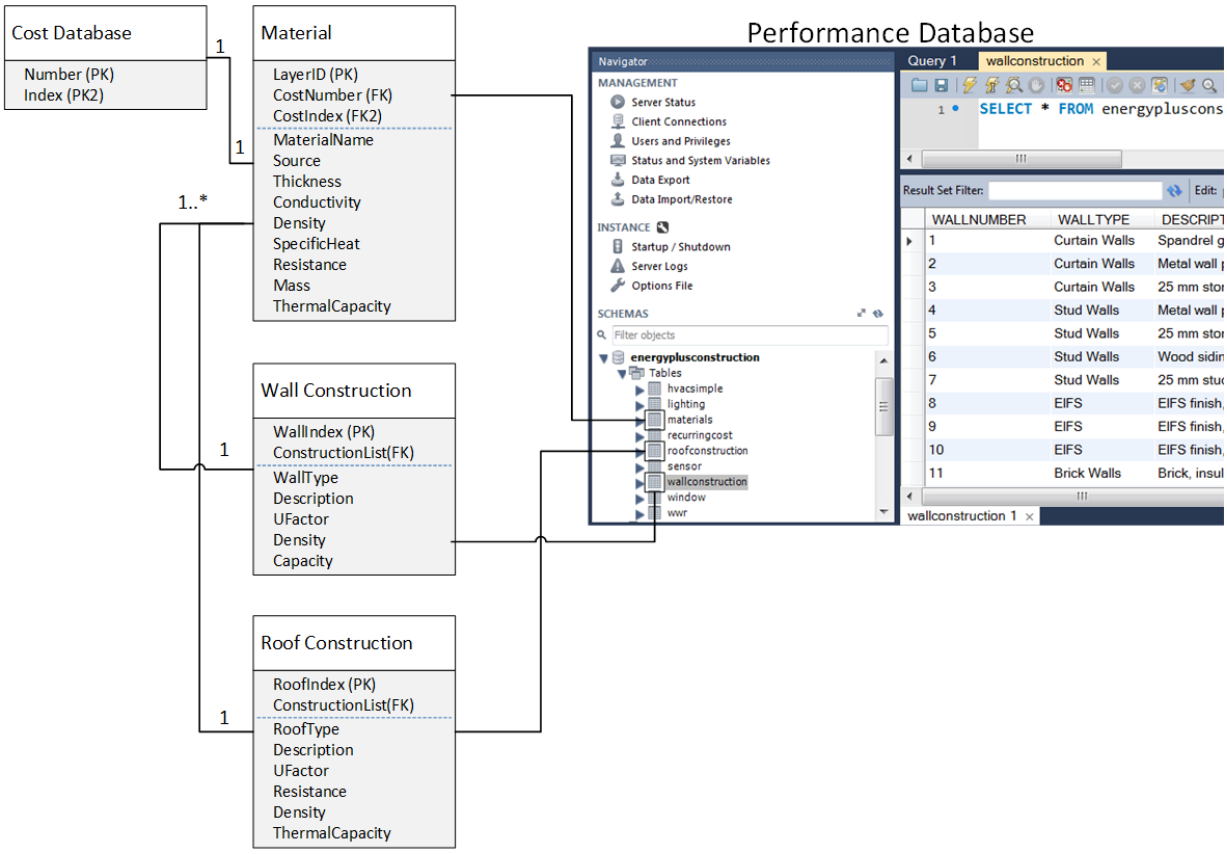

Figure 3.3: Example of opaque construction database and its relation to the cost database

thermore, for systems that require aggregating various building products, such as wall and roof construction, one set of keys is necessary for completing the data link. Figure 3.3 shows an example of the opaque constructions (Wall and Roof constructions) database and their relations to the cost database.

3.2.1 Passive system data

Passive systems focus on building envelope related aspects determined by the architectural design so as to reduce building energy demand (Chen et al., 2015). The passive systems usually require a one time cost and little or no maintenance needed after the installation. Such system includes walls, roofs, windows and shading systems (Blumenfeld and Thumm, 2014).

There are currently 39 wall, 19 roof and 4 floor constructions in the building system database. The insulation level varies from R-0.3 to R-6.5. All the constructions use the layer-by-layer

method in EnergyPlus, which requires the assembly information of a construction. Furthermore, the thermal properties of each layer are calculated through a detail parameter set, which includes the material's density (kg/m^3), thickness (m), conductivity (W/mK) and specific heat (J/kgK) etc. All this data is collected from ASHRAE 90.1 2010 standard (ASHRAE, 2010), DOE commercial reference buildings (DOE, 2017), ASHRAE Fundamental Handbook 2009 (ASHRAE, 2009) and the ASHRAE advanced energy design guides (AEDG) (ASHRAE, 2016a).

Similarly, six distinct type of window systems are recorded in the building system database. These windows are assembled according to the same sources as the opaque constructions. However, with an exception that the spectral data of each glazing are collected from the International Glazing Database (IGDB) v53.0 (LBNL, 2017). The IGDB is a collection of optical data for over 5000 glazing products and it is currently maintained by the Lawrence Berkeley National Lab. The selected windows range from double clear to quadruple. The thermal transmittance (U-Value) of these window starts from 3.13 W/m^2K to 0.781 W/m^2K, the solar heat gain coefficient (SHGC) ranges between 0.7 to 0.3 and the visibility transmittance (Vt) covers from 0.4 to 0.8. Besides the envelope systems, window to wall ratio (WWR) is also considered as part of the passive systems. The options includes 10% to 90% WWR in a step of 10%.

Lastly, the daylight shelf system is included in the building system database. The daylight shelves are one of the many daylighting devices for bringing more daylight into a building. They are typically installed as an inside shelf, an outside shelf, or both on south facing windows (Meresi, 2016). The shelves reflect the exterior light onto the ceiling of a room to achieve extended daylight penetration distance and increase uniformity in daylight distribution levels.(LBNL, 2016). In EnergyPlus, daylight shelves are modeled via the "*DaylightingDevice:Shelf*" object, where it requires a shelf host window, a heat transfer surface (inside light shelf), an attached shading surface (outside light shelf) and a shelf construction (LBNL, 2016). In order to add daylight shelves to an existing window, the window must be separated into upper window and lower window sections. The height of the upper window section decides where the daylight

shelves are mounted. In EnergyPlus, daylight shelves are simulated separately for daylighting and the zone heat balance; however, the calculations vary between the inside and outside daylight shelves. The inside shelf is assumed to reflect all the transmitted light from the upper window onto the ceiling of the room as diffuse light. This means no beam or downgoing flux can pass the end of the shelf. On the other hand, the daylighting of the outside shelf is calculated by integrating over the sky and ground and summing the luminance contribution of each sky or ground element(UIUC and LBNL, 2016). The daylighting interactions are assumed to be between shelves and the upper window except the lower window receives shading from the outside shelf. For heat balance calculation, the inside shelf is defined as an inter-zone heat transfer surface (partition) and the outside shelf is simulated as an external shading device.

Three numeric parameters are included for the daylight shelf design. They are the height (h) of the upper window, the projection (p_{in}) of the inside shelf and the projection (p_{out}) of the outside shelf. A threshold has been set for each of the parameters. For h, it can be a value between 10% to 30% of the original window height (Meresi, 2016). Any value that is outside of this range is considered a no daylight shelf system. For p_{in} and p_{out}, the value is limited between $0.5m$ to $1.5m$. If the projection of a shelf is less than $0.5m$, this shelf will not be modeled. The cost of the shelf is quoted based on the construction material cost from RSMeans construction cost database (RSMeans, 2015). The construction of the light shelf consists of one lightweight concrete layer, which is identical to the daylighting shelf example file in EnergyPlus.

3.2.2 Active system data

The active systems are those that consume external energy resources to maintain the indoor environment quality of a building (Chen et al., 2015). Such systems include heating, ventilation, air-conditioning (HVAC) systems, lighting and other building service systems. These systems typically have high capital cost and have to be properly operated and maintained (Blumenfeld and Thumm, 2014).

Three lighting and six HVAC systems are collected in the building system database. The lighting systems are selected according to the ASHRAE AEDG (ASHRAE, 2016a), and their prop-

erties are derived from the manufacturers' specification (GE, 2016). Besides lighting systems, a daylighting control system that can dim the lighting fixtures, is included in the building system database. The specification for daylighting control system is based on the examples in the EnergyPlus installation package and the EnergyPlus input output document (LBNL, 2016). The height of daylighting reference point is set at a desk height ($0.8m$) and the location of the daylighting reference point is set to the center of the room. The illuminance setpoint for the daylighting reference point is 500 lux, which is a typical value for general office work (LBNL, 2016). A continuous daylighting control type is assumed. This type of control dims the overhead lights continuously and linearly from the maximum electric power and light output to minimum electric power and light output (0.1) as the daylight illuminance increases (LBNL, 2016). The choice for daylighting control system is in a boolean or integer type, where 1 indicates "Yes" and 0 indicates "No".

The HVAC systems are more complex than most of the active systems in EnergyPlus. One of the advantages of EnergyPlus is its modularization feature, which allows energy modelers to model a large variety of advanced HVAC systems. However, this feature creates problems for generalizing the HVAC system creation process in various building layouts because different HVAC systems may have different system connection methods and different control logics. Therefore, an automatic HVAC system generation system is developed according to (Xu et al., 2016b) to generalize the creation of various popular HVAC systems in a building energy model. The system consists of a pre-defined thermal zone format, a HVAC-XML data schema and an idf translator that translates XML data into .idf format. The pre-defined thermal zone format is designed to capture the HVAC components connections. There are five elements in the proposed thermal zone format (Table 3.1). They are block, zone function, zone identification, zone's mechanical ventilation group and its thermal condition group. The first three elements store a zone's architectural information and the last two elements indicate a zone's HVAC system information. For instance, Floor6%Office%601%DOAS6%VRF6E2 indicates the number 601 thermal zone is located on the 6^{th} floor and it is an office room. Regarding to its mechani-

Table 3.1: Thermal zone name convention

Name element	Remark
Block	Block composed of a number of thermal zones. e.g, Floor6
Function	The primary function of a thermal zone. e.g, Office
Identification	The label of a particular thermal zone. e.g, 602
Ventilation	Zone group of mechanical ventilation. e.g, DOAS
Thermal	Zone group of indoor thermal conditions. e.g, VRF6E2

cal system information, this zone belongs to the DOAS6 zone group for mechanical ventilation and the VRF6E2 zone group for indoor thermal condition. There are some reserved characters for the last two elements, which are designed for the zones that require special mechanical conditions. For example, an ”EXT” in the ventilation group element means an exhaust system is required in this zone. This zone name convention allows tools to quickly construct basic zone activity assumptions and some common HVAC systems.

The HVAC data is stored in an XML format. The design of this XML data schema focuses on providing quick data conversion between EnergyPlus .idf data structures and HVAC property data structures. The design quality attributes of the HVAC system XML data schema includes:

1. Adaptable to common HVAC systems' property data
2. Extensible and easy to modify with EnergyPlus version upgrades.

The XML format has elements including:
<**dataset**>: dataset is the parent element that contains the entire data of one specific HVAC system. It has two attributes:

1. **setname**: specify the HVAC product name of this dataset
2. **version**: specify EnergyPlus version for this dataset

Example: <dataset setname = “Manufactuer VRF 4Ton” version = “V8.3”/>.
<**object**>: object is a child of <object>element. This element represents the objects in EnergyPlus. It has two attributes:

1. **description**: the name of the EnergyPlus object
2. **reference**: the object reference. This attribute indicates the sub-system that this object

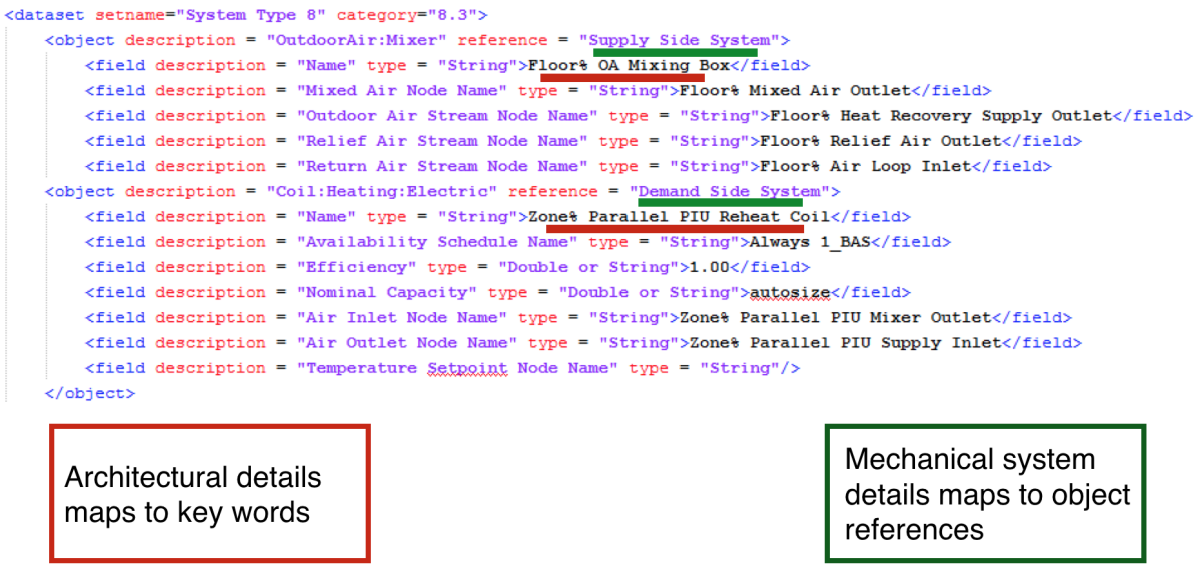

Figure 3.4: EnergyPlus HVAC XML schema and its connections to thermal zone name

belongs to.

Example: <object description = "AirLoopHVAC" reference = "Supply Side System">.

<**field**>: field is a child element of <object>. This element represents the individual field under an object in EnergyPlus. It also has two attributes:

1. **description**: the key of a field
2. **type**: data type, this includes "String", "Double" and "Integer".

Example: <field description = "Gross Rated Cooling COP" type = "Double">3.2</field>.

The data schema can directly link to the EnergyPlus HVAC system model based on a two-layer logic process. The first layer identifies HVAC system type and EnergyPlus version to extract the corresponding dataset at **dataset** element. The next step applies auto generation strategies to different sub-systems and thermal zones. Figure 3.4 shows an example of the second connections process. The sub-system, supply side system, is created by analyzing both the ventilation group, and the thermal condition group ("*Zone%*" or "*Floor%*") in the zone name. Currently in the building system database, six different types of HVAC systems are collected and stored. The selection of the systems is based on ASHRAE AEDG (ASHRAE, 2016a) and ASHRAE

90.1 2010 standard (ASHRAE, 2010). The system specifications are collected from multiple sources including the DOE commercial reference buildings (DOE, 2017), EnergyPlus example files, and manufacturer's specifications (Toshiba Carrier, 2016; Carrier, 2016). All the property of systems have met the minimum requirements set by ASHRAE 90.1 2010 standard (ASHRAE, 2010).

3.2.3 BiPV system data

The use of building integrated photovoltaic (BiPV) system is increasing due to its contribution towards net zero building in urban areas, where most of the buildings have limited rooftop area but large facade areas (Ng and Mithraratne, 2014). The selected photovoltaic technology in this thesis is applicable to opaque and mono-crystalline silicon (m-Si)-based solar cells encapsulated between multiple glass layers (i.e., glass-glass encapsulation). The objective here is to provide parametric evaluations of systems integrative energy performance of BiPV elements. Therefore, the PV heat transfer integration mode is selected as "Integrated Outside Face" within EnergyPlus. In such an integration mode, the solar cells are treated as integral elements of the building envelope assemblies with bi-directional thermal interactions, where solar cell temperatures are effected by conductive heat flux within the envelope assembly, while electrical energy generated by solar cells are taken as a heat sink term and removed from heat transfer surfaces. So as to achieve this thermal interaction, the PV integrated envelope assemblies are defined by a "*Construction: InternalSource*" in EnergyPlus (LBNL, 2016), which allows locating an internal heat source or sink element, such as a PV element, within the assembly. The front glass of the BiPV system selected as a clear uncoated monolithic glass with relatively high front-side solar and visible transmittances at normal incidence (0.903 and 0.912, respectively). Currently, Solar World 185 watt BiPV product is collected in the building system database (SolarWorld, 2016). It is m-Si PV with a peak power rating of 185 Wp and a solar conversion efficiency of 16.32% under the Standard Test Conditions. A simple DC-to-AC inverter model with a constant operating efficiency of 0.94 is assumed for the entire BiPV system. It should be noted that the BiPV system life time in this thesis is assumed to be 25 years. This was set in accor-

dance with literatures (Ng and Mithraratne, 2014) as well as IEA recommended life expectancy (Fthenakis et al., 2011). In addition, the performance degradation of BiPV system in the 25 year life span is not considered in this thesis.

3.3 Utility tariff model in EnergyPlus

The EnergyPlus's economics module is capable of modeling complex utility cost tariffs. Unlike an average energy cost value, the well established tariff model can accurately represent the monthly energy cost based on both energy consumption and monthly peak demand (Xu et al., 2016a). It also allows energy modelers to set tariff qualifiers which capture the energy performance of a building (typically the peak demands in 6 or 12 consecutive months) and determine the tariff that this building should subscribe to. In addition, block rates, ratchet and seasonal rates can be modeled as well. For the full capability of the EnergyPlus utility model, readers are encouraged to explore in (LBNL, 2016). Therefore, with a tariff model, the optimization process will not only minimize the building's annual energy consumption, but also reduce its peak demands.

To demonstrate the accuracy of the utility tariff model in EnergyPlus, an energy model, whose monthly energy consumption is calibrated in accordance with the ASHRAE Guidenline 14-2002 threshold (Chong et al., 2015), is used to estimate the monthly energy cost with a detailed local tariff model and the average energy price from the EIA average of the electricity price (EIA, 2016). The results in Figure 3.5 suggests that the utility tariff model could achieve less than 5% coefficient of variation of the root mean square error (CVRMSE) compared to the results by using the average energy price, which is more than 30% CVRMSE.

3.4 LCC model in EnergyPlus

The LCC is one of the most frequently used economic methods for project evaluations. However, it requires effort and data to initialize such a study. In this thesis, the LCC follows the

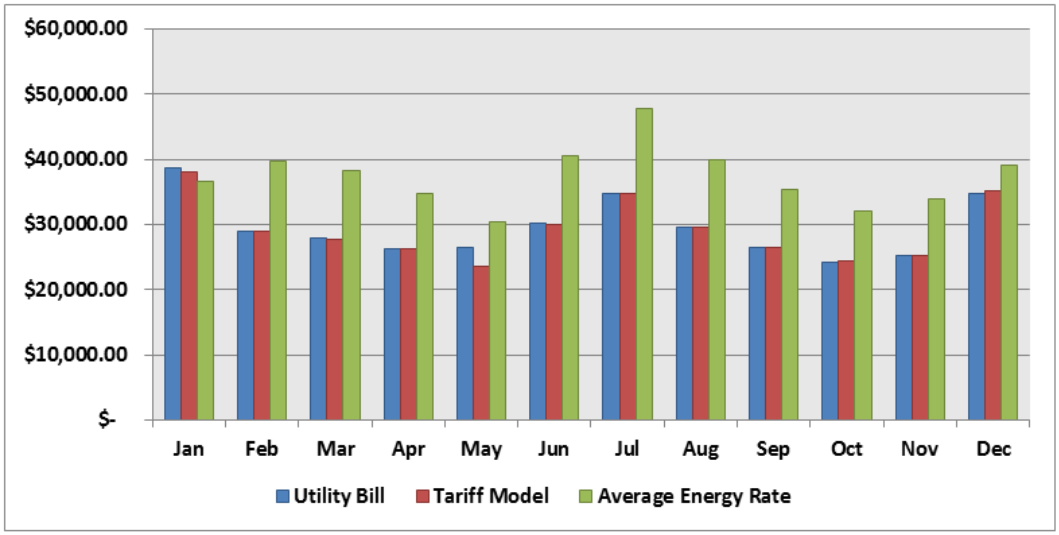

Figure 3.5: Prediction accuracy comparison between utility tariff model and average energy rate approaches

guideline that is provided in (Fuller and Petersen, 1995). The formulation of LCC study is:

$$f_1(X) = c_{rep} - c_{res} + c_e + c_{om\&r} \tag{3.1}$$

$$f_2(X) = c_{ei} + c_{hi} + c_{li} + c_{rest} \tag{3.2}$$

Where,

X is a design solution,

$f_1(x)$ is the building operation costs,

$f_2(x)$ is the capital cost,

c_{ei} is the envelope costs,

c_{hi} is the HVAC system costs,

c_{li} is the lighting system costs,

c_{rest} is the other costs,

c_{rep} is the present value of capital replacement costs,

c_{res} is the present value of residual value less the disposal costs,

c_e is the present value of energy costs,

Table 3.2: Life cycle cost analysis important parameters and sources

Parameter	**Description**	**Source**
Base date	date when the study starts	Design Team
Service date	date on which project starts	Design Team
Study length	expected life span of the project	(Fuller and Petersen, 1995)
Adjusted value of currency	constant dollars or current dollars	Design Team
Interest Rate	discount rate	NIST 2016 Supplement/ (Rushing et al., 2016)
Depreciation	reduction in the value of an asset	(IRS, 2016)

$c_{om\&r}$ is the present value of non-fuel operating, maintenance and repair costs.

$$X = \left\{ x \in \mathbb{Z}^{sc} | x^{ij}, i \in \{1..c\}, j \in \{1..s\} \right\} \tag{3.3}$$

Where,

$\mathbb{Z}^{sc}$ is the constraint set,

x is the design parameter,

s is the building system types,

c is a system cost information.

The $\mathbb{Z}^{sc}$ is the constraint set, which contains the pre-defined building system types s and their cost c. The design parameter x is specified as discrete or continuous independent variables that can only take the values from $\mathbb{Z}^{sc}$.

The parameters in LCC could largely affect the final outcome. This task also collects these critical parameters from various reliable sources. Table 3.2 shows the LCC parameters and their sources that are used in this thesis.

3.4.1 Discounting in LCC analysis

The essential idea of performing life cycle cost analysis for buildings is to justify the short-term investments by considering the long-term cost savings impacts on the present value. Therefore,

it is critical to discount the future costs to its present value. In this LCC model, two types of discounting operations are included.

- Discounting one-time amounts to a present value. This type of discounting method is used to calculate the present value of costs occurring at irregular or non-annual intervals. Examples include fan replacement at end of 15 years or residual value of a system at the end of the study period.
- Discounting a series of annually recurring amounts to a present value. Examples include annual system checkup, energy costs etc.

Equation 3.4 shows the single present value (SPV) factor that can be used to calculate the present value of a future cash amount occurring at the end of year t, F_t, given a discount rate of d (Fuller and Petersen, 1995).

$$PV = F_t \times \frac{1}{(1+d)^t} \tag{3.4}$$

Equation 3.5 presents a a uniform present value (UPV) factor for calculating the present value of a series of equal cash amounts, A_0, that recur annually over a period of n_y years, given a discount rate of d (Fuller and Petersen, 1995).

$$PV = A_0 \times \frac{(1+d)^{n_y} - 1}{d(1+d)^{n_y}} \tag{3.5}$$

These calculation processes has been integrated in the life cycle cost module in EnergyPlus. The validation of the life cycle cost module was conducted in (Cho et al., 2011) by comparing its outputs against the building life cycle programs (BLLC5) (NIST, 2016).

Chapter 4

ammNSGA-II, an advanced multi-objective optimization algorithm

4.1 Overview

The adaptive meta-model NSGA-II is one of the most advanced meta heuristic optimization algorithms developed for tackling the optimization problems with computationally expensive fitness functions. This type of algorithms has been tested in many real-world engineering problems, whose fitness functions involve solving differential algebra equations (DAE) with approximation techniques. Such examples can be found in aeronautics designs (Giannakoglou, 2002), airfoil design (Emmerich and Naujoks, 2004), and building design (Gilan and Dilkina, 2015; Brownlee and Wright, 2015).

Figure 4.1 depicts the workflow of the proposed framework and highlights the position of the ammNSGA-II algorithm. The algorithm takes in cost information and energy simulation results from the cost estimation model and life cycle cost analysis model. Then it will generate a group of optimal design solutions for design team and clients review. In this chapter, a detailed description for the development of a mixed type ammNSGA-II algorithm for building system design optimization is presented.

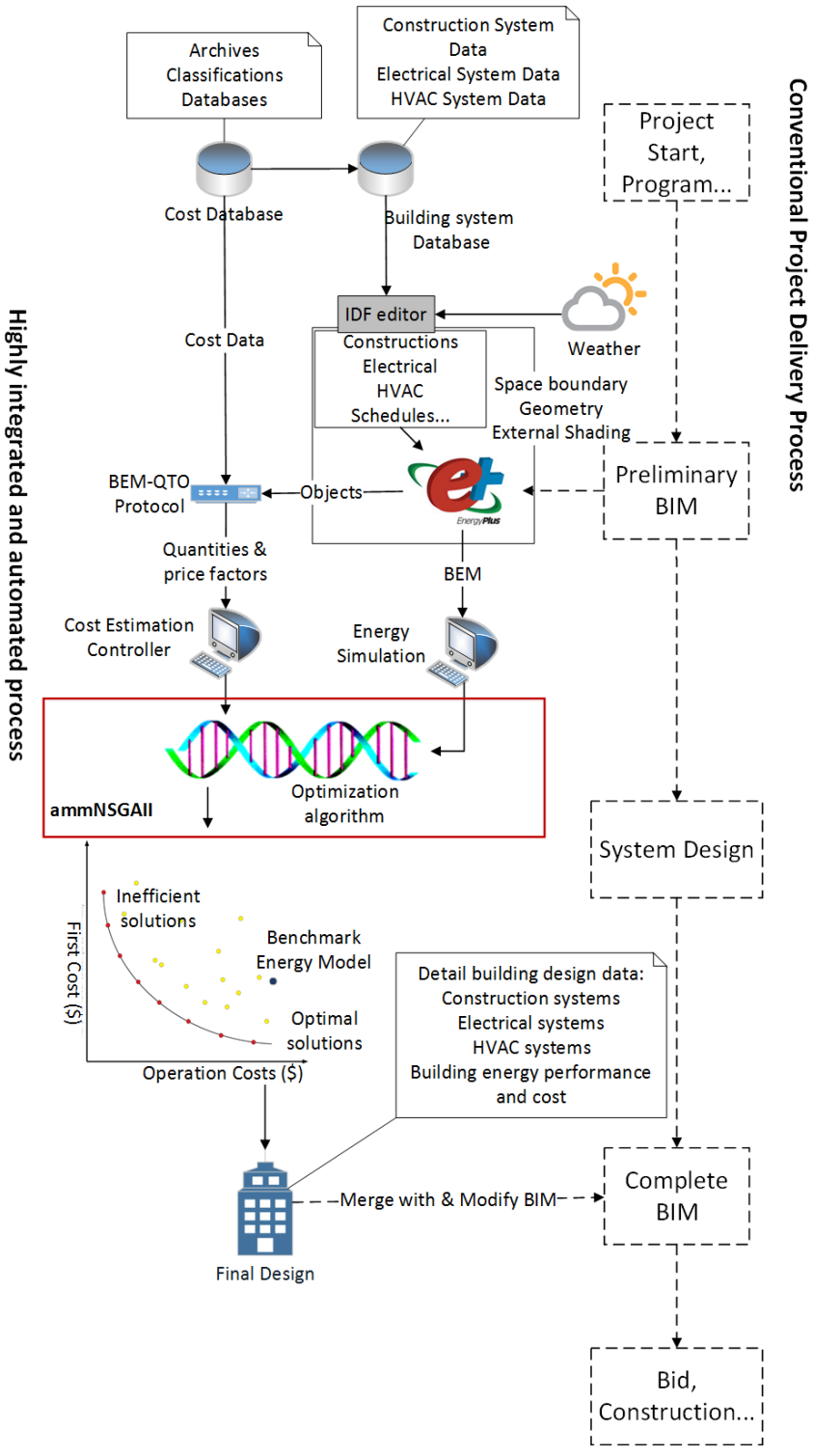

Figure 4.1: Proposed building system design optimization framework: optimization (Dashed line: processes that are not considered in this thesis.)

4.2 Meta-heuristic algorithm

The optimization algorithms can be categorized into deterministic or stochastic. A deterministic algorithm works in a mechanical deterministic manner without any random nature, such as a hill-climbing algorithm (Yang, 2011). On the contrary, stochastic algorithms add randomness into its process. Therefore, the algorithm may generate different outputs from time to time, even though the initial point remains the same. In recent optimization literature, such type of algorithms are often being referred to as metaheuristic algorithms (Glover and Kochenberger, 2006). The word "metaheuristic" first appeared in (Glover, 1986). It can be considered as "*an master strategy that guides and modifies other heuristics to produce solutions beyond those that are normally generated in a quest for local optimality*"(Glover and Laguna, 2013). Summarized in (Yang, 2011), there are two distinct advantages of metaheuristic algorithms.

- Quality solutions to difficult optimization problems can always be found in a reasonable time.
- Global optimality can be achieved in problems that have a discontinuous solution space.

For the majority of building system design problems, evaluation of the fitness function involves solving differential algebra equations (DAE) with approximation techniques, which is not only computationally intensive but also introduces the discontinuity relation between fitness functions and design parameters (Wetter, 2004). Therefore, metaheuristic optimization algorithms are the ideal algorithms for solving building system design problems. Many popular algorithms are classified as metaheuristic which includes the simulated annealing type that searches along a markov chain and converges under appropriate conditions (Kirkpatrick et al., 1983), particle swarm optimization, which searches by adjusting the trajectories of a swarm of intelligent agents (particles) on a solution space (Eberhart and Kennedy, 1995), and genetic algorithms etc. Among these algorithms, genetic algorithms (GAs) are probably the most popular with a diverse range of applications (Yang, 2011). The algorithms are developed based on Charles Darwin's natural selection theory that models the biological evolution (Holland, 1992). By

mimicking gene reproduction, crossover and mutation behaviors, the algorithm's mathematic foundation shows that the GAs can achieve exponential search power in the solution space (Goldberg and Holland, 1988).

The essential components of a genetic algorithm are selection, crossover and mutation operators. These components are often referred to as genetic operators. The selection operator preserves the elite design solutions in a generation, which ensures the offsprings have the optimal solutions. On the other hand, crossover is one of the operators used in producing offspring (i.e, candidate design solution alternatives). A typical crossover proceeds in two steps. First, members of the newly reproduced design solutions in the mating pool are mated in a pair at random. Second, every pair of design solutions exchange a group of their design parameters with each other (Goldberg and Holland, 1988). The key idea of this operator is to enhance the exploration process by recombining the "high-performance" group of design parameters. The selection and crossover can efficiently search and recombine the "better performance" group of design parameters along the generation. However, occasionally they may become overzealous and lose some potentially useful combinations of design parameters, which is often referred to as the premature convergence issue. The mutation operator is intended to protect against this issue through a random alteration in the value of design parameters (Goldberg and Holland, 1988). A typical procedure of GA can be summarized in seven steps.

1. Encode parameters (design option) into GAs data format.
2. Define the fitness function (energy, cost or predicted mean vote) to evaluate each chromosome (design solution).
3. Create a population of chromosomes (a group of design solutions).
4. Evaluate the fitness of every chromosome in the population.
5. Create a new population by performing selection, crossover and mutation.
6. Replace the old population with the new population
7. Repeat step 4,5,6 for a number of iterations

8. Decode the best chromosome to obtain a solution to the problem.

4.3 Multi-Objectives optimization

Most of the building system design optimization problems have multiple goals. It is possible to optimizing one goal with constraints from the other goals. However, this approach limits the flexibility of solution evaluation in multiple dimensions. For instance, the goals for a medium size office is to minimize the energy consumption with a limited budget. By setting energy as the main goal and budget as one of the constraints, the design team could potentially find a solution to achieve a design that has relatively low energy consumption within the target budget. However, it does not offer "what-if" situations, e.g, "will the energy consumption reduced drastically if the budget can be stretched by 5%?" Multi-Objective optimization is designed to answer such questions. Instead of one fitness function, Multi-Objective optimization has two or three fitness functions that are evaluated in parallel in the process. Pareto optimality is a frequently used method for analyzing Multi-Objective optimization results (Evins, 2013). This method introduces a set of design solutions as an optimal solution set. In this solution set, a unique situation occurs where a single objective adversely affects other objectives. Figure 4.2 shows a typical Pareto Front curve. It can be observed that there is no solution in this optimal solution set, which has both lower capital and operation costs than any other solutions in the same set. However, by analyzing this Pareto Front curve, one can learn that in a span of 25 years, design solution "case 3" demands 4% higher capital cost but yield 10% lower operation costs than design solution "case 1".

To equip an algorithm with the ability for evaluating multiple fitness functions, a design solution sorting algorithm must be applied. The current most popular sorting algorithm is the non-dominated sorting algorithm, which ranks a design solution based on the number of the design solutions in a population it dominates. The definition of dominance can be described in two conditions. Assume one design solution is X^1 and the other is X^2.

- If all the outcomes of the fitness function $f(X^1) \leq f(X^2)$ and

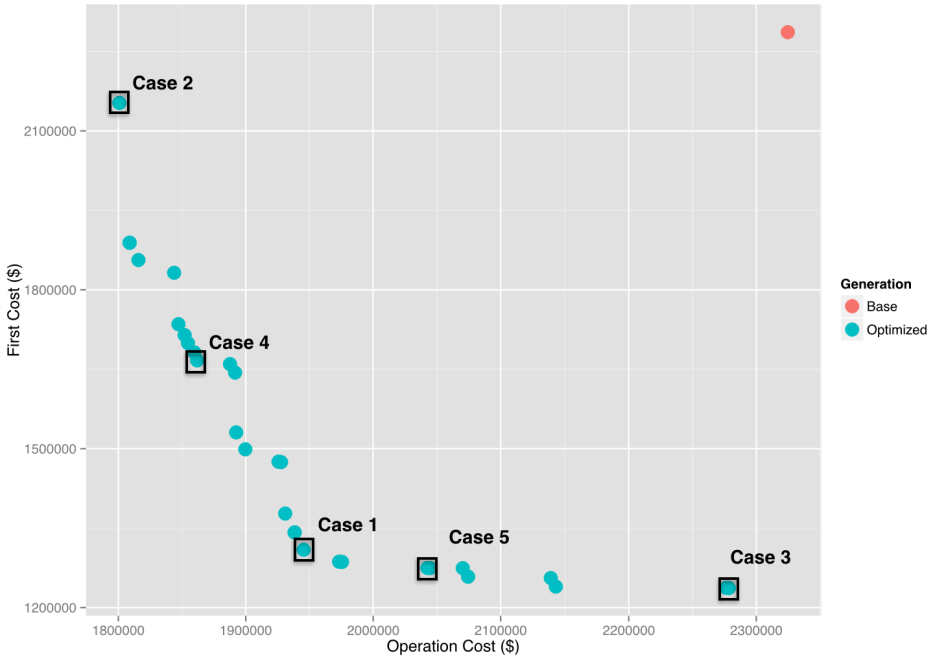

Figure 4.2: The pareto front curve (adopted from (Xu et al., 2016a))

- If at least one $f(X^1) < f(X^2)$

Then X^1 dominates X^2 .

There are many metaheuristic algorithms that are equipped with the non-dominance sorting algorithm to achieve a Multi-Objective evaluation capability. The non-dominant sorting genetic algorithm II (NSGA-II), proposed by (Deb et al., 2002), is one of the most popular algorithm that has been applied in many real-world engineering problems (Roberti et al., 2017; Esfe et al., 2017; Chan et al., 2016).

4.4 ammNSGA-II algorithm framework

The NSGA-II algorithm has combined the search capability of a genetic algorithm with an advanced sorting algorithm. It is robust but, not fast, especially when the fitness functions are computationally expensive. In this thesis, a new method called adaptive meta-model NSGA-II (ammNSGA-II) algorithm is proposed to speed up the conventional NSGA-II algorithm so that the optimization process for problems with a heavy computational requirement can be com-

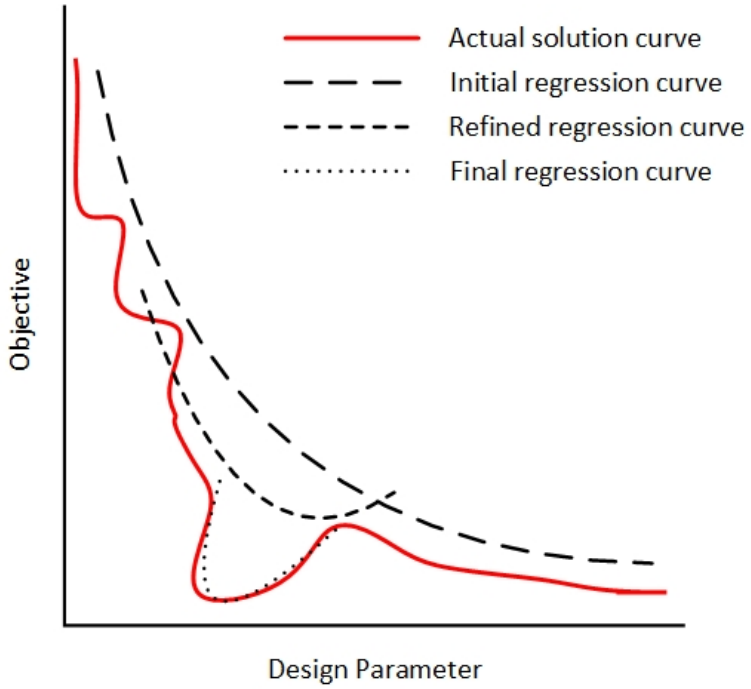

Figure 4.3: The coarse-to-fine adaptive meta-modeling theory.

pleted in a short timeframe. Unlike the convention NSGA-II algorithm, ammNSGA-II algorithm integrates the optimization components and machine learning modules. This concept is based on a "coarse-to-fine" search theory, which is proposed in (Deb and Nain, 2007). The theory states that the accuracy of meta-models could be compromised at the beginning stage of an optimization process due to the lack of sufficient data points for training. However, they can be refined in later stages when the search is conducted in a smaller but more focused region. Figure 4.3 demonstrates the concept of the "coarse-to-fine" theory. The initial regression curve in Figure 4.3 does not provide enough accuracy to predict the actual solution value, however, it provides the algorithm with a search direction to move to. As the optimization continues, the regression curve is refined to a higher accuracy in predicting target values. Eventually, a final regression curve can successfully predict the values in the optimal region.

The optimization components include an elite selection mechanism, crossover operator, mutation operator and solution ranking algorithm. Additionally, the machine learning modules equip regression models and a k-fold cross validation scheme. The functions for each component will

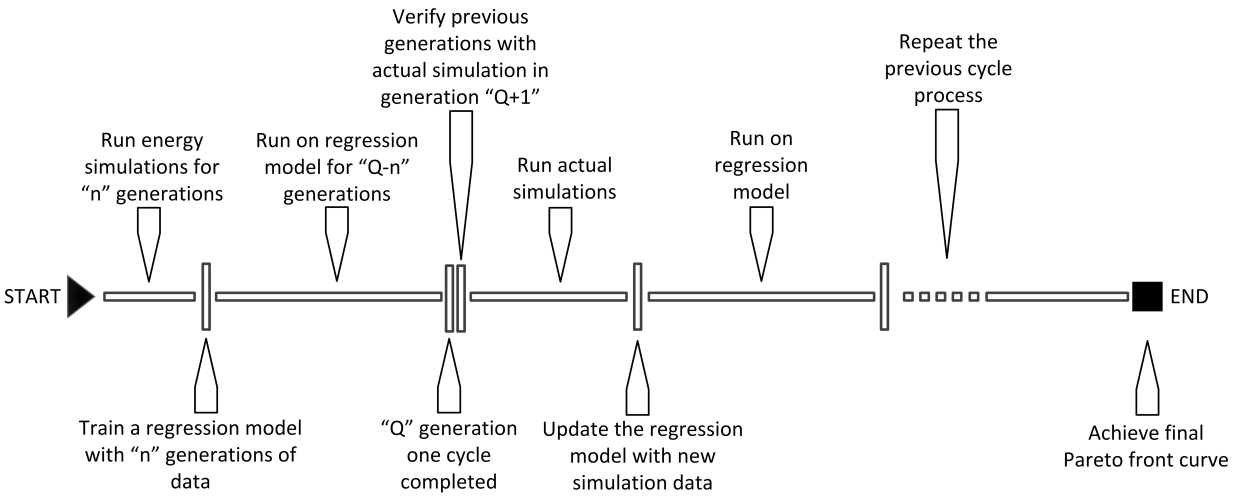

Figure 4.4: The procedure of adaptive meta-model NSGA-II (adopted from (Xu et al., 2016a))

be detailed in the following sections.

4.4.1 Optimization procedure

The optimization procedure of ammNSGA-II contains two hyper-parameters n and Q. Figure 4.4 depicts the overall process of the proposed ammNSGA-II algorithm. At the beginning, the ammNSGA-II behaves similar to a conventional optimization. A population is raised by randomly selecting from pre-defined design options and their operation costs are evaluated through energy simulations. Meanwhile, external storage is created for storing all the design solutions at each generation. At generation n, the ammNSGA-II pauses the optimization process and then trains the meta models with data retrieved from the external storage. Once regression models are built, the ammNSGA-II replaces the energy simulation in the fitness functions with newly trained meta models and restarts the optimization process until Q's generation is reached. Every Q^{th} generation is called one optimization cycle. The cycle will continue until a maximum evaluation number is reached.

4.4.2 GeneAS scheme for mix-type data

Most of the building system design optimizations are complex not only because of the computationally expensive fitness functions, but also the design parameters that needs to be explored.

These design parameters can be a set of systems such as HVAC systems, which are transferred into binary or integer data types before passing to the algorithm, or design variables such as the height of a piece of shade that should be recognized as numeric data types. However, the typical NSGA-II algorithm can only work with one type of parameter due to the data processing limitation from the crossover and mutation operations. In order to equip ammNSGA-II with the ability to handle mixed type of parameters, the combined genetic adaptive search (GeneAS) scheme proposed in (Deb and Goyal, 1996) is adopted. In a GeneAS scheme, each parameter to be encoded depends on its type nature in the optimization process, and the crossover and mutation operators apply their operations parameter by parameter.

- For a binary or integer parameter, the binary-genetic operations are performed
- For a numeric parameter, the numeric-genetic operations are performed.

4.4.3 Crossover operator

Crossover is one of the operators used in producing offspring (i.e, candidate design solution alternatives). A typical crossover proceeds in two steps. First, members of the newly reproduced design solution in the mating pool are mated at random. Second, each pair design solutions exchange a group of their design parameters (Goldberg and Holland, 1988). The concept of this operator is to enhance the exploration process by recombining the "high-performance" group of design parameters. Several operations are available for performing the random mating with binary or integer parameters such as one-point crossover, two-point crossover, or half uniform crossover (HUX). However, these crossover operations cannot be used for numeric parameters. For those type of parameters, operators such as simulated binary crossover (SBX) can be implemented to perform the same task. The SBX operator is designed with respect to the properties of a single point crossover by ensuring the average design parameter value holds in the process, and the spread factor (β), which controls the spread of likely offspring, is more likely equal to 1 (Deb and Kumar, 1995).

$$\beta = \begin{cases} (2\mu)^{\frac{1}{\eta_c+1}} & \text{for } \mu \leq 0.5 \\ (\frac{1}{2(1-\mu)})^{\frac{1}{\eta_c+1}} & \text{for } \mu > 0.5 \end{cases} \tag{4.1}$$

$$\begin{aligned} p_1' &= 0.5[(1+\beta)p_1 + (1-\beta)p_2] \\ p_2' &= 0.5[(1-\beta)p_1 + (1+\beta)p_2] \end{aligned} \tag{4.2}$$

Where,

β is the spread factor,

μ is a random number between 0 and 1,

η_c is the distribution index,

p' is offspring value,

p is parent value.

In Equation 4.1, μ is a number randomly drawn from the set of $[0, 1)$ and the η_c is the distribution index which determines how close the offsprings are to their parents. p' and p are the values for offspring and parents respectively. The mathematical formation of Equation 4.1 implies a high possibility of achieving a β that is close or equal to 1. The β calculated in Equation 4.1 is used in Equation 4.2 for calculating the values of design parameters in offspring. Equation 4.3 combines the two equations in Equation 4.2. It implies that the average design parameters values are the same for both parents and offspring.

$$\frac{p_1' + p_2'}{2} = \frac{p_1 + p_2}{2} \tag{4.3}$$

4.4.4 Mutation operator

The mutation operator is primarily used to maintain the diversity of design solutions. A bit-flip algorithm is ordinarily used for parameters with integer data type. The algorithm simply replaces the original value of a design parameter by selecting a random integer value within the allowable range of this design parameter. For numeric design parameters, a polynomial mutation operator with a user-defined index variable (η_m) is often used to perturb a design solution in a parent's vicinity. The calculation consists of three steps.

1. Generate a random number μ between 0 and 1.

2. Calculate a parameter δ as follows:

$$\delta_q = \begin{cases} [2\mu + (1-2\mu)(1-\delta)^{\eta_m+1}]^{\frac{1}{\eta_m+1}} - 1 & \text{for } \mu \leq 0.5, \\ 1 - [2(1-\mu) + 2(\mu-0.5)(1-\delta)^{\eta_m+1}]^{\frac{1}{\eta_m+1}} & \text{for } \mu > 0.5. \end{cases} \tag{4.4}$$

   Where,

   μ is a random number between 0 and 1,

   δ is normalized differences,

   η_m is the distribution index for mutation.

   In Equation 4.4, the η_m controls the distances of the mutated value with its parent. A larger η_m shows a higher probability that the mutated value is closer to its parent. As demonstrated in (Deb and Agrawal, 1999), a value between $[20, 100]$ for η_m is sufficient for most of the problems. The δ can be calculated in Equation 4.5.

$$\delta = min[(p - p_l), (p_u - p)]/(p_u - p_l) \tag{4.5}$$

   Where,

   p_u is the upper bound of a parameter p,

   p_l are the upper and lower bounds of parameter p.

3. Calculate the mutated offspring as follow:

$$p' = p + \delta_q(p_u - p_l) \tag{4.6}$$

In GeneAS, the polynomial mutation operator (Equation 4.4 and 4.6) has been integrated into the operator with a mutation clock scheme. The mutation clock scheme requires that the probability of a bit followed by a mutated bit should be determined by using an exponential probability distribution (Deb and Deb, 2014).

4.4.5 Regression models

Two candidate machine learning algorithms, linear regression and support vector machine, are included in the framework.

Linear Regression

Linear regression (LR) is a commonly used method where energy performance is estimated by building characteristics (Braun et al., 2014; Zhao and Magoulès, 2012). The Mathematical representation of LR is shown in Equation 4.7. In this equation, y_i is the output vector, and x stands for the input vector. β and ε denotes parameters estimated from the data. The selection of the LR model is performed through a greedy search using Akaike-based criterion (AIC) as shown in Equation 4.8 (Hall et al., 2009). In this equation, I represents the number of instances considered in the regression model and k is the number of attributes.

$$y_i = X^T\theta + \alpha_i \tag{4.7}$$

Where,

y_i is the output vector,

X is the design solution,

θ is the slope vector,

α is the intercept vector.

$$AIC = (I - k) + 2k \tag{4.8}$$

Where,

I is number of instances (design parameters),

k is the number of attributes (design options).

Support Vector Machine

Support vector machine (SVM) is one of the popular supervised machine learning algorithms that is often used in the building field (Dong et al., 2005). In this study, LibSVM was used for

SVM training and predicting (Chang and Lin, 2011). The algorithm constructs a set of hyper-planes in high dimensional space to separate training data into different classes with a functional margin, which offers high generalization. Consider a set of training points, $((x_1, z_1), ..., (x_i, z_i))$ where $x_i \in R^n$ is a feature vector and $z_i \in R^1$ is the target output. Under the given parameters $C > 0$ and $\varepsilon > 0$ (Chang and Lin, 2011) , $\varepsilon - SVR$ can be formulated as:

$$\begin{aligned} \min_{\omega,b,\xi,\xi^*} \quad & \frac{1}{2}\omega^T\omega + C\sum_{i+1}^{l}\xi_i + C\sum_{i+1}^{l}\xi_i^* \\ \text{s.t.} \quad & \omega^T\omega(x_i) + b - z_i \leq \varepsilon + \xi_i, \\ & z_i - \omega^T\varphi(x_i) - b \leq \varepsilon + \xi_i^*, \\ & \xi_i\xi_i^* \geq 0, i = 1, ..., l. \end{aligned} \tag{4.9}$$

Where,

ω is the support vectors,

ξ_i is the slack variables,

ε is the soft margin.

The formation of equation 4.9 represents the Lagrange Multiplier. In this equation, ω denotes the support vectors, which are the input vectors that lie within the margin's boundary. ξ_i is a slack variable that controls the sensitivity of the algorithm to outliers, and lastly ε provides a soft margin which alters hard constraints into ranges.

The SVM hyper-parameters were tuned with a set of pre-simulated data to ensure the algorithm's prediction performance. A polynomial kernel was used in this test. Different combinations of C (0.0625, 1, 16) and degree in kernel function (3, 4, 5) were tested. The results indicated no significant difference in prediction errors among these combinations. Therefore, the default value $C = 1$ and $d = 3$ were used in this thesis.

4.4.6 Cross-validation

The selection of regression models is performed through a k-fold cross validation method according to their prediction errors. The k is set to 10 according to the "caret" tool default settings (Kuhn, 2008). In the model selection process, this method is performed on LR and SVM. The

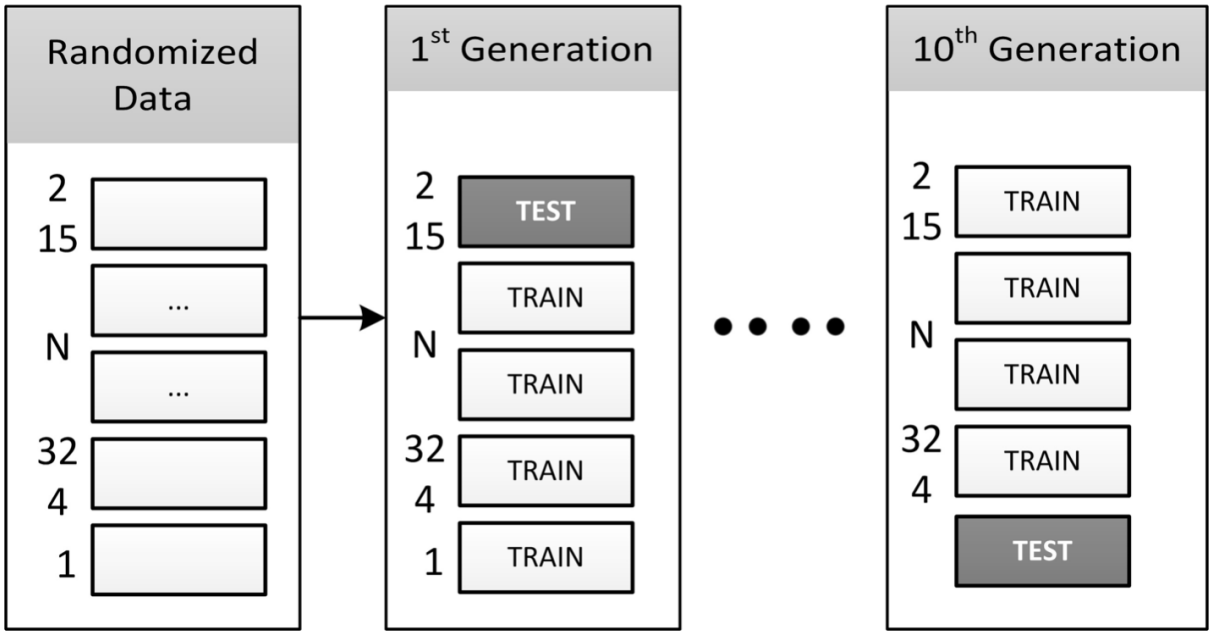

Figure 4.5: k-fold cross validation procedure

model with the smallest calculated prediction error is selected and used for prediction. The process of this method is demonstrated in Figure 4.5.

- Rearrange the index of the instance in a random order and split these randomized data into 10 equally sized partitions.
- Perform 10 iterations of the evaluations. At each iteration, the method leaves one partition out as the testing case and uses the rest of the data to train the regression model.
- Accumulate the calculated prediction errors as the accuracy metric for the regression model with this dataset.

The prediction error is a function of the differences between the actual and the predicted output values. It is typically used as an accuracy metric for evaluating the regression model's generalization property, which prevents the model from under-fitting and over-fitting issues. In this study, normalized root mean square error (NRMSE) is used as the prediction error (Equation

4.10).

$$RMSE = \sqrt{\frac{\sum_{t=1}^{n_t}(\hat{y}_t - y)^2}{n_t}}$$
$$NRMSD = \frac{RMSE}{y_{max} - y_{min}} \tag{4.10}$$

Where,

$\hat{y}_t$ is the predicted value at time t,

y is the simulated value at time t,

n_t is the number of training data,

y_{max} is the maximum target value in the training data,

y_{min} is the minimum target value in the training data.

In the regression model selection process, a 10-fold cross validation method is performed on SVM and LR models with respect to each objective. The model with the smallest calculated accuracy metric in one objective is selected and used for predicting this objective.

4.5 Algorithm performance validation

The validation process was conducted on a medium-size office building in Pittsburgh, PA. The case study demonstrated that the proposed ammNSGA-II algorithm could achieve up to 60% time savings and 25 times higher convergence performance. Details regarding this case study can be found in Appendix C.

Chapter 5

Building baseline energy model generation

5.1 Overview

This chapter introduces a system that can automatically generate baseline energy models according to the ASHRAE standard 90.1 2010 performance rating method (PRM). Figure 5.1 depicts the role of this system in the optimization result analysis. Once the multi-objective optimization generates a Pareto Front curve, a baseline energy model is created through an envelope, a lighting and an HVAC engine for comparison. Such comparison could inform the design team and clients about the quality of the generated optimal design solutions. In order to automate this process, envelope, lighting and HVAC system generation engines are developed and the methods are described in this chapter.

5.2 Automatic generation method

5.2.1 Envelope system engine

The building envelope engine takes care of all the construction requirements. Figure 5.2 shows the workflow of this module. The engine first analyzes each building and fenestration surface to identify their types (wall, roof or partition, etc.), surrounding environment and thermal properties. The processed data is prepared and stored in a data structure for the next step. Then, the

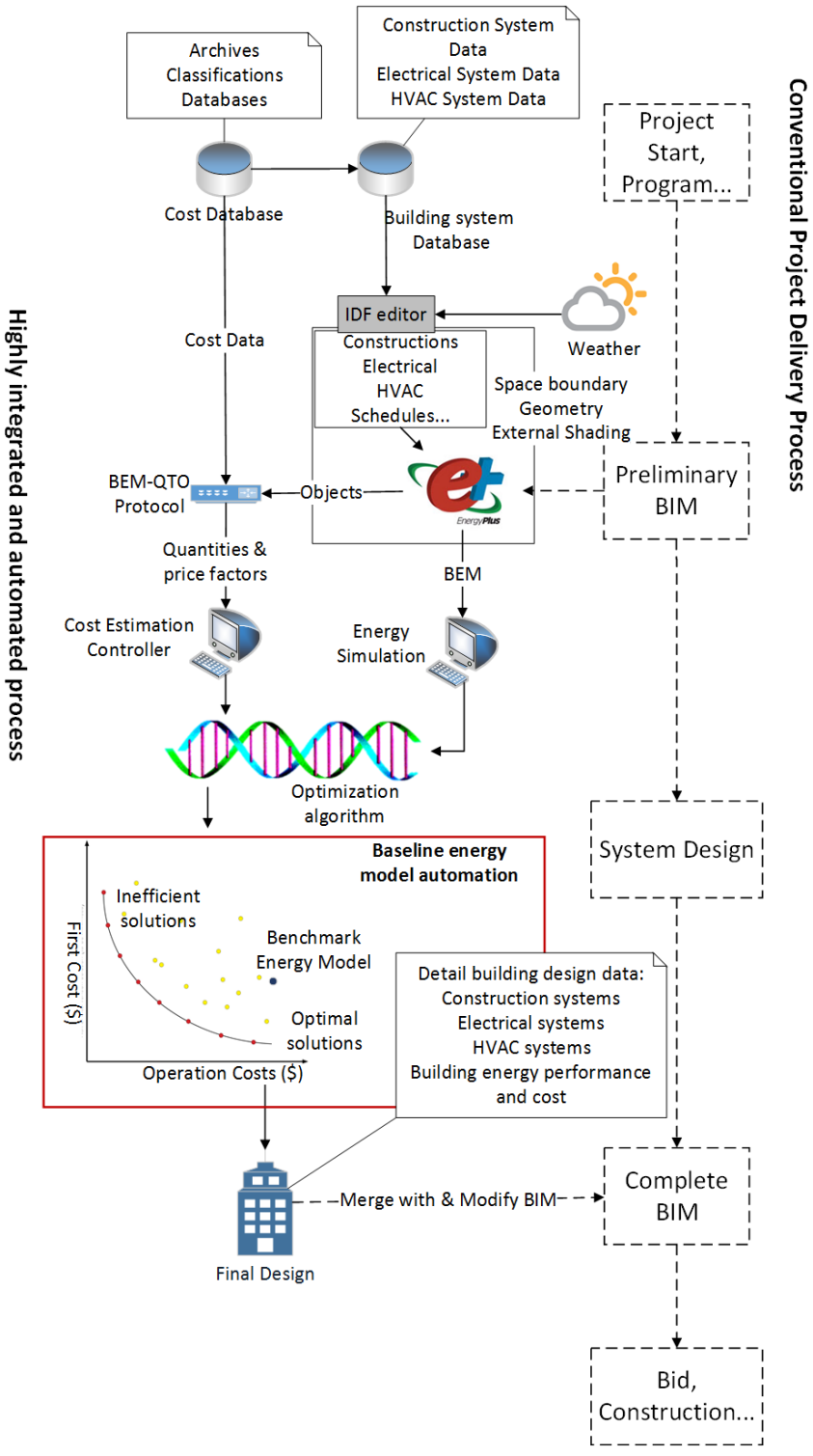

Figure 5.1: Proposed building system design optimization framework: baseline generation (Dashed line: processes that are not considered in this thesis.)

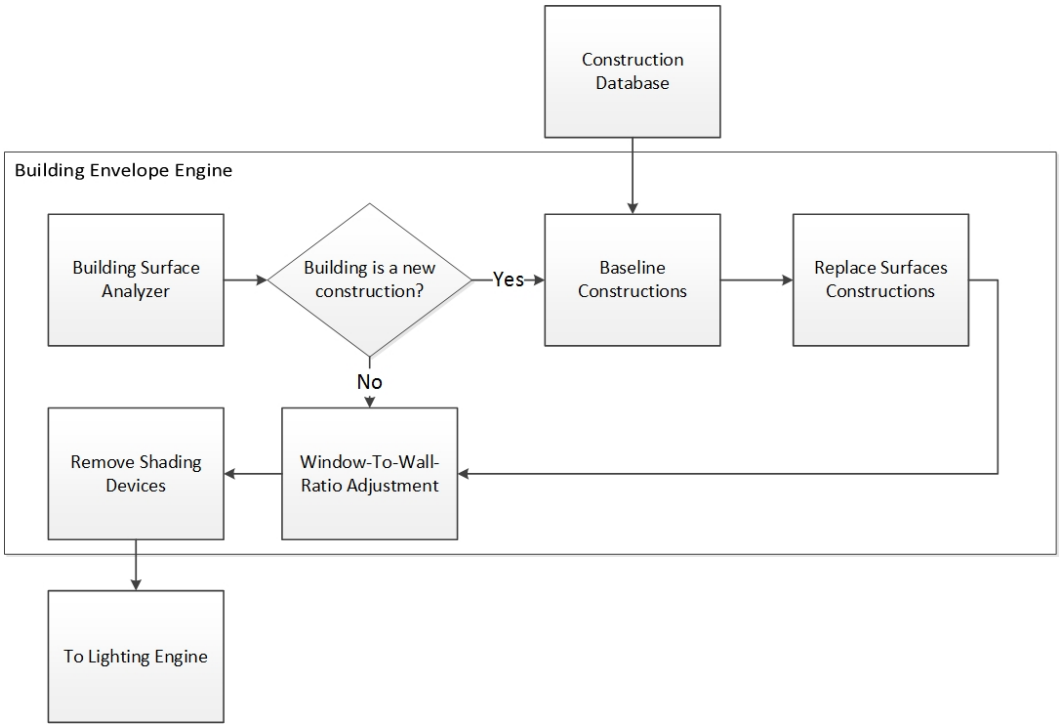

Figure 5.2: Building envelope engine process diagram

engine checks the condition of the building to determine the necessity of activating the baseline constructions generation process. If this is a new construction, the baseline envelopes will be extracted from a construction database based on the climate zone that the building resides in. The opaque envelopes are created using a layer-by-layer method. This method requires the envelope engine to specify each material layer's thermophysical and surface properties and assemble all layers in a design order (outside-to-inside). Baseline fenestration is created using a simple window method. The simple window method in EnergyPlus uses U-factor, solar heat gain coefficient (SHGC) and visible transmittance (Vt) as the 3 inputs to extrapolate a single layer window's optic and thermal properties. This object is typically used when specific property levels are being targeted (LBNL, 2016). The assembled baseline constructions will then replace the design constructions in the baseline energy model. However, if the project is an existing building, these steps will be skipped. Once the envelope check is completed, the envelope engine will start a window to wall ratio (WWR) checking process. If the overall WWR is more

than 40%, dimension adjustment on the windows are performed to reduce the window area. Lastly, overhangs and fins are removed from the design model to eliminate shading impacts according to the requirements of ASHRAE standard 90.1 2010 (ASHRAE, 2010).

5.2.2 Lighting system engine

The lighting engine replaces lighting power density (LPD) following either the building area method or the space-by-space method defined in ASHRAE 90.1 Chapter 9. The values of LPD are provided in the ASHRAE standard 90.1 Table 9.5.1 and Table 9.6.1. For the building area method, the lighting engine can directly read the building type from user inputs, and map the correct LPD value to the "*Lights*" objects in EnergyPlus. However, if the space-by-space method is selected, the space function, following the common space types specified in the ASHRAE standard 90.1 such as "Office", has to be included in the thermal zone name. Exterior lighting power and its controls are also accounted for in the baseline model. However, at the current development stage, the exterior lighting systems are directly replicated from the design model to the baseline models.

5.2.3 HVAC system engine

HVAC engine is the most complex module. It is due to the complicated mechanism of the baseline HVAC system selection as well as their design specifications in ASHRAE standard 90.1 2010. For instance, in the ASHRAE standard 90.1 2010, there are 45 out of 64 clauses and 19 out of 27 exceptions that describe the baseline HVAC system. According to these rules, 18 distinct HVAC system types and a total of 416 different HVAC configurations can be produced. Furthermore, excluding the scenario of having multiple baseline HVAC systems in a building, 1744 logic process branches are required to be implemented in this automation process to define HVAC systems and their performance data correctly. Figure 5.3 shows the selection logic for commercial buildings. In this Figure, the major decision factors for selecting a baseline HVAC system are floor numbers, floor area and sources of heating and cooling energy. Besides system selection, system components in a baseline system can also be varied based on different

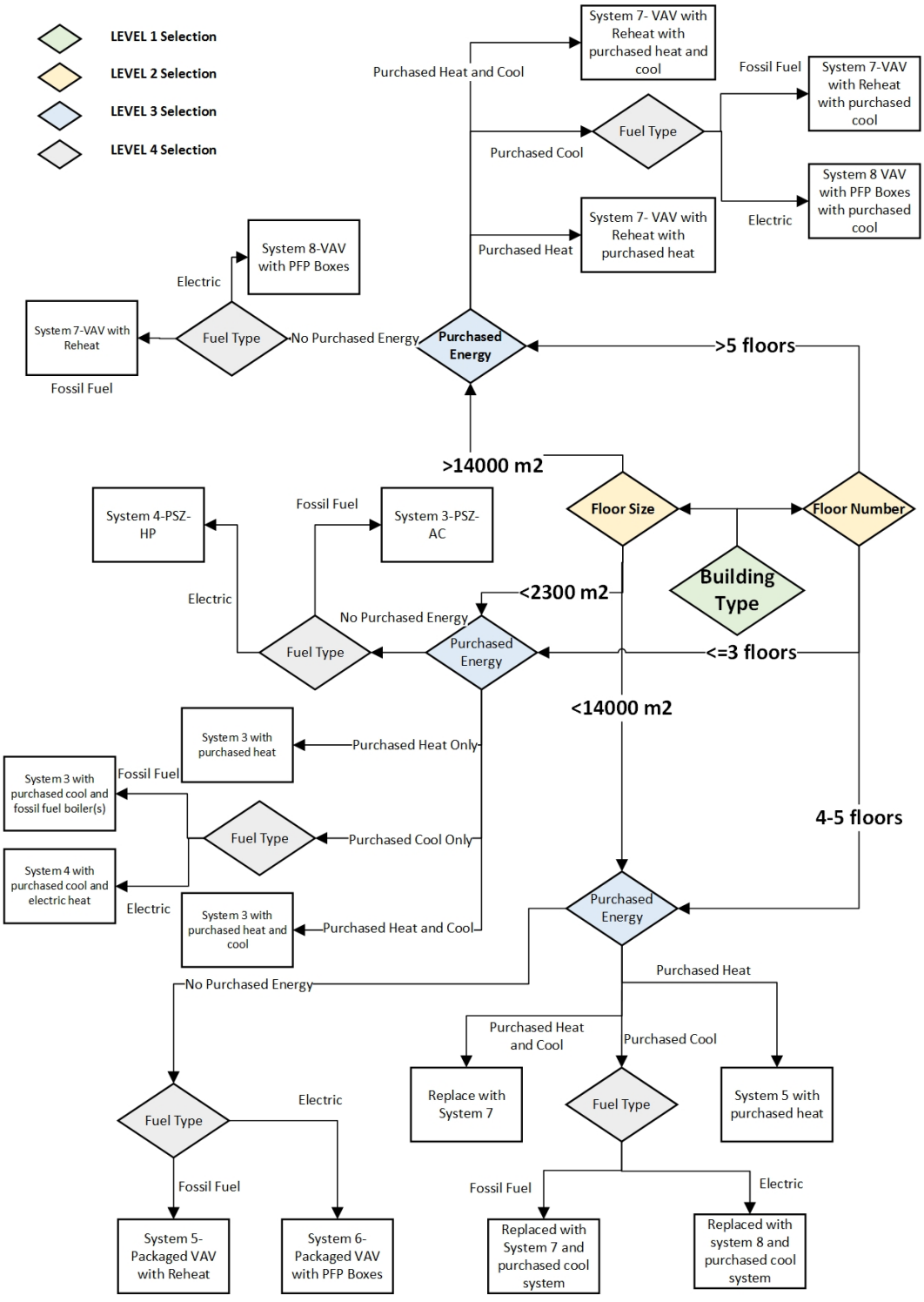

Figure 5.3: Baseline HVAC system type selection logic for commercial buildings

Table 5.1: Baseline HVAC system components variations

Component	Decision Source	Standard 90.1 2010 Reference
Economizer	Climate Zones	Table G3.1.2.6A; Table G3.1.2.6B
Preheat Coils	Design Case	G3.1.2.4
Supply Fan	Design Case	G3.1.2.9.1; G3.1.2.10; G3.1.2.10.1
Exhaust fan	Design Case	G3.1.2.9.1; G3.1.2.10; G3.1.2.10.1
Boiler	Sizing Result	G3.1.3.2 (for System 1,5,7)
Chiller	Sizing Result	G3.1.3.7 (for System 7 and 8)
Hot Water Pumps	Floor Area	G3.1.3.5
Chilled Water Pumps	Sizing Result	G3.1.3.10

sources. Table 5.1 indicates the sources of the HVAC system components variations' sources and their reference in the ASHRAE standard 90.1 2010 version.

Besides the selection of HVAC systems, the data under each baseline HVAC is stored in a designated XML format described in section D.3. Based on the XML schema, the HVAC data is divided into supply, demand, and plant loops and recorded in the "reference" attribute inside the "object" element as described in D.3. The HVAC engine firstly examines and groups the conditioned thermal zones. Then, the demand loops are generated, which are installed at the thermal zone level, inside each group of thermal zones. A supply loop is then constructed and linked to every demand loop in a thermal zone group. The supply loop is typically an air handling unit or a unitary system, which usually connects the demand-side HVAC components via both the "*AirLoopHVAC:ZoneSplitter*" and the "*AirLoopHVAC:ZoneMixer*" objects in EnergyPlus. A plant loop may need to be installed in some of the baseline HVAC systems such as System Type 7 (Figure 5.4). Once the HVAC engine detects a plant loop in the database, it creates not only the plant loop equipment but also the method for connecting the supply loops. "*BranchList*" is the object for connecting supply and plant-side systems. Figure 5.4 shows the system type 7 template as an example of such creation logic. In Figure 5.4, the text section specifies the system features followed by a list of fixed specifications identified for this baseline HVAC system.

System 7 – VAV with Reheat
This section shows the system type 7 building logics.
System 7 is Packaged rooftop VAV with reheat.
Fan Control: VAV
Cooling Type: Chilled water
Heating Type: Hot-water fossil fuel boiler

Template Design:
System Connections
System Specifications and compliance with
G3.1.2.1: Equipment Efficiency
G3.1.2.2 Equipment Capacity
G3.1.2.2.1 Sizing Runs
G3.1.2.9.1: Baseline System Design Air Flow
G3.1.3.3 Hot Water Supply Temperature
G3.1.3.4 Hot-Water Supply Temperature Reset
G3.1.3.8 Chilled Water Design Supply Temperature
G3.1.3.9 Chilled Water Supply Temperature Reset
G3.1.3.13 VAV Minimum Flow Setpoint
G3.1.3.15 VAV Fan Part-Load Performance

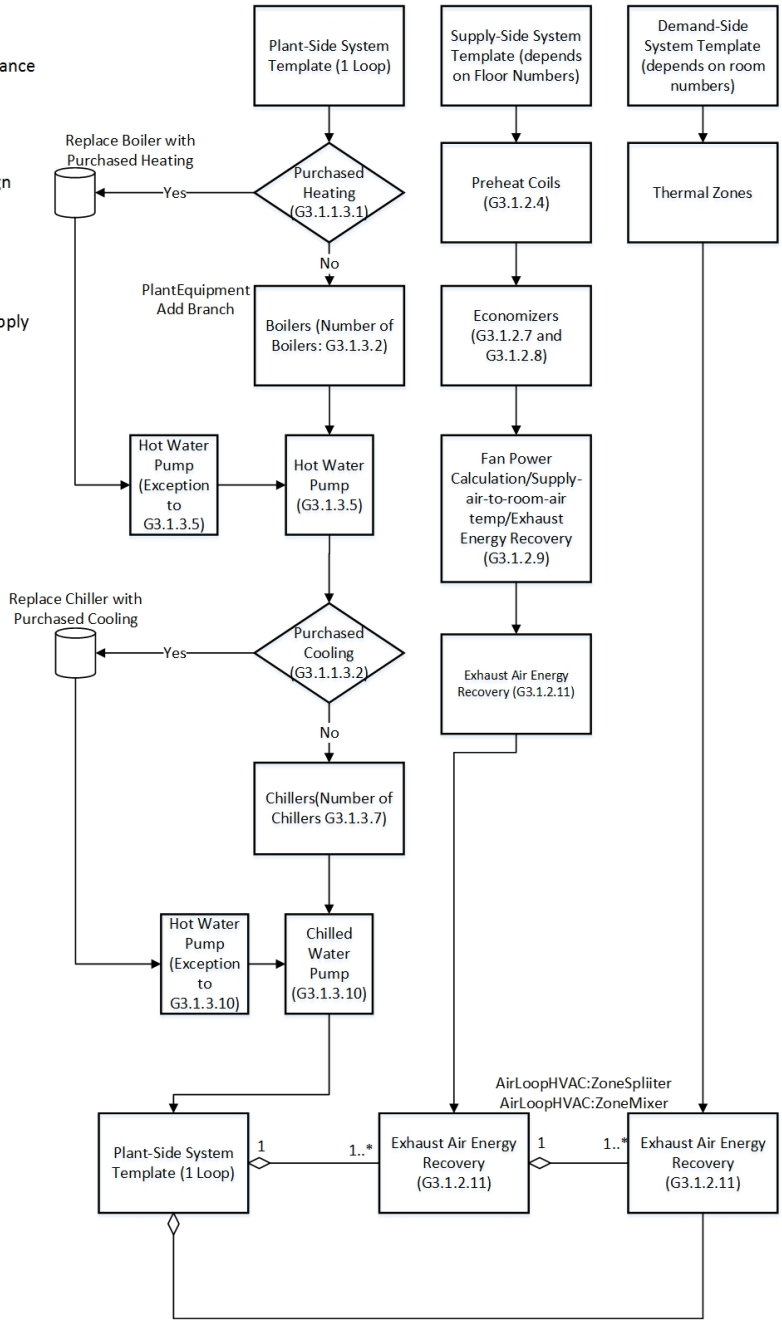

Figure 5.4: Baseline HVAC System Type 7 creation logic

The three processes in Figure 5.4 are the plant, supply and demand loops creation processes. It should be noted that in System Type 7, the demand loops also connect to the plant loop because the heating source of reheat coils in the air terminals are from boilers.

Chapter 6

Optimization on a new construction project: Center for Sustainable Landscapes (CSL)

6.1 Project overview

The proposed platform utilizes the ammNSGA-II optimization algorithm that builds on a cost database, strategically linked to EnergyPlus with an LCC module and a building system database, is tested with case studies. This chapter focuses on a new construction project, the Center for Sustainable Landscapes (CSL) at Phipps Conservatory, a net-zero energy building that received the LEED Platinum and Living Building Challenge designation. The goal of this case study is to explore the potential combined capital and operational costs reduction by performing optimization on an integrated building system. The design parameters include exterior wall, roof, window, window to wall ratio (WWR), light shelf, lights, daylight control, HVAC and building integrative photovoltaic system (BiPV).

6.2 Building description

The CSL is a two-floor office building located at 1 Schenley Dr., Pittsburgh, PA, U.S. It is owned by the Phipps Conservatory and Botanical Gardens, which is a non-profit organization in Pittsburgh. The designed building embraced high-insulation envelopes, lighting and HVAC systems to minimize the site energy consumption effectively. Also, with the help of onsite photovoltaic solar panels and wind turbines, it successfully achieved zero energy consumption. Figure 6.1 depicts the energy flow diagrams between the building and its renewable energy systems. Its main HVAC system, including the tri-coil unit, the under floor air distribution system and the hot water radiant system, consumes the energy generated from geothermal wells (A), photovoltaic array (B) and wind turbines (E). Besides the geothermal wells, the other two renewable systems connect to a power control center (red box). If the CSL electricity demand is lower than generated, the power control center can supply the excess power to the main campus, located next to the power control center.

6.3 The EnergyPlus model

A CSL energy model in EnergyPlus format is obtained from previous research conducted by (Lam et al., 2014). The energy model contains open plan offices, classrooms, research space and conference rooms. In total, there are 20 thermal zones that occupy around 2000 m^2 of gross floor area. The real building has been operating for more than four years. In 2015, the measured total energy consumption was around $70kWh/m^2$. The CSL energy model was calibrated against monthly energy consumption. The procedure of the energy model calibration is detailed in (Zhao, 2015). The model was first created in DesignBuilder version 4.7 and then exported into an EnergyPlus data format (.idf). Figure 6.2 shows the rendered geometry in the DesignBuilder interface.

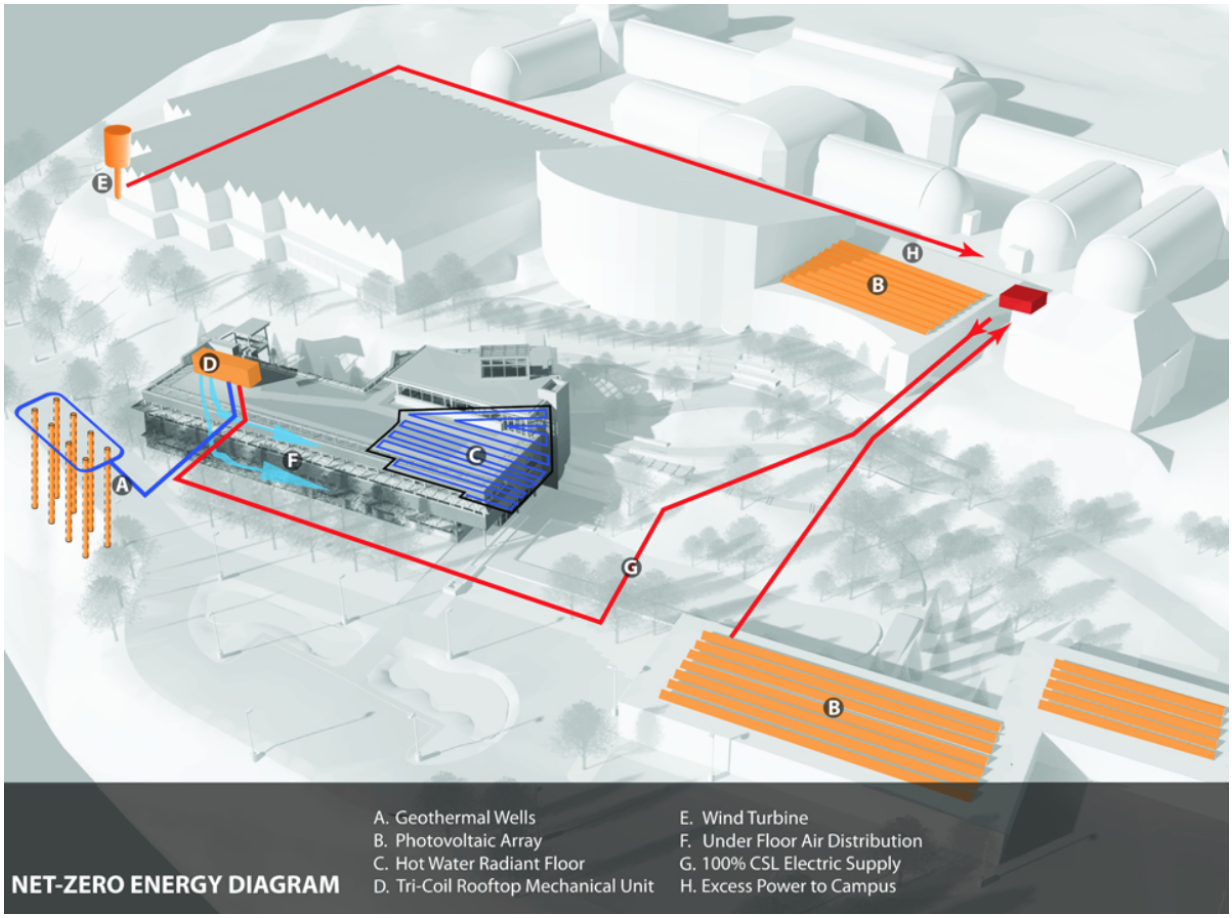

Figure 6.1: The net zero energy diagram of CSL (courtesy of the Design Alliance.)

6.4 Design parameters for CSL

Table 6.1 lists the design options under each design parameter and the thermal properties and costs for each option. This list of design parameters is formed based on the recommendations from ASHRAE advanced energy design guides (AEDG) (ASHRAE, 2016a) in ASHRAE climate zone 5 (ASHRAE, 2010) and the real building design. The maintenance and replacement cost information is dynamically extract from Table A.1 in Appendix A based on the selected design options. For example, a concrete wall will extract the concrete patch as the maintenance task. In addition, a BiPV system, which is not in the real building, is proposed as an integrative renewable energy source to the case study. In total, there are nine categories of design

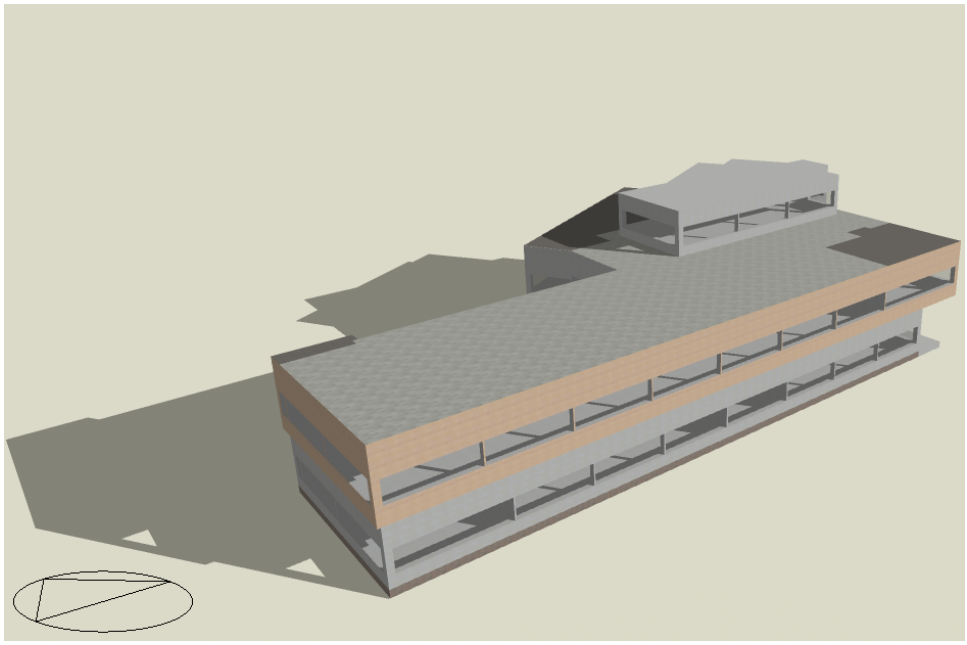

Figure 6.2: Rendered CSL building geometry in DesignBuilder v4.7

parameters with 56 design options. The properties for walls and roofs are extracted from the (ASHRAE, 2009). The properties of window systems are collected from the default dataset in EnergyPlus (UIUC and LBNL, 2016), manufacturers specifications (Euroglas, 2016) and DesignBuilder dataset (DesignBuilder, 2016). Lighting fixtures and BiPV system are also extracted from manufacturers specifications (GE, 2016; SolarWorld, 2016). In addition, the light shelf system design parameters are recommended in (Meresi, 2016). Lastly, the HVAC system selected in this study contains a whole package of the system, including both primary and secondary systems. The efficiencies of the HVAC system are based on calibrated operation data or manufacturers' specifications. If the data is not available, then the minimum efficiency data in ASHRAE 90.1 2010 performance rating method is used (ASHRAE, 2010).

It should be noted that the cost information is extracted from "*RSMeans construction cost estimating data book*" in 2015 and adjusted for the differences in consumer price index (CPI) to 2016 dollar values (RSMeans, 2015). The cost data only includes the material cost. This is because the labor, equipment and overhead costs for some of the advanced building systems (e.g, VRF system) are currently not available in the "*RSMeans construction cost estimating data*

Table 6.1: Design Options for each Design Parameters (Part-1)

Design Parameters	Design Options	Property	Unit Cost
Walls[a]	Wall R-0.3	U-3.11	$\$189.65/m^2$
6 options	Wall R-1.5	U-0.673	$\$222.65/m^2$
	Wall R-2.1	U-0.467	$\$242.89/m^2$
	Wall R-2.6	U-0.418	$\$265.34/m^2$
	Wall R-3.8	U-0.266	$\$302.44/m^2$
	Wall R-6.5	U-0.153	$\$448.73/m^2$
Windows[a]	Double Clear (DC)	U-3.13, SHGC-0.73, Vt-0.8	$\$242/m^2$
6 options	Double Tinted (DT)	U-2.58, SHGC-0.37, Vt-0.53	$\$290/m^2$
	Double Low-e Clear (DLC)	U-1.40, SHGC-0.41, Vt-0.61	$\$356/m^2$
	Heat Reflective Clear (HRC)	U-1.40, SHGC-0.25, Vt-0.45	$\$409/m^2$
	Triple Glazing (TG)	U-1.31, SHGC-0.57, Vt-0.47	$\$480/m^2$
	Quadruple (Q)	U-0.73, SHGC-0.46, Vt-0.62	$\$862/m^2$
WWR[b]	40%, 50%, 60%,	For each orientation	-
6 options	70%, 80%, 90%		
Light shelf	Shelf height	10% to 30%	-
numeric	Inside shelf projection	0.5m to 1.5m	-
	Outside shelf projection	0.5m to 1.5m	-
Roof	Metal Roof R-2.2	U-0.452	$\$46.52/m^2$
4 options	Metal Roof R-3.1	U-0.323	$\$58.68/m^2$
	Metal Roof R-4.9	U-0.227	$\$71.18/m^2$
	Green Roof R-5.3	U-0.189	$\$142/m^2$
Lights	T8	$LPD^{a} - 10.2W/m^2$	$\$150/m^2$
3 options	T5	$LPD - 7.5W/m^2$	$\$220/m^2$
	LED	$LPD - 4.5W/m^2$	$\$390/m^2$
Light control	Yes		$\$268/Each$
2 options	No		
BiPV[b]	Yes	Each orientation	$\$4.5/W$
2 options	No		
HVAC[c]	VAV with Chillers and Boilers		$\$1,233/kW$
3 options	DOAS+VRF System		$\$1,541/kW$
	VAV+GeoHP System		$\$1,891/kW$

[a]: R: overall thermal resistance (m^2K/W), U: overall coefficient of thermal transmission (W/m^2K), SHGC: solar heat gain coefficient (dimensionless), Vt: visible transmittance, LPD: lighting power density (W/m^2)

[b]: WWR: window to wall ratio, BiPV: building integrated photovoltaic system,

[c]: HVAC: heating ventilation, air conditioning system, VAV: variable air volume system, DOAS: dedicated outdoor air system, VRF: variable refrigerant flow system, GeoHP: geothermal heat pump.

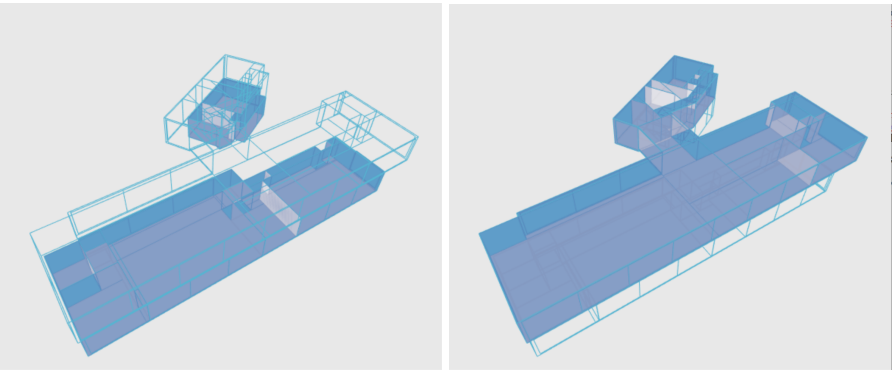

Figure 6.3: HVAC air side zone layout. Left: first floor, Right: second floor

book". For HVAC systems, only the components that are available in EnergyPlus (e.g, chiller, boiler, VRF air conditioner, etc.) are included in the cost estimation. Most of the design parameters are integer type except for the three parameters under the light shelf system. In the "Design Options" column, a design with an underline indicates that it is installed on the target building. It shows that CSL is currently equipped with most of the advanced systems in the available set of design options. Such "deluxe" design can effectively lower the annual energy consumption. Not including the light shelf system, the total number of system combinations can reach up to 54 million.

6.5 Model assumptions

In addition to the ASHRAE 90.1 baseline model, the calibrated EnergyPlus model is another base case model for comparison in this case study. All the calibrated operation data, e.g, the occupant and lighting schedules, remain identical in the optimization. The HVAC system installed in the current building consists of two air handling units. One controls the first floor and the other controls the second floor (Figure 6.3). This HVAC air side zone layout, including the DOAS and VAV, is also unchanged in the study.

Table 6.2: Life Cycle Cost Model Parameters

Field	Input
Discounting Convention	End of Year
Inflation Approach	Constant Dollar
Real Discount Rate	0.03 (Rushing et al., 2016)
Base Date	2016 January
Service Date	2018 January
Study Length	25 Years
Price Escalation	NIST Handbook 135 Table Ca-1, Census Region 1
Electricity Tariff	Duquesne Light 2016 Rate GS (Duquesne Light Co., 2016)
Natural Gas Tariff	Equitable Gas 2016 Rate GSS (People Natural Gas, 2016)

6.6 Life cycle cost model parameters for CSL

Apart from the energy model assumptions, there is a life cycle cost model (LCC) and a detail utility tariff model built in the EnergyPlus. The LCC is constructed using the parameters published in the "*NIST Handbook 135*" (Rushing et al., 2016). Table 6.2 lists the important LCC parameters defined in this study. It should be noted that the study length is set to 25 years. This is because most of the systems included in this study can last for a minimum of 25 years. In addition to the LCC model, utility tariff models that represent published local utility tariffs (Table 6.2) are also included in the economic module of EnergyPlus.

The optimization is conducted on a desktop with a configuration of i7 quad-core 3.5 GHz CPU and 16 GB RAM. A maximum thread pool mechanism is used so that the optimization can utilize all available computer powers to evaluate the fitness functions of design solutions concurrently. Using EnergyPlus for energy simulation takes about 4 minutes. Therefore, a full enumeration of the parameter space, which consist of more than 50 million possible design combinations, using a one-at-a-time strategy would require 200 million minutes to complete. This is equivalent to 400 years. With the concurrent strategy and the advanced ammNSGA-II algorithm, the full optimization is completed in 4 hours.

6.7 Results analysis on CSL case study

6.7.1 Overview

The same optimization is repeated five times with different initial starting design solutions. This strategy ensures the optimization results can cover a broad range of design combinations in the solution space. Figure 6.4 shows the design solutions, whose energy and cost performances are evaluated by EnergyPlus in the five optimizations, are color-coded by the index of generations (iterations). The red color dots indicate design solutions that are generated in the initial set of the optimizations, and the purple color dots are generated close to the end of the optimizations. It can be observed that through generations, the design solutions move towards the bottom left corner of the plot. This pattern shows that the optimization algorithm is effectively searching for all the combinations of the building system to find design solutions that can minimize both operation and capital costs. Furthermore, the total operation costs for these generated design solutions is reduced from $530,000 to $44,000 in a 25-year term. Along with the reduction in operation costs, the capital cost increases from $600,000 to $2,000,000. Among the generated design solutions, many of them show that the optimization of an integrated building system design can help clients make "smart" decisions. These decisions save not only operation costs but also the capital cost. To strengthen this argument, two examples are selected from the generated design solution pool (Table 6.3). These two solutions both have a VAV as HVAC system. However, the overall envelope insulation level in design solution 48 is higher than design solution 2. Also, design solution 48 uses T5 lighting fixtures with daylight control system to reduce the interior load further. Although it seems that design solution 48 requires a higher capital cost on these additional investments, the results shows a different story. By investing extra capital on better insulations and higher efficiency lighting system, design solution 48 saves more capital cost on its HVAC system by purchasing a smaller size of the VAV system.

One may argue that the BiPV system in design solution 2 is a high-cost investment system

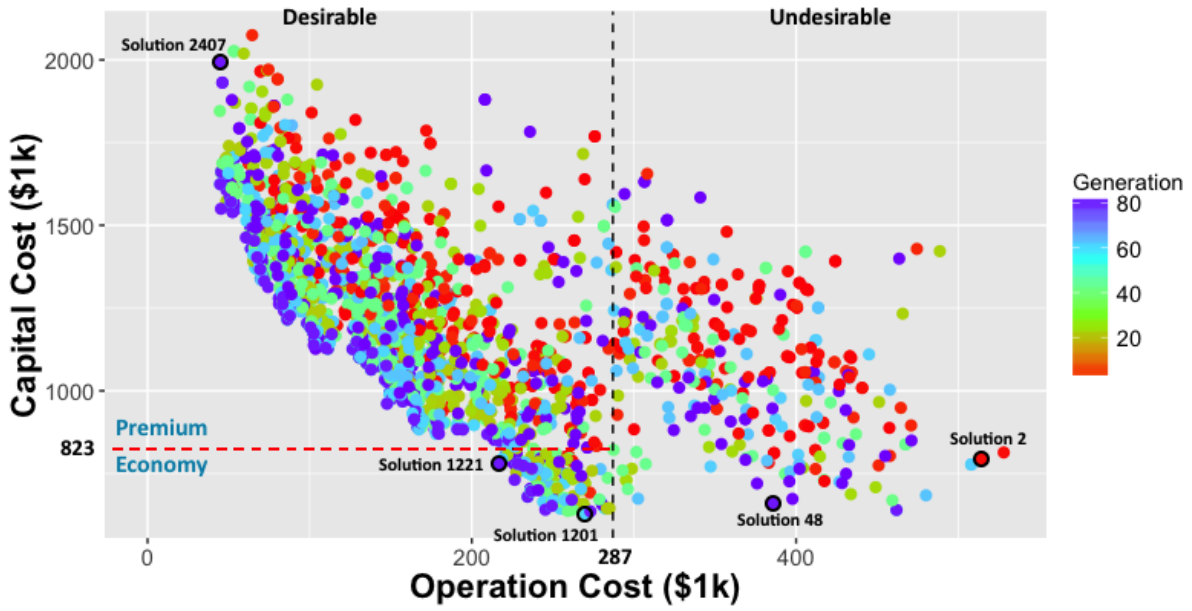

Figure 6.4: Generated design solutions for CSL

Table 6.3: Comparison between two design solutions that are under $1 million budget

Solution Index	Insulation Level	WWR	HVAC	Lights	BiPV	LightShelf
2	Wall: R-0.3	South: 40	VAV	T8	South: No	Inside:
Operation: $528k	Roof: R-2.2	North: 60		**Daylit Sensor:**	North: No	0.53m
Capital: $813k	Window:	East: 70		Off	East: No	Outside:
	DC	West: 40			West: Yes	N/A
48	Wall: R-2.1	South: 40	VAV	T5	South: No	Inside:
Operation: $385k	Roof: R-4.9	North: 50		**Daylit Sensor:**	North: No	N/A
Capital: $659k	Window:	East: 90		On	East: No	Outside:
	DLC	West: 50			West: No	1.3m

which may be the reason for its higher capital cost. However, the West facade has a gross wall area of 160.50 m^2, which is four times smaller than the south and north gross wall area. With 40% WWR, the total estimated cost of the BiPV system for design solution 2 is $118,000. Therefore, the design solution 2 has a higher capital cost even without the BiPV system compared to the design solution 48. Also, removing BiPV system in the design solution 2 will enlarge the differences in the operation costs.

6.7.2 Compared with the ASHRAE baseline model

In Figure 6.4, a black dashed line ($287,000) and the red dashed line ($823,000) form the cost performance of the baseline model. The baseline model is generated according to the ASHRAE standard 90.1 2010 Appendix G performance rating method. Without a renewable energy system, the maximum operation cost saving compared to the baseline model reaches around 40%, which is close to the estimation (30%-50% saving) given by the Building Technology Office (Building Technologies Office, 2014). Based on the operation costs of baseline model (black dashed line), Figure 6.4 can be separated into two sections.

1. Undesirable solutions: the design solutions that have higher operation costs than baseline model.
2. Desirable solutions: the design solutions that have lower operation costs than baseline model.

In addition, based on the capital cost of the baseline model (red dashed line), these desirable design solutions can be further divided into two sub-types.

1. Desirable premium solutions: the desirable solutions that require higher capital cost than baseline model.
2. Desirable economy solutions: the desirable solutions that require less capital cost than baseline model.

Undesirable solutions are probably the least appealing solutions to clients and design teams since they are expensive and inefficient. On the other hand, Desirable solutions are perhaps the attractive solutions to clients and design teams. Further divided the desirable solutions, desirable economy solutions present an integrated building system that outperforms the baseline design in both capital and operation costs. Design solution 1201 represents the highest capital cost saving (23% or $196,000), and it still manages to achieve 4% operation costs saving ($12,000). This design solution upgrades roof insulation (R-5.3), window (Double Tinted), lighting (T5) and HVAC system (Table 6.4). A higher window to wall ratio is also observed

Table 6.4: Design solution 1201, 1221 and 2407 compare with ASHRAE 90.1 baseline design

Solution Index	Insulation Level	WWR	HVAC	Lights	BiPV	LightShelf
Baseline	Wall: R-2.6	South: 40	System Type 6	T8 ($12W/m^2$)	South: No	Inside:
Operation: \$287k	Roof: R-3.3	North: 40		**Daylit Sensor:**	North: No	N/A
Capital: \$823k	Window:	East: 40		Off	East: No	Outside:
	U:1.9, SHGC: 0.4	West: 40			West: No	N/A
1201	Wall: R-2.1	South: 40	DOASVRF	T5	South: No	Inside:
Operation: \$256k	Roof: R-5.3	North: 50		**Daylit Sensor:**	North: No	N/A
Capital: \$678k	Window:	East: 50		Off	East: No	Outside:
	DT	West: 60			West: No	1.5m
1221	Wall: R-2.1	South: 40	DOASVRF	LED	South: No	Inside:
Operation: \$217k	Roof: R-4.9	North: 50		**Daylit Sensor:**	North: No	0.5m
Capital: \$780k	Window:	East: 60		On	East: No	Outside:
	DLC	West: 60			West: Yes	1.06m
2407	Wall: R-6.5	South: 80	GEOHP	LED	South: Yes	Inside:
Operation: \$44.3k	Roof: R-5.3	North: 40		**Daylit Sensor:**	North: Yes	0.8m
Capital: \$1991k	Window:	East: 70		On	East: Yes	Outside:
	Quadruple	West: 40			West: Yes	N/A

in design solution 1201, which further increases its capital cost of the envelope system. Nevertheless, it seems the upgrades can effectively reduce the size of the HVAC system, thus achieving an instant capital cost saving. On the other hand, design solution 1221 further upgrades the lighting (LED) and window (Double Low-E Clear) as well as adds a BiPV system on the West facade (Table 6.4). The capital cost is increased by \$100k. However, this design solution maximizes operation costs saving by 23% (\$70,000) with less on capital cost (5% or \$45,000) compare to the ASHRAE baseline design.

Unlike desirable economy solutions, desirable premium solutions have higher capital cost but lower operation costs. The trade-offs between premium cost and operation cost saving could be an interesting factor that attracts the design team to investigate these design solutions. Also, if the target of the project is to achieve net-zero building, desirable premium solutions are certainly the only design solutions that the design team should be considered. The highest operation costs saving over the ASHRAE baseline design reaches 84% (\$243,000) in design solution 2407. This design solution has configured with all the best design options under each design parameter (Table 6.4). As trade-offs, the capital cost for this design solution is increased by

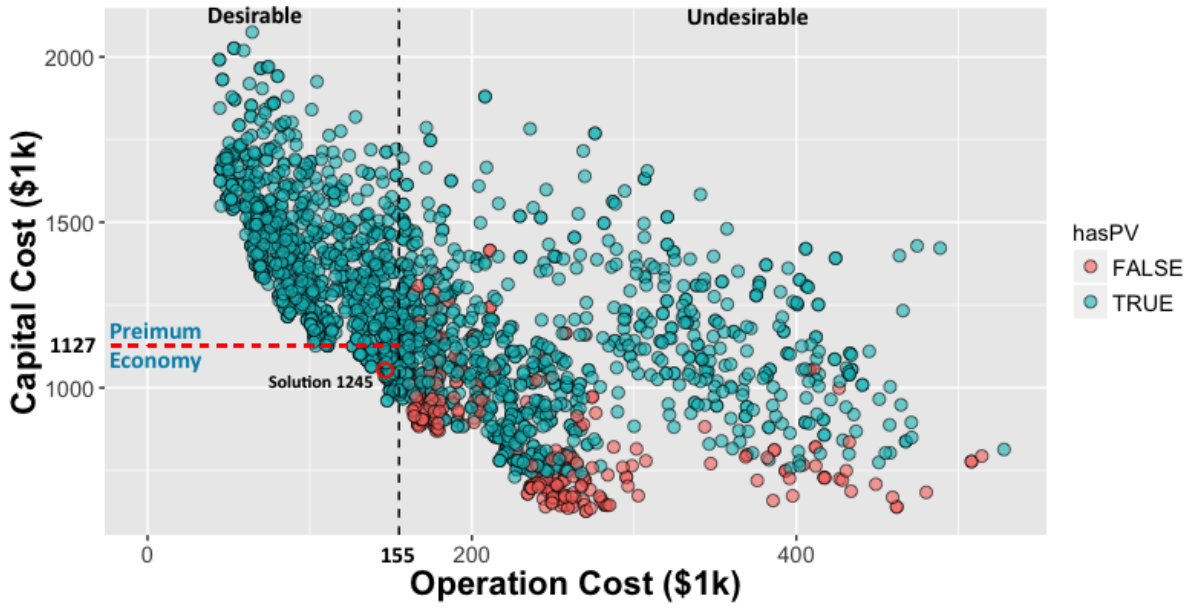

Figure 6.5: Comparing the generated design solutions with the real building design

142% ($1,168,000). The expensive capital cost is mainly due to the advanced BiPV systems. However, it should be noted that the window to wall ratio is largely increased. It is probably because the high insulation level of the quadruple glazing allows less energy loss from openings. In addition, it also shows the algorithm is optimizing the cost trade-off between high investment and operation cost savings of BiPV system.

6.7.3 Compared with the real building design

Figure 6.5 shows the comparison between the real design and the generated design solutions. The real design is equipped with many high efficiency systems, which maximizes the energy saving of the building. This can be observed as the operation costs (black dashed line) is ahead of most the generated design solutions. There are still almost a hundred of design solutions that have lower operation costs than that of the real design. All these design solutions have BiPV systems to reduce the consumption of net site energy. On the contrary, the real design surpasses the energy and cost performance of all the design solutions that have no BiPV system. Furthermore, capital cost (red dashed line) of the real design out-performs some of these generated

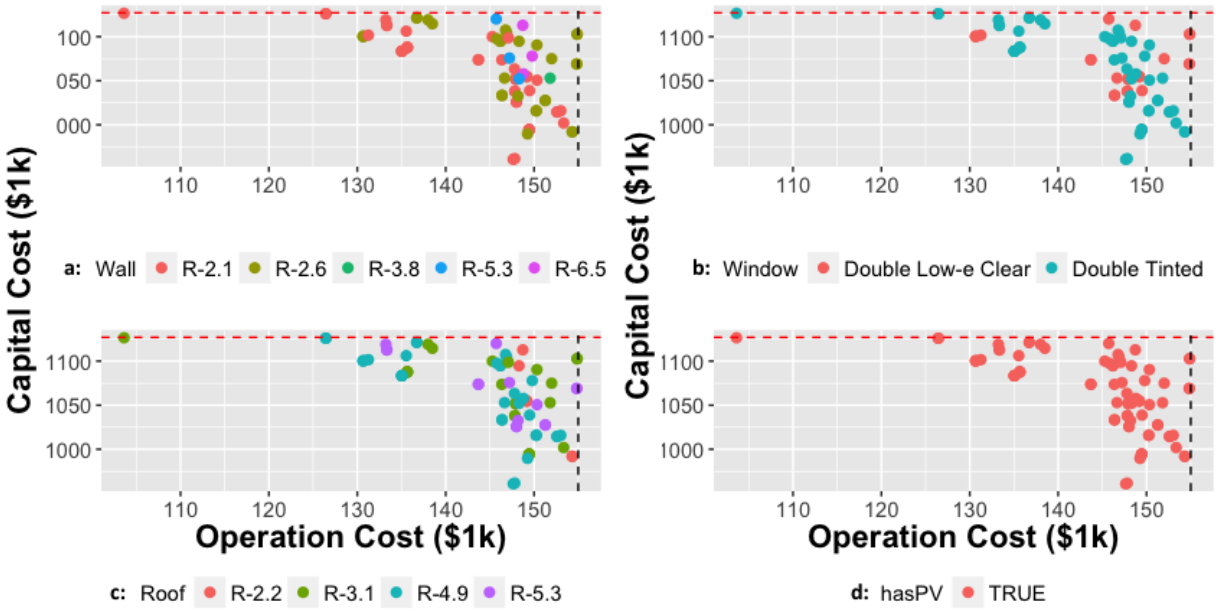

Figure 6.6: Design options for desirable economy solutions: Wall, Roof, Window and BiPV

design solutions, which proves that integrating advanced building systems does not equate to the high price premium.

Among all the generated design solutions, the desirable economy solutions are the most interesting design solutions that clients and design teams could consider. This is because these design solutions save not only long-term operation costs but also capital cost compared to the real design. Figure 6.6 shows the envelope and BiPV design choices of the desirable economy solutions. Figure 6.6a illustrutes that most of the designs select lower wall insulations (R-2.1 or R-2.6). Similarly, for windows, triple glazing or quadruple glazing are not selected for the desirable economy solutions. On the contrary, all the desirable economy solutions contains BiPV systems. This implies that the algorithm trades the capital costs of wall and window systems for advanced BiPV systems. Furthermore, a higher roof insulation may be economically preferred since most of the designs choose R-4.9 or R-5.3. Figure 6.7 lists the rest of the design choices including the daylight control, lighting fixture, HVAC and light shelves. It can be observed that besides light shelves, all the other systems prefer high efficiency options among the desirable

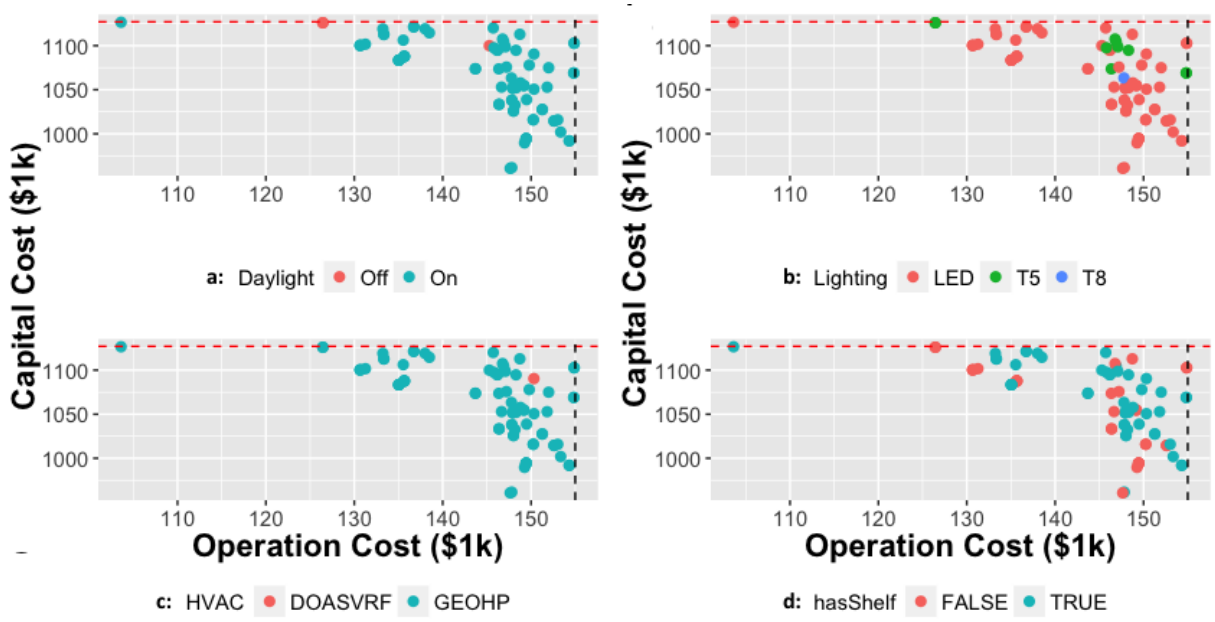

Figure 6.7: Design options for desirable economy solutions: Daylighting Sensor, Lighting fixture, HVAC and Light Shelves

economy solutions. Most of the design solutions choose to have daylight control with LED lighting fixtures and geothermal heat pump systems. Besides viewing the design choices for

Table 6.5: Comparison between design solution 1245 with real design

Solution Index	Insulation Level	WWR	HVAC	Lights	BiPV	LightShelf
1245 Operation: $150k Capital: $1016k	Wall: R-3.8 Roof: R-4.4 Window: DT	South: 50 North: 40 East: 40 West: 60	GEOHP	LED **Daylit Sensor:** On	South: No North: No East: No West: Yes	Inside: N/A Outside: 1m
Real Operation: $155k Capital: $1121k	Wall: R-6.5 Roof: R-5.3 Window: TG	South: 50 North: 30 East: 40 West: 40	GEOHP	LED **Daylit Sensor:** On	South: No North: No East: No West: No	Inside: N/A Outside: 1m

each design parameter, the comparison can also be made by comparing the integrated design solutions. Table 6.5 lists the detail building systems selected from one of the desirable economy solutions and the real building design. The major differences come from the building envelope, where design solution 1245 has a lower insulation level on the wall, roof, and windows. Also,

design solution 1245 has a slightly higher overall window to wall ratio than the real design. The lower insulation level does pose large impacts on the building peak heating load (from 66kW to 86kW). However, at the same time, this design solution reduces the peak cooling load from 157kW to 133kW. The reduction in cooling load is mainly due to the double tinted windows, whose SHGC (0.37) is nearly 40% lower than windows in the real design (0.6). Therefore, the lower insulation level has negligible impacts on the capital cost of the HVAC system. In this case, it creates more room in the budget for the BiPV systems, which results in lower capital and operation costs. However, the double tinted window may not be a preferred choice due to its low visible transmittance. Such low visible transmittance could cause an unpleasant view for the tenants. This factor can be applied as a constraint to narrow down the available selections of design solutions. However, constraint optimization is not within the scope of this thesis.

6.7.4 Pareto front curve

Figure 6.8 shows the optimal design solutions among the results derived from the five replicated optimizations. The Pareto front curve plots the optimal design solutions in the solution space. Among these solutions, the total operation costs are quickly reduced from $270,000 to $44,300. Adversely, the capital cost climb rapidly from $627,000 to $1,991,000. The absolute improvement plot consists of absolute changes in operation costs, capital cost, and life cycle cost (LCC) compared to those of ASHRAE baseline design. Similarly, the percentage improvement curves show the improvement of both capital and operation costs over the ASHRAE baseline design. Table E.1, E.2, E.3 and E.4 in the Appendix E show the details about these design solutions on the Pareto front curve.

To understand the trade-offs in Figure 6.8, the very first observation should start at the right side of the plots. The design solution 30 shows cost saving for both capital and operation costs and its absolute saving from capital cost is larger than that from operation costs. However, this is not the optimal LCC saving. The design solution 29 in Figure 6.8 indicates the highest LCC saving among all the optimal solutions (red dashed line). It is not the cheapest option, and it is also not the design solution that saves the most operation costs. However, it optimizes the trade-

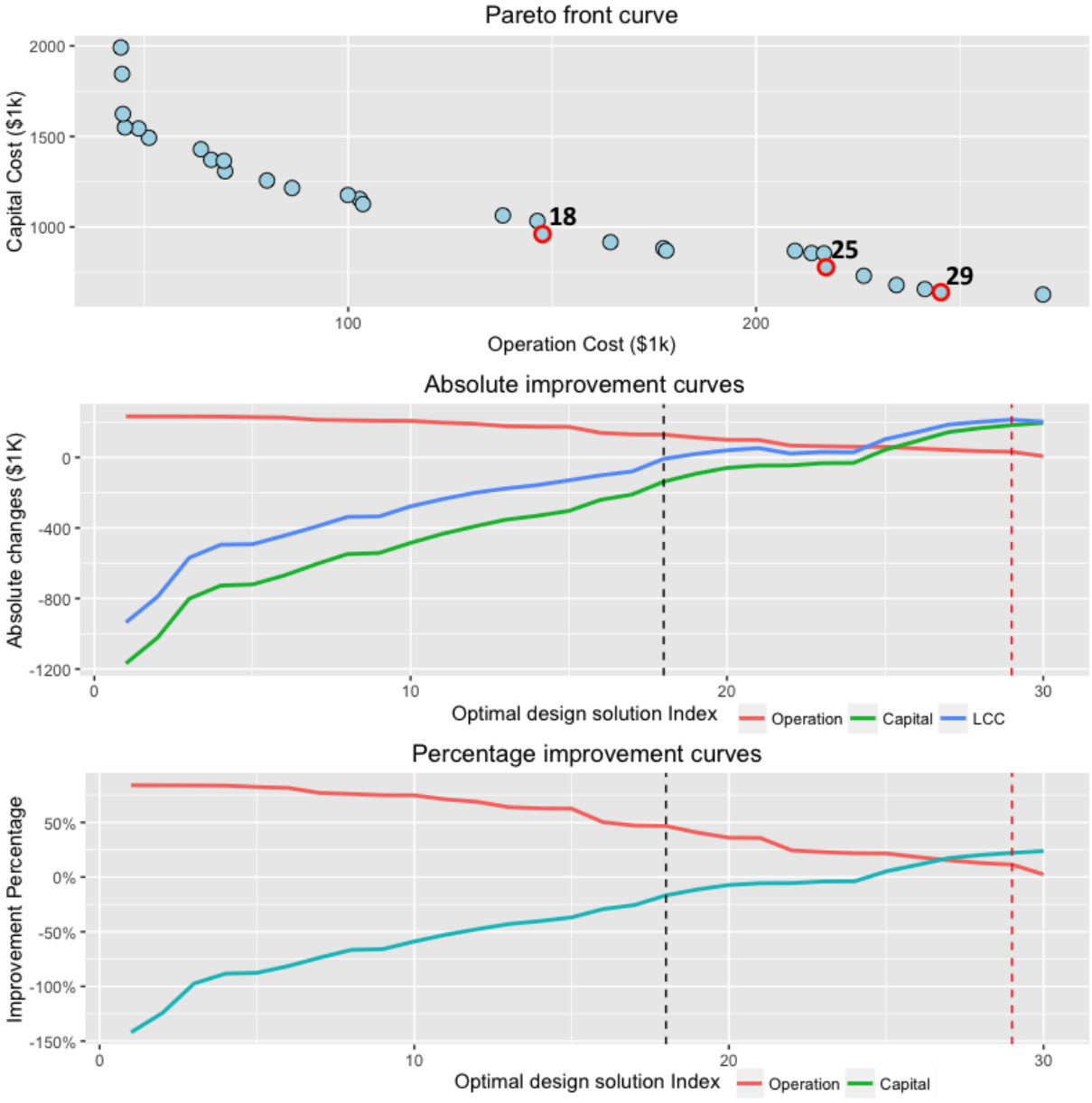

Figure 6.8: Pareto front curve, percentage and absolute improvement curves

offs between the capital and operation costs. Further to the left, the operation cost saving is increasing at a constant 3% rate (percentage improvement curves) while the capital cost saving is decreasing at around 3.3% (percentage improvement curves). At design solution 25, the capital cost saving is diminished, which means that the rest design solutions require higher capital cost than the ASHRAE baseline design. However, as the optimization algorithm continuously increases the price premium to trade for lower operation costs, it finally reaches a break-even point at the design solution 18 (black dashed line), where the saving from operation costs is offset by the increased price premium. Beyond this point, all the remaining optimal design solutions (1-17) show a negative LCC. From the investment point of view, the analysis should end at design solution 18. This is because a further stretch on the budget to trade smaller saving in 25-year term is not an appealing option. However, there are many reasons that clients may consider to stretch their budget to reach a certain level of operation cost saving such as meeting the regulation constraints or fulfilling requirements for certifications. These design solutions also demonstrate the cost to bring the design to net-zero for a middle-size office building. Nevertheless, by providing the Pareto front curve with the improvement curves, clients or the design team can easily focus on a certain optimal area and find a best design solution that satisfies all the building stakeholders.

6.7.5 BiPV system in optimal design solutions

Figure 6.9 presents the same Pareto front curve with the BiPV system indicator. A red dashed line indicates the capital cost of the ASHRAE baseline design and the black dashed line shows the operation costs of the ASHRAE baseline design. The first observation is that only the design solutions with the BiPV systems can achieve operation costs of $150,000, which is close to 50% of the baseline design. However, the BiPV systems are not a cheap design option. For instance, Table 6.6 indicates a detail system comparison between design solution 26 and design solution 27 in Figure 6.9. Both design solutions use the medium to high insulation systems with close to 40% overall WWR. Also, both design solutions have LED lighting fixtures with daylight control and DOAS + VRF hybrid HVAC system. Design solution 27 has a 1.5 meter out-

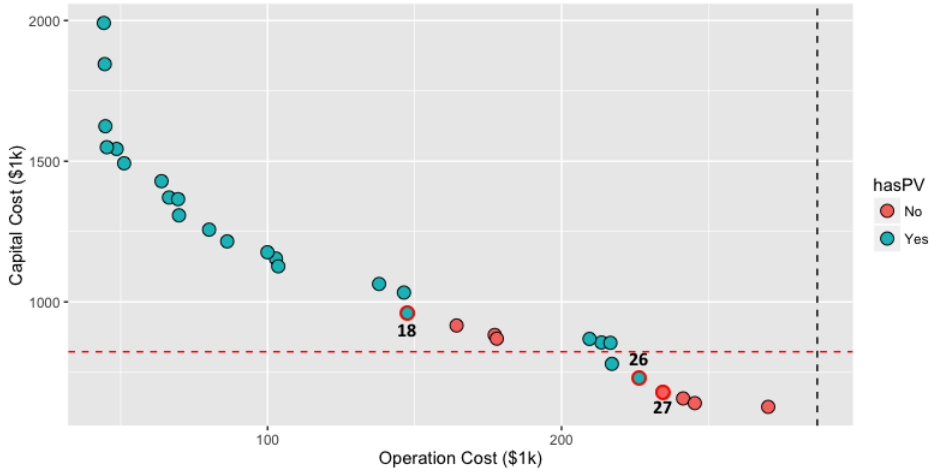

Figure 6.9: Compare optimal solutions with baseline in BiPV perspctive

side light shelf on its south facade. Similarly, design solution 26 has a 0.5m inside light shelf and a 0.5m outside light shelf. The major difference is the BiPV systems on the West facade in design solution 26, which increases the capital cost by $50,000 (7%). In return, there is only around $10,000 (4%) operation cost saving.

However, comparing design solution 26 with the energy and cost performance of ASHRAE baseline design, it not only lowers the capital cost by $100,000 but also achieves less operation costs ($61,000) in 25-year term. This proves that with an optimized integrated building system, the high investment of BiPV system can be justified. Also, the design solution 18, which is highlighted in Figure 6.9, demonstrates that it is impossible to achieve more than 50% operation costs saving without the BiPV systems.

6.7.6 Light shelf in optimal design solution

A light shelf system is installed in the real building. Therefore, an investigation on the energy impact of the light shelf system is included in the optimizations. Figure 6.10 shows the distribution of light shelf system in the Pareto front curve. Light shelves can be viewed from two different perspectives, the outside shelf, and the inside shelf. The outside shelf is acting as a shading device and daylight reflector at the same time. The inside shelf is used for reflecting the daylight to the indoor ceiling as well as the thermal mass in the room (UIUC and LBNL,

Table 6.6: Comparison between design solution 27 and design solution 26 in Figure 6.9 with ASHRAE baseline design

Solution Index	Insulation Level	WWR	HVAC	Lights	BiPV	LightShelf
Baseline	Wall: R-2.6	South: 40	System Type 6	T8 ($12W/m^2$)	South: No	Inside:
Operation: \$287k	Roof: R-3.3	North: 40		**Daylit Sensor:**	North: No	N/A
Capital: \$823k	Window:	East: 40		Off	East: No	Outside:
	U:1.9, SHGC: 0.4	West: 40			West: No	N/A
27	Wall: R-2.1	South: 50	DOASVRF	LED	South: No	Inside:
Operation: \$234k	Roof: R-4.9	North: 40		**Daylit Sensor:**	North: No	N/A
Capital: \$679k	Window:	East: 50		On	East: No	Outside:
	TG	West: 40			West: No	1.5m
26	Wall: R-2.1	South: 40	DOASVRF	LED	South: No	Inside:
Operation: \$226k	Roof: R-3.1	North: 40		**Daylit Sensor:**	North: No	0.5m
Capital: \$730k	Window:	East: 50		On	East: No	Outside:
	DLC	West: 40			West: Yes	0.5m

2016). In Figure 6.10, it seems that the impact of the light shelf system has a strong relation to the window glazing selections. Since most of the optimal designs choose double Low-E clear and triple glazing windows with high Vt, the analysis focuses on these two subsets of the entire Pareto front curve. The double Low-E clear window has a lower SHGC (0.41) than that of the triple glazing (0.57). It seems that the outside shelf is preferred than the inside shelf in design solutions with a triple glazing window due to the extra shadings. This is because a longer piece of the light shelf can provide more shades to the window. Therefore, it relieves the negative impact from a high SHGC in the cooling season. Also, the majority of the design solutions prefer investing in high insulation walls (R-2.6 to R-6.5) or roofs (R-4.9 to R-5.3) instead of having an inside light shelf as an additional piece of thermal mass.

6.7.7 LCC model sensitivity analysis

The LCC model sensitivity analysis focuses on predicting the effect of changes in the interest rate on net present value (NPV). This procedure is often used in investment decision making related to the investment project evaluation under a condition of uncertainty (Marenjak and Krstic, 2010). In this study, the interest rate is varied from 1% to 17% with a step of 2%. The analysis is conducted within the Pareto front curve. The 30 design solutions (Table E.1, E.2,

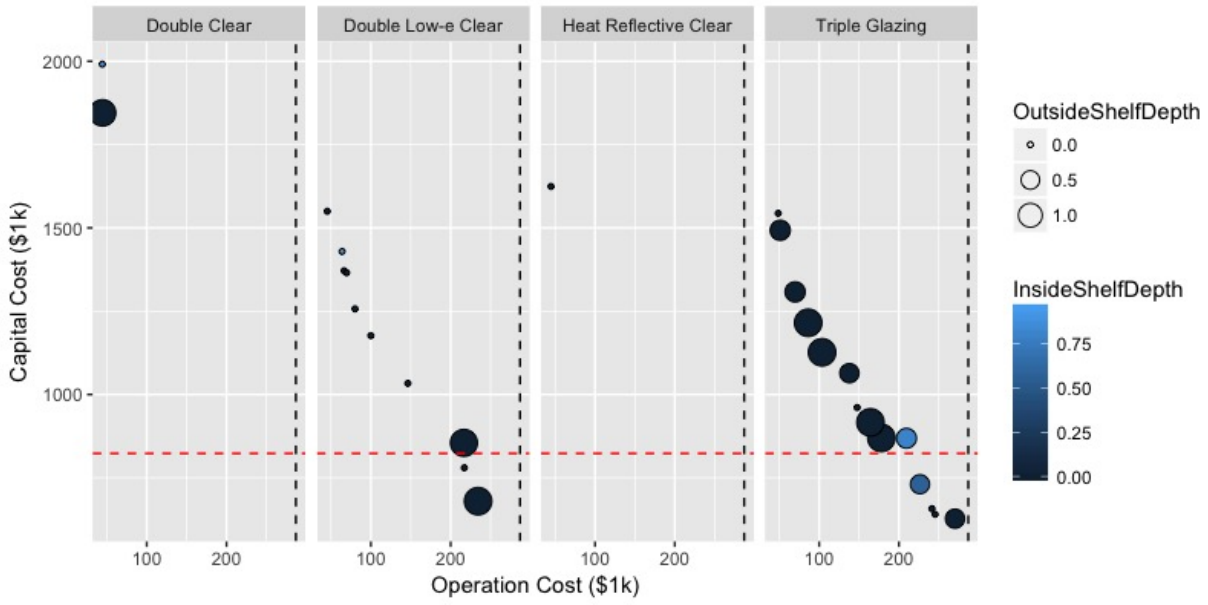

Figure 6.10: Compare optimal solutions in light shelf system perspective (divided by windows)

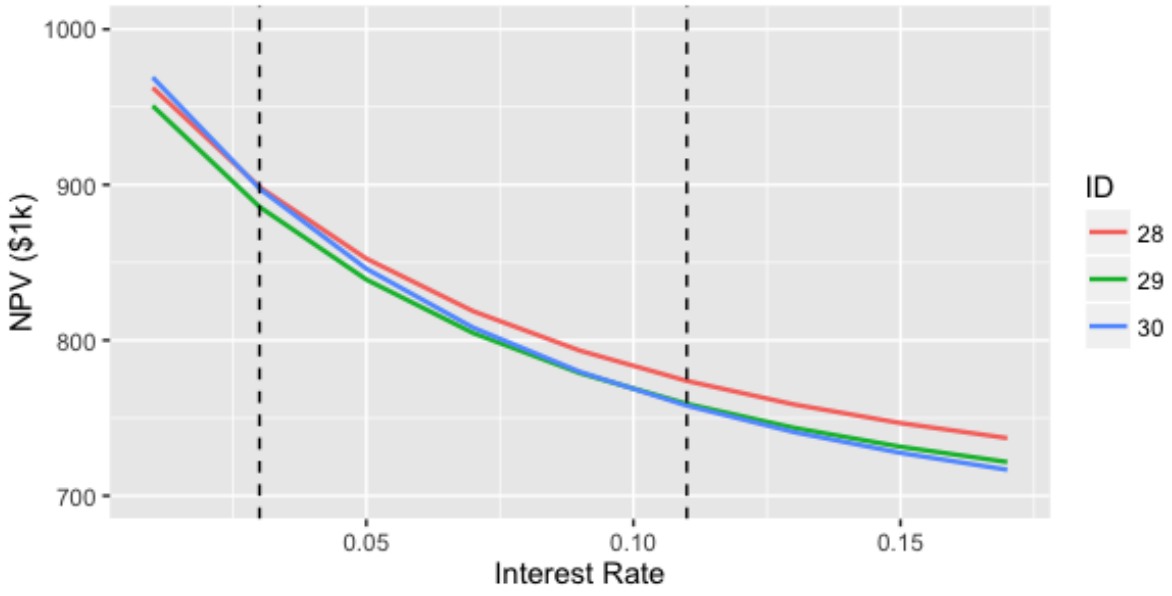

Figure 6.11: Net present value sensitivity analysis for design solution 28, 29 and 30

E.3 and E.4) are sorted based on operation costs in an ascending order. In Appendix E, Table E.5 lists the NPV for all the optimal design solutions (1-30) at different interest rates. In a design solution, a higher interest rate yields a lower NPV. Depends on the weight of operation costs in the total life cycle costs, the drop rate of NPVs are different. For instance, the operation costs are small compared to the capital cost in design solution 1. Therefore, its NPV drops 2% between 1% to 17% interest rate. On the contrary, design solution 30 drops more than 26% within the same range of interest rates. These results demonstrate that design solutions with lower operation costs are more resistant to the market risk.

Furthermore, as the interest rate increases, some of the cases become logical choices. Figure 6.11 shows the analysis results for design solution 28, 29 and 30. It shows that the design solution 30 is the least favored design solution among the three if the interest rate is lower than 3%. However, it is also an ideal design solution if the interest rate exceeds 11%. By navigating through the different interest rates, investors get a better understanding of the risk of each design solution.

6.7.8 Algorithm performance comparison

The ammNSGA-II algorithm is designed to improve the speed and convergence performance in solving building design problem. To demonstrate the algorithm's performances, an additional optimization is replicated and performed with the conventional NSGA-II algorithm. The Pareto front curve comparison is shown in Figure 6.12. The red dots represents the design solutions generated from ammNSGA-II, and the green dots shows the design solutions generated from NSGA-II algorithm. A reference Pareto front curve is constructed according to the method described in (Deb and Nain, 2007). This method extracts the best design solutions from a pool of optimal design solutions generated by the five replicated studies. Visually, it can be observed that the red dots are much closer to the reference Pareto front curve than the green dots. Using the normalize convergence metric (Equation C.2) and spread metric (Equation C.3) for comparison, the ammNSGA-II outperforms the NSGA-II with almost 3 times smaller convergence metric and 2 times smaller spread metric (Table 6.7). These mean the results generated from

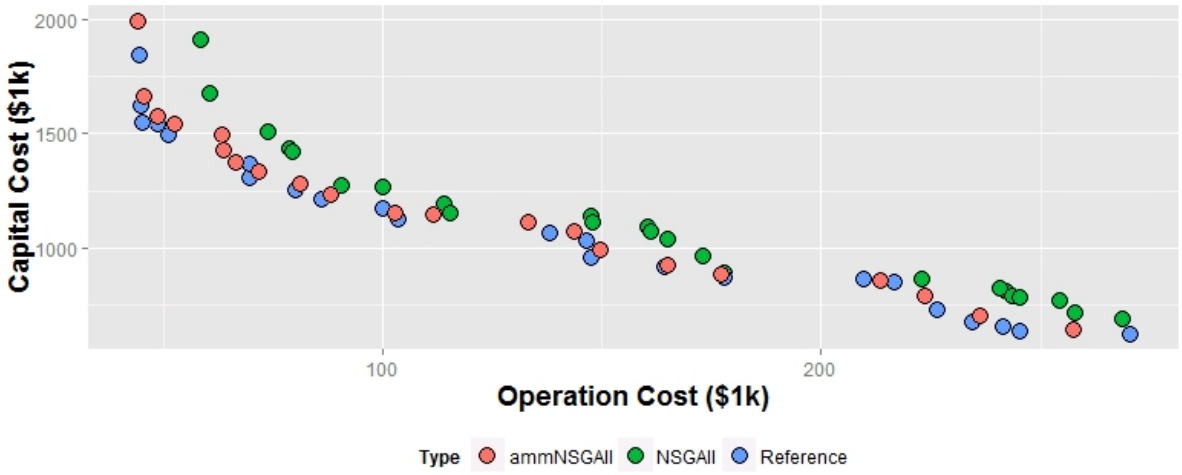

Figure 6.12: Compare the performance of ammNSGA-II and NSGA-II algorithms

Table 6.7: Algorithm performance comparison for CSL

Algorithm	Speed (hr)	Convergence ($\bar{C}(P^{(t)})$)	Spread (Δ)
NSGA-II	5.3	0.07	0.95
ammNSGA-II	4	0.02	0.45

ammNSGA-II is closer, and its shape is more similar to the reference Pareto front curve. Also, the faster convergence grants the ammNSGA-II the advantage of generating more duplicated design solutions at the later stage. With a mechanism that skips evaluation for duplicate design solutions, ammNSGA-II can save around 1.3 hours than NSGA-II out of 5 hours.

6.8 Summary of the CSL case study

- The real design of CSL is amazingly close to the global optimal. The only reason that the design does not reside on the Pareto front curve is that the design did not consider the BiPV system. Nevertheless, this case study demonstrates that through an integrated design process, a building could achieve low operation costs with reasonable capital cost.
- Multiple cases (Design solution 2 vs. Design solution 48, Design solution 1243 vs. Real design) support that an integrated building system optimization can find a design solution that offers more appealing long-term operation costs and capital cost than the current

standard.

- Pareto front curve demonstrates the trade-offs between capital cost and operation costs, which provides clients and the design team a visual approach to select the most desired optimal solutions that satisfy the project goals.
- The high capital cost of the BiPV system can be justified not only by long-term operation costs but also by the short-term capital cost via optimization (Design solution 1245 vs. Real design, optimal design solution 26 vs. Baseline energy model), which fully explores the energy and cost interactions among the various building systems.
- The LCC model sensitivity analysis demonstrated that depending on the interest rate used in the study, the design solution that generates the lowest net present value could be changed. In addition, the study shows buildings with higher operation costs are more fragile to the fluctuation of the market.

Chapter 7

Optimization on a retrofit project: One Montgomery Plaza

7.1 Project overview

This chapter focuses on a retrofit project. The One Montgomery Plaza is a large-scale office building owned by the Montgomery County. The building was built in 1973 and 2 years ago, the Montgomery County decided to retrofit the building in order to reduce the building's energy consumption. Similar to the previous case stud, the proposed platform is utilized in this case study to search for optimal renovation plan.

7.2 Building description

The One Montgomery Plaza is a multi-story office building located in Norristown, PA, U.S. Norristown has a heating dominant climate with a nearly 3000 heating degree day ($HDD18$). The building is a public property owned by the Montgomery County, PA. The facility houses county offices as well as other tenants. The building was built in 1973 and currently, requires a major renovation due to issues discovered in its envelope and HVAC systems. It consists of two towers, one has eight stories on the north, and the other has ten stories on the south. The total floor area of this building is 28,000 m^2 with 18,000 m^2 of conditioned building area. The

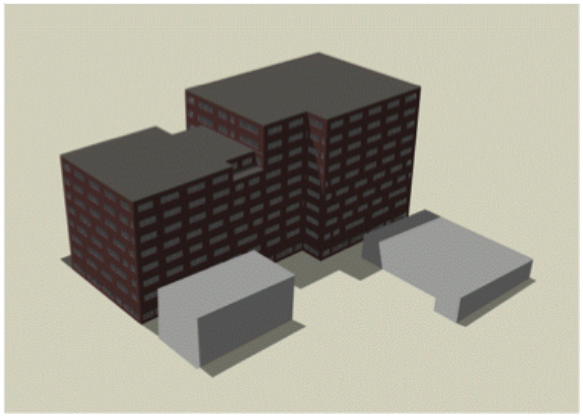

Figure 7.1: Rendered image of One Montgomery Plaza in DesignBuilder v4.7

building energy model is built in DesignBuilder v4.7 (Figure 7.1).

The HVAC system in One Montgomery Plaza is a dual duct VAV system and is modeled according to actual configurations in EnergyPlus. Figure 7.2 shows the chilled water plant loop modeled according to the actual configurations with the two chillers supplying chilled water to cooling coils located within the two AHUs of One Montgomery Plaza. The heating system is provided via hot water supplied by two boilers connected in parallel as shown by the hot water loop in Figure 7.3.

7.3 Energy model calibration

The One Montgomery Plaza energy model was calibrated at monthly resolution against the measured data (Chong et al., 2015). The calibration was conducted for the period of Mar-16 to Dec-18 in 2013. The calibrated model had cooling, heating as well as lighting and equipment energy within 5% of measured data and fan energy by 8%. Also, the coefficient of variation of the root mean square error (CVRMSE) and Normalized mean bias error (NMBE) recommended by (ASHRAE, 2002) were employed to demonstrated the robustness of the calibrated model in monthly resolution. The calibration results indicated that the NMBE was 2.46%, and CVRMSE was 13.6%, which were lower than 5% NMBE and 15% CVRMSE thresholds set by the ASHRAE guideline 14 (ASHRAE, 2002). This case study has been in-

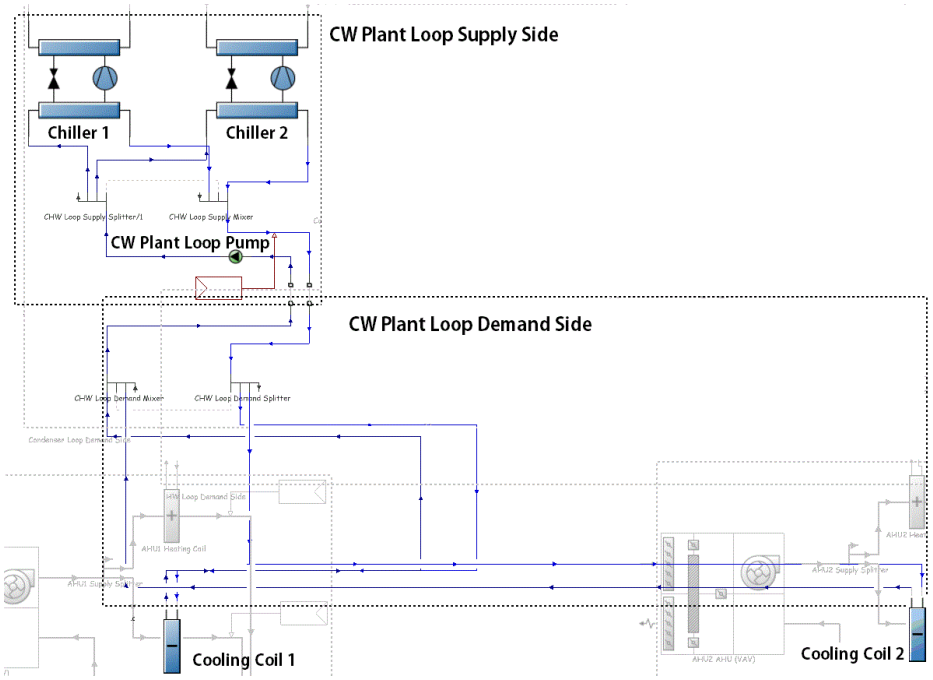

Figure 7.2: Chilled water loop of One Montgomery Plaza modeled in DesignBuilder

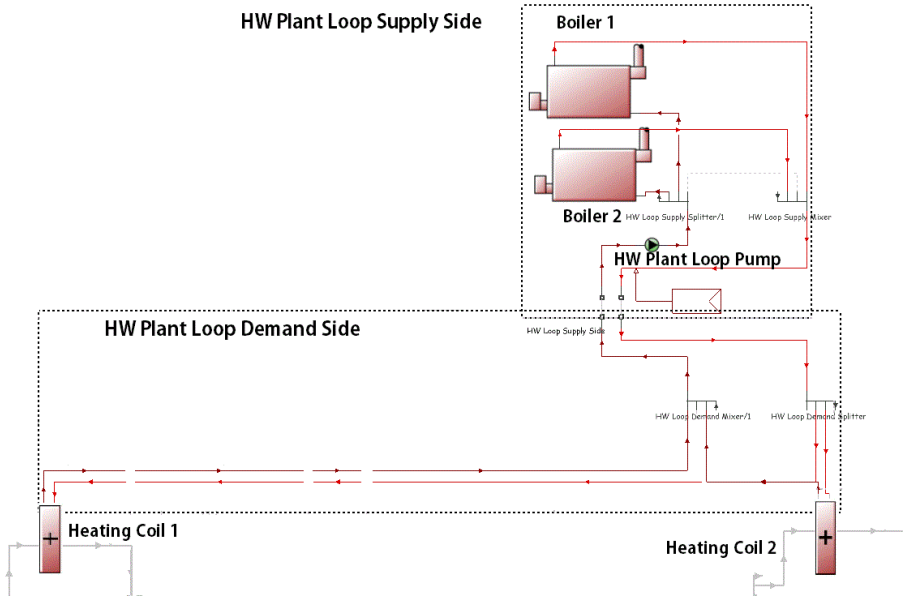

Figure 7.3: Hot water loop of One Montgomery Plaza modeled in DesignBuilder

Table 7.1: Design Options for each Design Parameters in One Montgomery Plaza

Design Parameters	Design Options	Property	Unit Cost
Insulation	R[a]-2.5	U-0.36[a]	$\$0/m^2$
3 options	R-3.3	U-0.25	$\$16.15/m^2$
	R-5.3	U-0.18	$\$20.88/m^2$
Windows	Double Clear (DC)	U-3.13, SHGC[a]-0.73, Vt[a]-0.8	$\$0/m^2$
6 options	Double Tinted (DT)	U-2.58, SHGC-0.37, Vt-0.53	$\$290/m^2$
	Double Low-e Clear (DLC)	U-1.40, SHGC-0.41, Vt-0.61	$\$356/m^2$
	Heat Reflective Clear (HRC)	U-1.40, SHGC-0.25, Vt-0.45	$\$409/m^2$
	Triple Glazing (TG)	U-1.31, SHGC-0.57, Vt-0.47	$\$480/m^2$
	Quadruple (Q)	U-0.78, SHGC-0.46, Vt-0.62	$\$862/m^2$
Lights	Current	LPD[a] $- 10.2W/m^2$	$\$0/m^2$
3 options	T5	$LPD - 7.5W/m^2$	$\$220/m^2$
	LED	$LPD - 4.5W/m^2$	$\$390/m^2$
Light Control	Yes		$\$268/Each$
2 options	No		$\$0/Each$
BiPV[b]	Yes	South, East, West	$\$4.5/W$
2 options	No		
Chiller	Current	COP[c]-5.5	$0
2 options	New	COP-8.4	Sizing
Boiler	Current	80% AFUE[c]	$0
2 options	New	92% AFUE	Sizing

[a]: R: overall thermal resistance (m^2K/W), U: overall coefficient of thermal transmission (W/m^2K), SHGC: solar heat gain coefficient (dimensionless), Vt: visible transmittance (dimensionless), LPD: lighting power density (W/m^2).

[b]: BiPV stands for building integrative photovoltaic system

[c]: COP: coefficient of performance (dimensionless), AFUE: annual fuel utilization efficiency (%)

tegrated into a proposed DesignAdvisor tool HVAC interface, and it can be found in the link: `http://128.2.109.83:8888/HVAC_CMU/DesignAdvisorDEMO.html`.

7.4 Design parameters for the One Montgomery Plaza

Table 7.1 lists the design parameters for this study. The list is extracted from the top ten sensitive parameters for office buildings in the Energy Asset Score Tool (Wang et al., 2015). The underlined design options are the currently installed systems. Therefore, their costs are set to $0 per unit. Similar to the previous case study, the unit cost includes only the material cost. The

list contains a subset of the database, which includes most of the design options that have better efficiencies in their categories than the current systems in the building. In this list, there are seven design parameters. Two of them are passive system improvements including wall insulation and windows. The calibrated wall insulation is R-2.5, and in the proposed retrofit plan, R-3.3 and R-5.3 are considered. Similarly, high insulation windows are suggested for window replacement strategy. Other than passive systems, active system improvement strategies such as high efficient lighting systems, chillers, and boilers as well as daylight controls are also included. Furthermore, renewable energy system, building integrated photovoltaic (BiPV), is introduced into this retrofit project. The maintenance and operation cost information is dynamically extracted from Table A.1 in Appendix A based on the selected design options. In total, there are nearly 4000 possible combinations. Compared with the new construction, this project has a significantly smaller set of possible design combinations (54 million vs. 4000). However, the One Montgomery Plaza is a much larger office building with nearly 450 thermal zones. A single simulation of this building could take up to an hour depending on the system selected. It means that a full enumeration of the possible combinations requires approximately 170 days. The optimization is conducted on a desktop with a configuration of i7 quad-core 3.5 GHz CPU and 16 GB RAM. The total time required for performing one optimization is 50 hours.

7.5 Life cycle cost model parameters for One Montgomery Plaza

Table 7.2: Life Cycle Cost Model Parameters

Field	**Input**
Discounting Convention	End of Year
Inflation Approach	Constant Dollar
Real Discount Rate	0.03
Base Date	2016 January
Service Date	2017 January
Study Length	25 Years
Price Escalation	NIST Handbook 135 Table Ca-1, Census Region 1
Electricity Tariff	PECO 2016 Electric Tariff (PECO Energy Co., 2016a)
Natural Gas Tariff	PECO Gas Service 2016 (PECO Energy Co., 2016b)

Table 7.2 lists the life cycle cost (LCC) parameters defined for this retrofit project. Similarly,

the LCC is constructed using the parameters published in the "*NIST Handbook 135*" (Rushing et al., 2016). The local electric and gas tariff model are provided by PECO (PECO, 2016). It should be noted that the study length is 25 years in this retrofit project. It is because most of the systems included in this study can last for a minimum of 25 years.

7.6 Results analysis on the One Montgomery Plaza case study

7.6.1 Overview

Similarly, the same optimization for One Montgomery Plaza is repeated five times to prevent premature convergence. Figure 7.4 shows all the generated design solutions for One Montgomery Plaza. The "as is"solution represents no retrofit plan solution. The red dashed line shows the capital cost of this "as is" solution ($\$0$), and the black dashed line shows the present value of operation costs in 25 years ($\$9,481,399$) for this solution. The intersection of these two dashed lines plots the location of the "as is" solution in the solution space. All the other design solutions are on the top left region of this design solution. It indicates that the comparison in retrofit project is different from that of new constructions in two aspects.

- **Comparison metric**: Both new construction and retrofit projects should be compared with a standard-compliance design. Also, the retrofit project should compare with the current condition of the building.
- **Capital investment**: The capital cost of the new construction can be reduced from a standard-compliance design through the integrated building system design optimization; however, a retrofit design cannot have lower capital cost than the "as is" option.

Therefore, the optimization in this study would focus on helping design team find productive investments which can maximize the long-term saving with minimal capital investment. Table 7.4 shows the comparison between two generated design solutions. It can be observed that both solutions choose to upgrade the boilers and chillers. Besides boiler and chiller, design solution 680 also increases the thermal resistance of the building envelope. This additional upgrade reduces not only the operation costs by $0.2 million in 25 years, but also reduces the capital cost

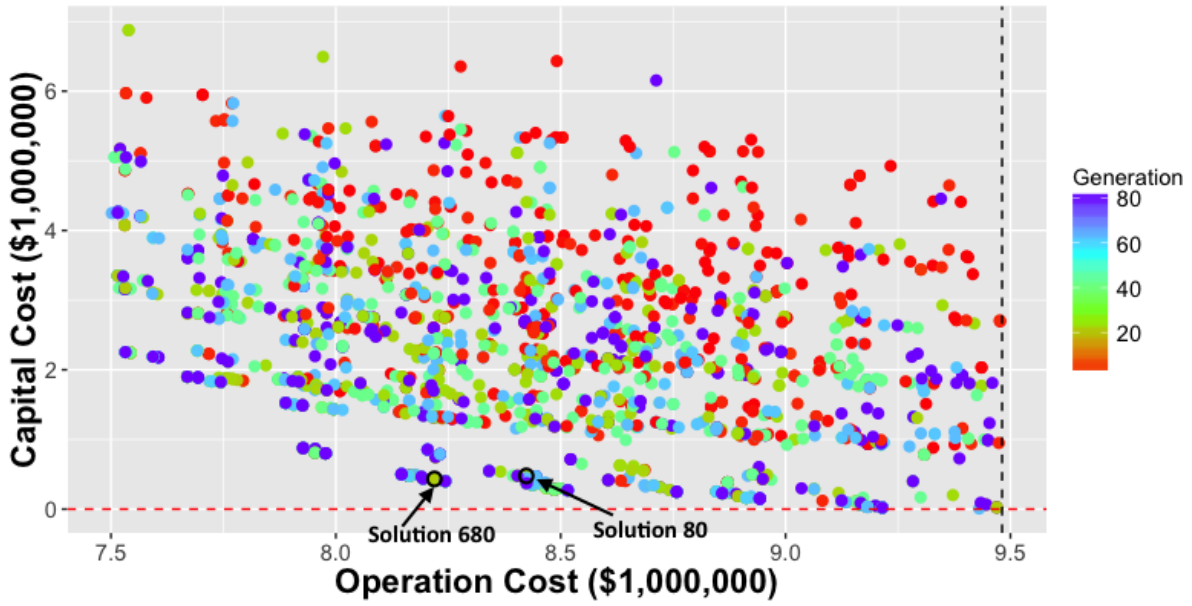

Figure 7.4: Generated design solutions for One Montgomery Plaza

Table 7.3: Comparison between design solution 80 with design solution 680

Solution Index	Insulation Level	Window	Lights	Heat	Cool	PV
80	Wall: R-2.5	DC	T8	New	New	South:No
Operation: $8.4M			**Daylit Sensor:**			East: No
Capital: $0.44M			On			West: No
680	Wall: R-5.3	DC	T8	New	New	South:No
Operation: $8.21M			**Daylit Sensor:**			East: No
Capital: $0.41M			On			West: No

by $0.03 million. This is mainly due to the capital cost trade-offs between load-reduction measures (insulation) and HVAC systems.

7.6.2 Compare to the ASHRAE baseline model

The generation of an ASHRAE baseline design for a retrofit project is almost the same as that of a new construction. The only difference is that the baseline design should use the existing envelopes, including wall, roof, and windows, etc., which could vary depending on the age of the building. Therefore, the capital cost for these systems is $0.0. The lighting system in One Montgomery Plaza ($11W/m^2$) has a similar power density value as the ASHRAE 2010 baseline design requirement ($12W/m^2$). Therefore, it is not necessary to replace the lighting

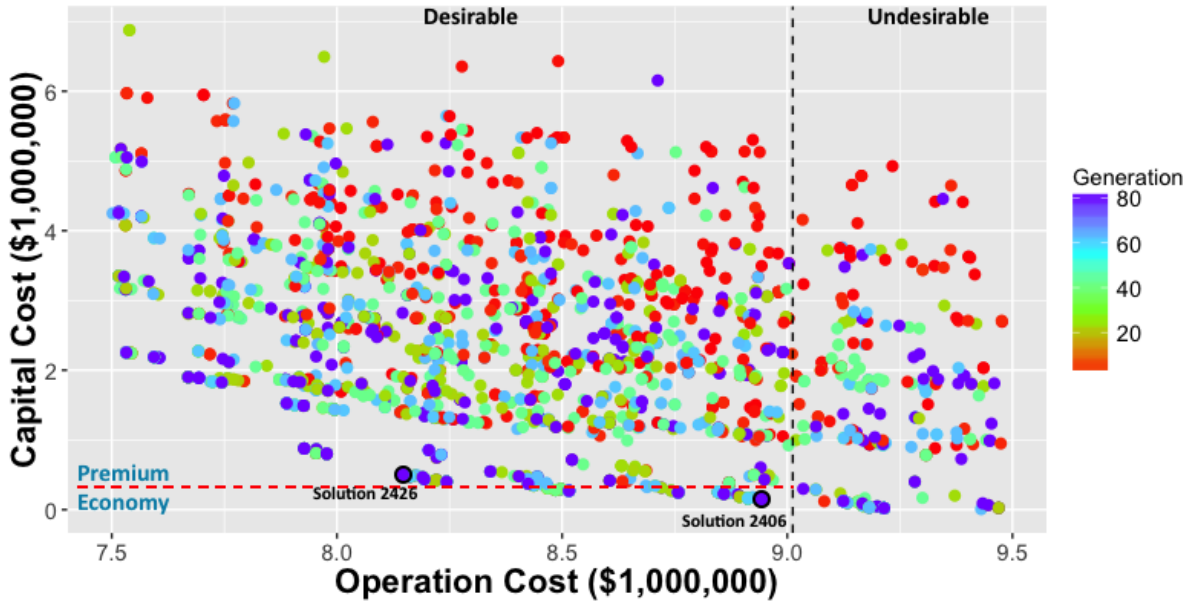

Figure 7.5: One Montgomery Plaza generated design solution compare with ASHRAE baseline design

system as well. In addition, the baseline design should not include any daylight control and renewable energy systems. Hence, the only change in capital cost is the HVAC system. For a fair comparison, the capital cost for the HVAC system is assumed to be equal to the material costs of chillers and boilers. The results from baseline design indicate that the cooling load is around $430tons$ and the heating load is $1700kW$. Therefore, the total chiller cost is estimated by using three $145tons$ reciprocating chillers, and the total boiler cost is calculated by using a $1,788,000kW$ gas-fired hot water boiler. It should be noted that the efficiency of a hot water boiler for ASHRAE baseline design is 82%, which is much lower than the design option listed in Table 7.1. Similarly, the coefficient of performance of the chiller is 6.1 in the baseline design instead of 8.4. The cost has been adjusted to reflect the standard efficiency equipment. For the boiler, the adjustment is multiplying the current price by 0.7. This number is derived from comparing the price of a condensing boiler with a regular boiler (HomeAdvisor, 2017). The same correction applied to the chiller as well. Therefore, the total chiller cost is $214,500, and the total boiler cost is around $115,500.

Figure 7.5 indicates the comparison between the generated design solutions with ASHRAE baseline design model. The comparison divides the generated design solutions into two types.

1. Undesirable solutions: design solutions that have higher operation costs than the baseline model.
2. Desirable solution: design solutions that have lower operation costs than the baseline model.

Furthermore, the desirable solutions can be divided into two types.

1. Desirable premium solutions: desirable solutions that higher capital cost than the baseline model.
2. Desirable economy solution: desirable solutions that have lower capital cost than the baseline model.

The undesirable solutions are the least appealing design solutions because their cost performance is worse than the baseline design. Desirable economy solutions could be the most popular solutions because they have lower capital and operation costs. On the other hand, desirable premium solutions may be attractive to the design team as well even though they require more capital cost than the ASHRAE baseline design. Table 7.4 compares two design solutions with the ASHRAE baseline design. The design solution 2406 is one of the desirable economy solutions. This design solution chooses to increase the wall insulation level and upgrade the lighting system instead of replacing chillers. The results show a $0.17M operation costs saving with nearly 25% less capital cost. It indicates that the replacement plan should focus on the integrated building system instead of a particular system. At the current stage, replacing lighting system and increasing insulation level could maximize the saving with minimal investment comparing with the designs that replace both chillers and boilers.

On the contrary design solution 2426 is one of the desirable premium solutions. This design solution achieves even lower operation costs with slightly more capital investments than the baseline design. On top of the design solution 2406, design solution 2426 adds higher insulations, daylight control and chillers, which immediately increases the capital cost by $0.2M. However,

Table 7.4: Comparison between design solution 80 with design solution 680

Solution Index	Insulation Level	Window	Lights	Heat	Cool	PV
Baseline	Wall: R-2.5	DC	$12W/m^2$	New	New	South:No
Operation: \$9.01M			**Daylit Sensor:**	82%AFUE	COP-6.1	East: No
Capital: \$0.33M			Off			West: No
2406	Wall: R-3.3	DC	T5($7.5W/m^2$)	New	No	South:No
Operation: \$8.84M			**Daylit Sensor:**			East: No
Capital: \$0.25M			Off			West: No
2426	Wall: R-5.3	DC	T5($7.5W/m^2$)	New	New	South:No
Operation: \$8.19M			**Daylit Sensor:**			East: No
Capital: \$0.53M			On			West: No

in return, more than \$0.8M operation costs are saved with this design solution. Through such analysis, clients and design team can quickly identify better design solutions than the ASHRAE baseline design.

7.6.3 Important designs

Table 7.5: Information gain for each design variable

Item	Importance to operation costs	Importance to capital cost
Window	0.218	0.348
Insulation	0.035	0.004
Light	0.076	0.046
Daylighting Sensor	0.018	0.005
Chiller	0.37	0.009
Boiler	0.096	0.016
BiPV	0.004	0.311

Interestingly, in Figure 7.4, the design solutions are clustered. This pattern usually implies that one or multiple design parameters have significant impacts on one or both objectives. Table 7.5 shows the information gain of every design parameter on both objectives. The information gain is a metric that informs the importance of a given design parameter to the objectives. Table 7.5 suggests windows and chillers have the high impact on operation costs and windows and BiPV systems are most critical to the capital cost.

Figure 7.6 shows all the design solutions that are highlighted by their window types. Based on the unit cost and the thermal properties of a window, design solutions are separated into dif-

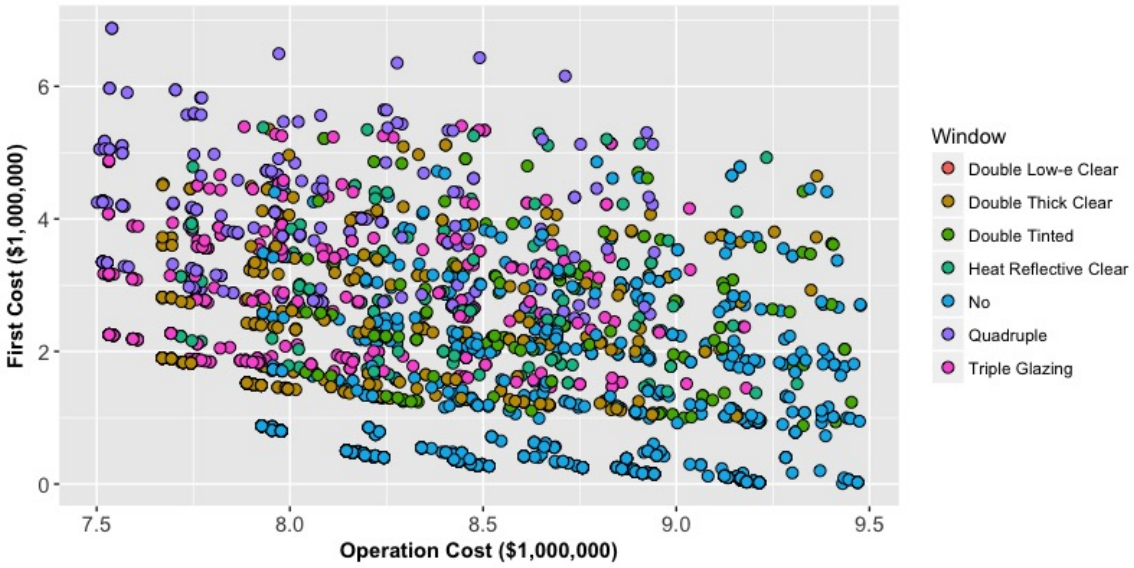

Figure 7.6: One Montgomery Plaza design solution plots by windows

ferent clusters. Remaining with current window options (“No”) have taken most of the bottom and right side area. On the other hand, design solutions with quadruple window, which has the best thermal properties among all the other windows, have occupied the most of the top left and middle area.

Unlike windows, chiller has a significant impact on operation costs. However, it seems it is not very relevant to the capital cost. Figure 7.7 indicates all the design solutions that are highlighted by chiller design. First of all, upgrading chiller does not guarantee a lower operation costs. It can be observed when the operation costs are around $8.5M, where the two types of design solutions are well mixed. However, this option is a must-have option if the client desire for a better operation costs saving. On the other hand, the differences between capital cost are not so obvious. A possible reason for this could be the high window and BiPV system costs, which reduce the relevance of chillers capital cost.

Lastly, the BiPV systems also play a major role in the capital cost. Figure 7.8 shows the design solutions with (“TRUE”) and without(“FALSE”) BiPV systems. Almost all of the design solutions that require more than $2M capital cost have BiPV system installed. However, it is surprising to find that the BiPV systems do not provide a significant amount of operation costs

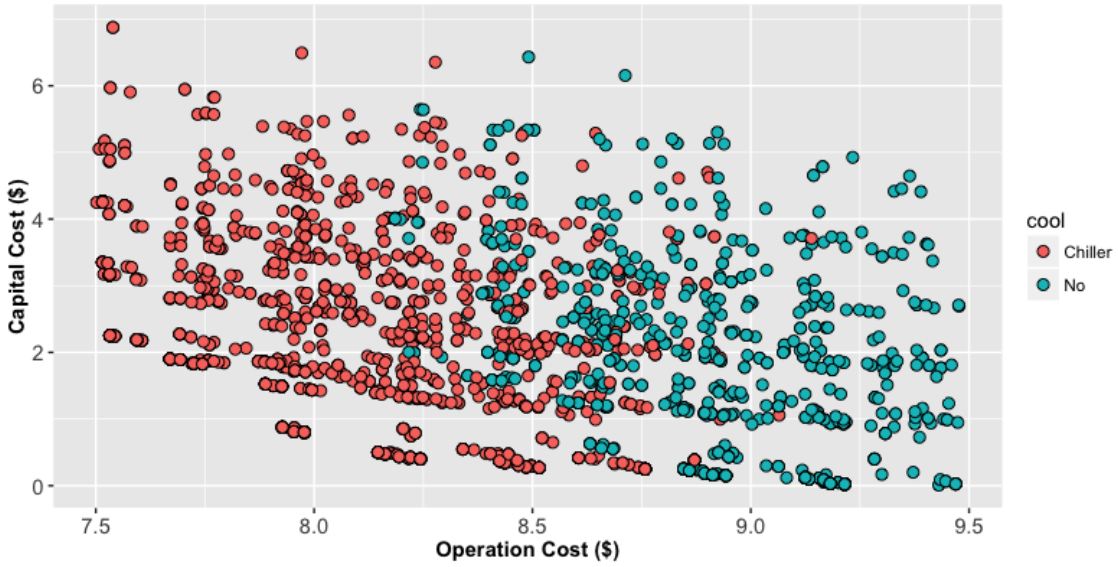

Figure 7.7: One Montgomery Plaza design solution plots by chillers

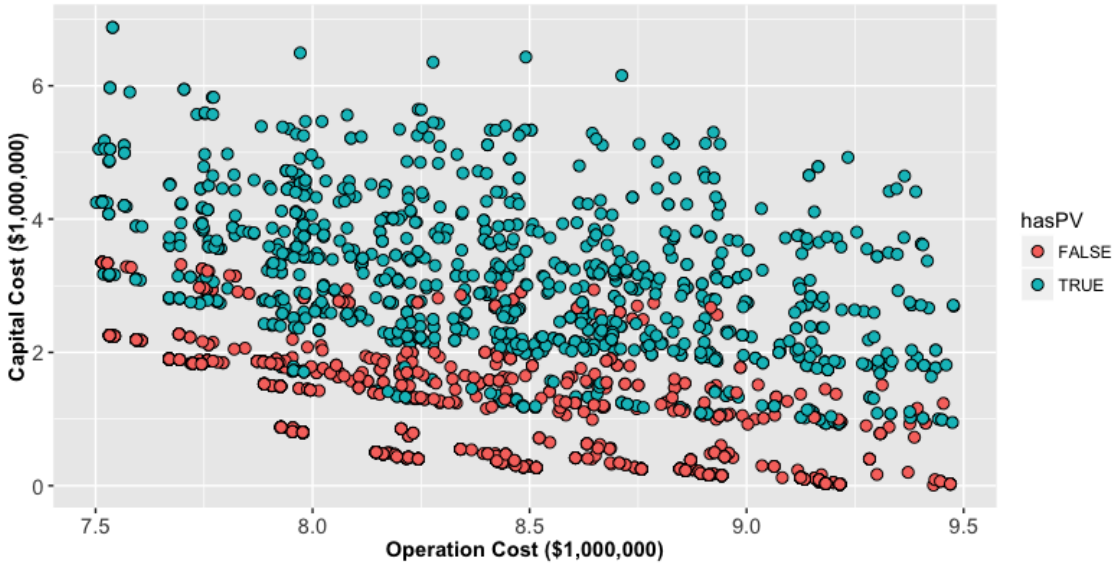

Figure 7.8: One Montgomery Plaza design solution plots by BiPV system

saving compare to the other design parameters. It partly because the One Montgomery Plaza has a high overall window to wall ratio (50%), but also because the electricity generated from the BiPV system is relatively small compares to the energy the building consumes in one year. Despite its high costs, design solutions still have to equip BiPV systems to reach minimum operation costs ($7.50M).

7.6.4 Pareto front curve

Figure 7.9 shows the optimal design solutions among the results derived from the five replicated optimizations. The Pareto front curve plots 26 optimal design solutions in the solution space. The full list of the 26 design solutions can be found in Appendix F, Table F.1, F.2 and F.3. The capital cost ranges from $0.0 to above $4.0M while the operation costs in 25 years dropped from $9.5M to $7.5M. The absolute improvement curves consist of changes in operation costs, capital cost, and life cycle cost (LCC) compared with the existing building. Similarly, the percentage improvement curves indicate the improvement of both capital and operation costs over the existing building.

The optimal design solutions are sorted by their operation costs in an ascending order. An optimal design solution index shows the standing of the design solution in the optimal design solution set. Therefore, the “as is” solution is plotted on the right side of the figures. Observing the absolute improvement curves from right to left, the operation and capital costs curves go into two opposite directions. The blue curve shows the absolute changes in the life cycle cost. At first, it climbs with the operation costs until the design solution 17. Afterward, it slowly falls to a break-even point at design solution 12, where the saving in operation costs is diminished by the increase of the capital investment. Last, it quickly falls with the capital investment. The black dashed line shows the design solution 17, which has the optimal life cycle cost performance among all the other design solutions.

Table 7.6 shows the design options under design solution 12 and 17. Compared with the design solution 17, design solution 12 enhances its thermal insulation, replaces windows with higher thermal insulation windows and upgrades lighting system. Although these upgrades enlarge the

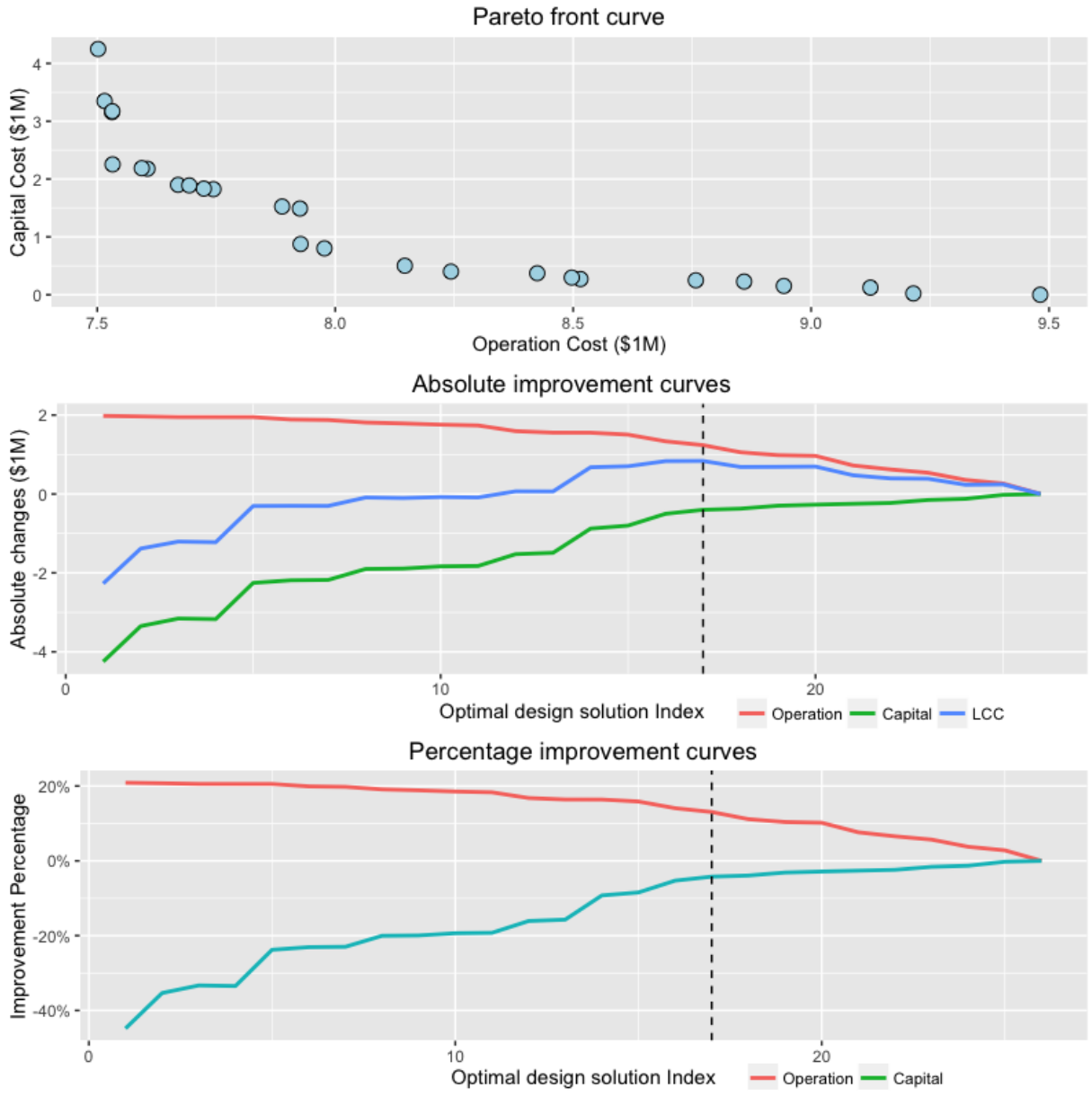

Figure 7.9: One Montgomery Plaza pareto front curve, percentage and absolute improvement curves

Table 7.6: Comparison between design solution 17 with design solution 12

Solution Index	Insulation Level	Window	Lights	Heat	Cool	PV
12	Wall: R-5.3	DLC	T5	New	New	South:No
Operation: $7.89M			**Daylit Sensor:**			East: No
Capital: $1.52M			On			West: No
17	Wall: R-3.3	No	No	New	New	South:No
Operation: $8.24M			**Daylit Sensor:**			East: No
Capital: $0.40M			On			West: No

operation costs saving by 3%, the capital cost increases around 10%. However, this is based on the assumption of 3% interest rate. The next section will further investigate the impact of interest rate on the decisions.

7.6.5 LCC model sensitivity analysis

In this study, the interest rate is varied from 1% to 17% with a step of 2%. The analysis is conducted within the Pareto front curve. There are in total 26 optimal design solutions, and they are sorted based on operation costs in an ascending order. Table F.4 in Appendix F lists the net present value (NPV) for all the optimal design solutions (1-26) at different interest rates. In the table, the NPV decreases significantly when higher interest rates apply. Another observation implies that the lower the capital cost, the larger the differences between R=1% to R=17%. For instance, the NPV of design solution 1 drops by around 50% from R=1% to R=17%. However, the NPV of design solution 26 drops almost 75%. Lastly, although some design solutions have a high NPV at lower interest rates, its NPV may drop faster and become lower than most of the other design solutions after increasing the interest rates. Figure 7.10 shows the NPV curves for design solution 15 to 20. In this Figure, the design solution 20 has the highest NPV when the interest rate equals to 1%. However, after R=11%, it achieves lower NPV than the other design solutions.

7.6.6 Algorithm performance comparison

To demonstrate the performance of ammNSGA-II algorithm in a larger scale office building, an additional optimization is replicated and performed with NSGA-II algorithm. Figure 7.11

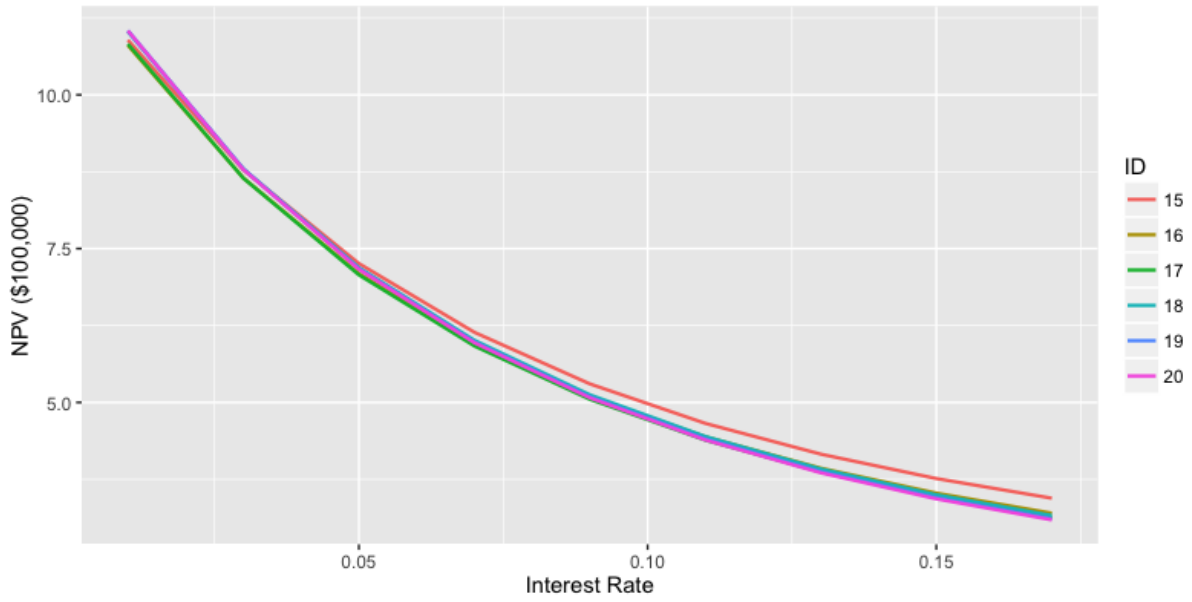

Figure 7.10: One Montgomery Plaza life cycle cost sensitivity analysis (15 to 20)

Table 7.7: Algorithm performance comparison for One Montgomery Plaza

Algorithm	Speed (hr)	Convergence ($\bar{C}(P^{(t)})$)	Spread (Δ)
NSGA-II	59	0.018	0.85
ammNSGA-II	50	0.002	0.60

shows the comparison results, where the red dots indicate the design solutions generated from ammNSGA-II algorithm, and the green dots denote the results of NSGA-II algorithm. The blue dots are the reference design solutions, which are found according to the method described in (Deb and Nain, 2007). It can be observed that the NSGA-II is quite comparable with ammNSGA-II in this case except for the middle region of the solution space. Compare the normalized convergence metric ($\bar{C}(P^{(t)})$), the advantage of using ammNSGA-II is not significant. It could be due to the smaller set of design combinations which allows NSGA-II finding optimal design solutions within the maximum number of evaluations. However, the ammNSGA-II does demonstrate its ability to find diverse design solutions by comparing the spread metric (Δ). Also, it seems that ammNSGA-II can reach optimal region earlier than NSGA-II. The algorithm typically preserves these optimal design solutions and reproduces them in the next generations. With a mechanism that skips evaluation for duplicate design solutions, the ammNSGA-II re-

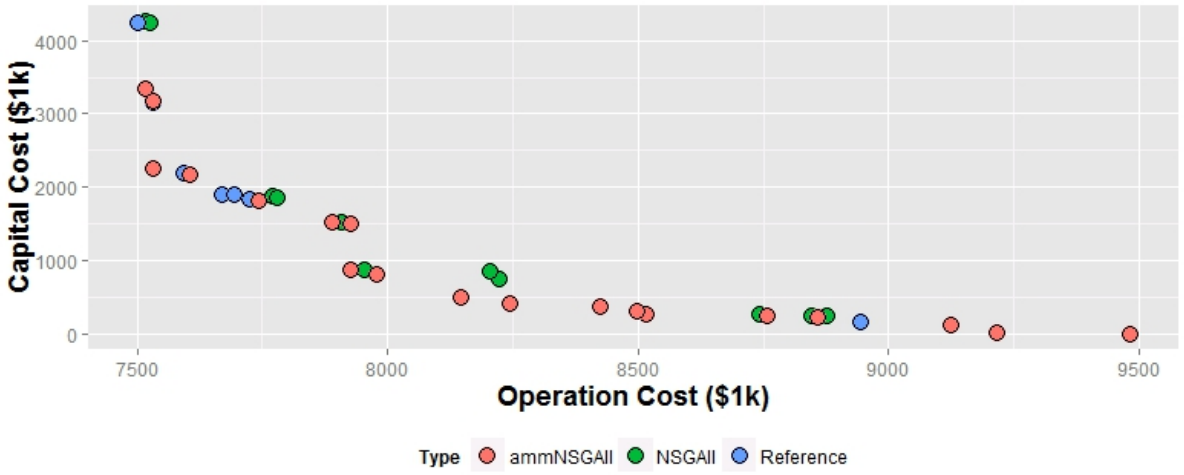

Figure 7.11: Compare the performance of ammNSGA-II and NSGA-II algorithms

sults in 10 hours less.

7.7 Summary of One Montgomery Plaza study

- The retrofit project has a different perspective on analyzing the cost benefit of design solutions since the capital cost performance of every design solution is worse than the "as is" solution. Therefore, the analysis should focus on minimizing the retrofit investment to trade for a more operational costs saving.
- Multiple cases (design solution 80 vs. design solution 680, baseline design vs. design solution 2406) demonstrate the effectiveness of an optimization algorithm in finding the design solutions with lower capital and operation costs than the current standard. They also illustrate that the capital cost of a higher investment choice (chiller) can be justified by not only the long-term operation costs but also the capital cost trade-offs between wall insulation and chiller.
- In this case study, the window system has a tremendous impact on both capital cost and operation costs. On the other hand, chiller has an enormous impact on operation costs and BiPV system can significantly affect the capital cost.

- The LCC model sensitivity analysis suggests that clients or design team could select a preferred design solution depending on the interest rates. It is realized by investigating the net present value of design solution 17 and design solution 20 at R=1% and R=17%.

Chapter 8

Conclusion

8.1 Contribution

This thesis presents a computation platform to optimize the cost performance of building system design through an integrated design approach. More specifically, the work has:

- Established a method to allow performing quantity take-off with a building energy model for an automatic capital cost estimation on designs that influence the building energy consumption.
- Integrated the economic module in EnergyPlus with a designed building system performance database, which contains passive, active and renewable building systems, for long-term operation costs evaluation.
- Developed a multi-objective meta-heuristic optimization algorithm, ammNSGA-II, for solving optimization problems with computationally expensive fitness functions.
- Analyzed the optimization results in a new construction and a retrofit project with an integrated design mindset to obtain an in-depth understanding of the platform capabilities in assisting building energy design decision.

The computation platform proposed in this thesis is a highly automated and fast process that helps design team, and client maximizing the operation costs saving with minimal capital cost

by:

- Organizing and managing the unique building system cost and performance data with a designed SQL relational data schema and XML data schema, allows fast sorting, retrieving and recombining operations on different types of building system data structure.
- Reusing the information generated in the process of a meta-heuristic algorithm by implementing machine learning techniques, which not only save time but also increase the algorithm convergence.
- Automating the tedious and error-prone process of creating ASHRAE 90.1 compliance baseline model.

A step by step instruction of using this platform is provided in Appendix G. This instruction includes the installation of third-party applications and packages, the installation of the platform, the creation of the EnergyPlus model, running optimization and results analysis method.

8.2 Summary of findings

The major findings achieved through the thesis work can be summarized as follows:

- Building energy model (BEM) can be used for building system quantity take-off (QTO). It is because 1) BEM is a multi-disciplinary model that covers the performance of the majority building systems including building envelope system, electric system, and HVAC system, etc., 2) BEM requires a full set of data for a successful energy simulation; its completeness allows performing high-quality QTO. However, one drawback of the BEM-based QTO is the lack of less energy related product descriptions, such as ducts and pipes.
- The developed ammNSGA-II algorithm successfully marry the machine learning technique with the conventional meta-heuristic algorithm to achieve higher convergence in less time.
- Integrated system optimization can effectively explore the energy and cost trade-offs among a group of interdependent building systems. Furthermore, with the system integra-

tion approach, the optimization can tunnel through the capital cost barrier that is defined in (Lovins, 2007). For example, compared design solution 2 with design solution 48 in the new construction case study, design solution 48 demonstrates a higher insulation level and a more efficient lighting system can reduce not only reduce operation costs, but also the capital cost through a smaller size of HVAC system.

In the case study of a new construction, the platform found multiple design solutions that achieved not only lower operation costs (4% to 23% savings) but also lower capital cost (5% to 23% savings) than the ASHRAE 90.1 baseline design through an integrated design optimization approach.

- The platform found a design solution that took advantage of the cost and performance trade-offs in an integrated design approach to achieve lower operation costs ($5000 savings) and capital cost ($100,000 savings) than the real design of the building, which was configured with the best design options in every design parameter.
- The high investment in the building integrated photovoltaic (BiPV) system could be justified not only by the long-term operation costs but also the capital cost trade-offs between systems in an integrated design. One of the optimal design solutions with the BiPV system revealed that 21% ($61,000) operation cost savings could be achieved with 12% ($100,000) less capital cost compare to the ASHRAE 90.1 baseline design.
- The sensitivity analysis of life cycle cost model indicated cheap design solutions with higher operation cost were more susceptible to the fluctuation of the market risk. The increase of interest rate not only reduced the total net present value for each design solutions but also changed the ranking of the optimal design solutions.

The findings could be generalized as design guidelines for a small new office buildings in Pittsburgh area through exploring the preferred design options that are selected in the desirable economy solutions. In comparison with baseline design, the results indicate the ASHRAE 90.1 2010 specified insulation level with high-efficiency lighting and HVAC system can effectively reduce both capital and operation costs. Furthermore, for projects whose target is net zero

buildings, installing BiPV system is probably a better option than stacking the insulation levels of the envelope. However, whether the high investment of BiPV system can be justified by capital cost trade-offs is also highly dependent on the window properties such as U-value, SHGC, and Vt, as well as the window to wall ratios.

In the case study of a retrofit project, the platform found the trade-offs between the operation costs and capital cost as well as the trade-offs within each objective.

- Unlike the new construction project, a retrofit project was about how many systems can be upgraded or replaced to achieve total life cycle cost savings within a given period. The optimization successfully targeted at a design solutions that minimized the capital cost ($400,000 investments) and maintained a lower life cycle cost ($800,000 savings) compared with the "as is" solution.
- For a large size office building, the information gain analysis showed HVAC system (Information Gain: 0.37), window system (Information Gain: 0.22) and lighting power density (Information Gain: 0.08) are the top 3 most sensitive design parameters related to the operation costs. This conclusion was similar to the study conducted by the Energy Asset Score Tool (Wang et al., 2015).
- The value of BiPV system was under-rated in this case study. It could be due to the relatively small amount of electricity generated by BiPV systems compared to the energy consumed by the building. However, it was necessary to have BiPV system if the design team and clients were targeting at more than 20% operation cost savings.
- Similarly, the sensitivity analysis of life cycle cost showed the building designs with higher operation costs are more fragile to the market risk.

The results of this case study could be used to guide the retrofit design for large office buildings in Philadelphia area. Table 7.5 provides the importance of the design parameters for both operation costs and capital cost. For operation costs, the window, chiller, and boilers are the most critical design parameters that the design team should consider. On the other hand, the windows, lights, and boiler have an enormous impact on capital cost. It should be noted that in this

study, the cost assumptions are based on multiplying the national average values by Philadelphia local cost index (RSMeans, 2015). Any additional information such as price discounts or unexpected events could alter the results significantly.

8.3 Future work

The following additional work can be conducted based on the outcome of this thesis:

- **Link the cost database with the commercial construction cost database.**

  The current version of the cost database is static, and it only allows manual entry, which means to update or add more cost items, it requires manual extraction of the information from the "*RSMeans cost data book*" (RSMeans, 2015). It requires at least one or two full-time employees to maintain the database to keep its cost information up-to-date. However, recently, RSMeans has released its online platform and API to access that platform. Through their web API, updating the database would be automated. It not only saves time and reduces the possible human errors, but also provides users a most up-to-date cost information with their cost optimization.

- **Include constraint functions in the optimization process**

  Constraints are common in the optimization, but they are not considered in this thesis. Thus, some of the optimal design solutions generated by the optimization may be not applicable for the particular project or sacrificing human comfort for energy savings (e.g. low visibility windows), etc. Future work could consider to include constraints in the optimization process to better filtering the optimal design solutions.

- **Automating the design parameter recommendations**

  The design parameters are manually selected for the optimizations in the current version of the platform. However, based on the recommendations given in the ASHRAE advanced energy design guides (AEDG), a rule-based expert system for design parameter selections can be implemented and automated. By integrating such system, the user can acquire the recommended design parameters for optimization just by specifying the

building type, size and climate zone.

- **Extension of the retrofit decision**

  The platform only optimizes the retrofit plans that can save operation costs in a long term (e.g., 10-25 years) while minimizing the investment. However, it does not consider whether the building is worth retrofitting. This statement means the residual value of the building could be lower than the value of the land. In this case, sell, or demolition of the building might be better options than upgrading the building. To add this level of decision making, the platform requires to have a detail time-series database that records the real estate market fluctuations as well as implementing the depreciation method provided by IRS for residual value calculation (IRS, 2016).

- **Uncertainty analysis of the cost**

  There are many uncertainties in the building design, especially for design cost estimations. The capital costs could be affected by local price change, material price fluctuations, and relations between the clients and manufacturers. Also, the operation costs might be different if the interest rate and utility cost changes or the uncertainties embedded in the performance of building system operations. Moreover, most of the factors do not have a linear relation to the cost. A conventional optimization results analysis is a deterministic approach for decision making. This means the uncertainties in the cost estimation is not considered in this thesis. However, to enable the uncertainties analysis on the optimal results, there are two key components should be established in the future. 1) A database that specifies the knowledge of the uncertainties for each factor (e.g., uncertainties of the interest rate; uncertainties of the material price) 2) A methodology that can be implemented in the optimization process to analyze the uncertainties in the optimal design solutions such as the reliability-based optimization proposed in (Deb et al., 2009).

Appendices

Appendix A

EplusQTO, an EnergyPlus-based building system cost estimation framework

A.1 EplusQTO Framework development

EplusQTO is a newly developed tool for performing building energy model (BEM) based quantity take off (QTO). In BIM-based cost estimation, there are two processes identified in most studies (Wu et al., 2014). One is building element quantification extraction, and the other is quantity take off with a cost database. To perform a similar task with building energy model (BEM), the framework has defined six elements. It includes (1) Building system quantification extraction; (2) Building system design cost database; (3) BEM to cost database mapping system; (4) Cost estimation controller; (5) Operation costs calculation; (6) User interface. Figure A.1 depicts the developed framework of the BEM-based cost estimation system. In this system, the infrastructure is written in JAVA, and the cost database is created in a relational data schema, which is managed through the mySQL v6.0 system. In EplusQTO, EnergyPlus and its simulation results provide building system information for quantity calculation. Through the data mapping layer, these extracted building systems and their quantities are mapped to the cost database in the framework. The detail process and method have been described in Chapter 2. A user interface is provided to users to interact with the framework. Thus users could provide

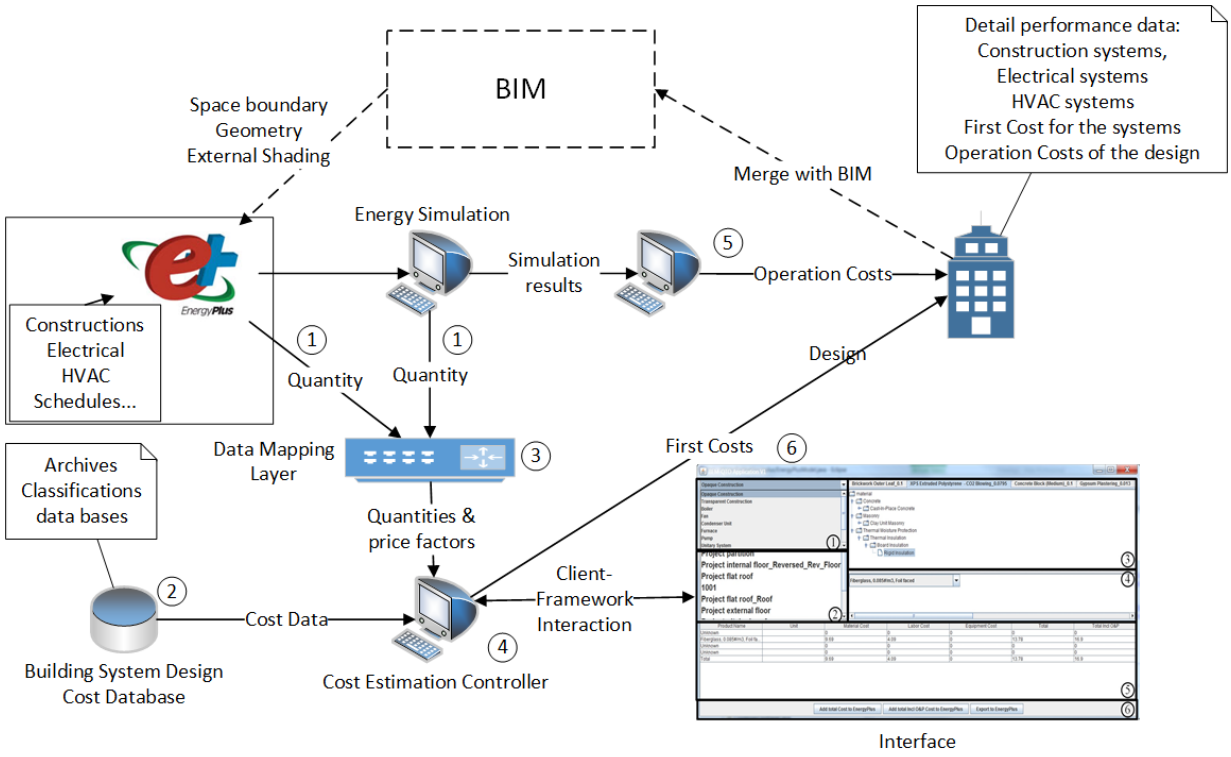

Figure A.1: The framework of BEM based cost estimation system

additional information to help the framework select the correct building system for cost estimation.

A.2 EplusQTO interface development

The user interface is developed to facilitate client-framework interaction. The interface is divided into two different types: (1) interface for building constructions cost estimation, (2) interface for building electrical and HVAC system cost estimation. Figure A.2 shows the graphic user interface for building constructions. In this interface, there are six main sections. Section 1 indicates different building system categories in this mapping framework. Section 2 shows objects found in a building energy model on the selected category. Section 3 displays the construction classification lists corresponding to a selected material layer under a construction object. Section 4 provides additional information for cost mapping. Section 5 shows the mapping results for each material layer and Section 6 offers user options to confirm the mapped

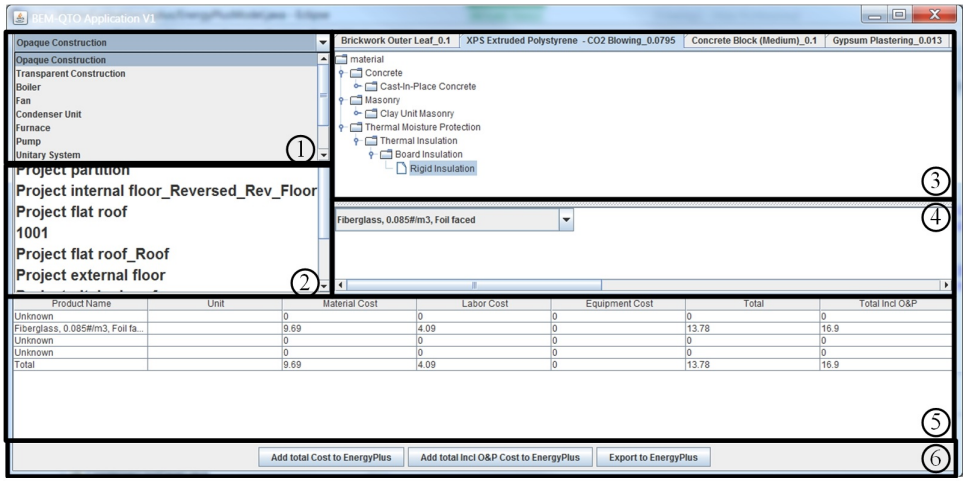

Figure A.2: GUI for building construction systems

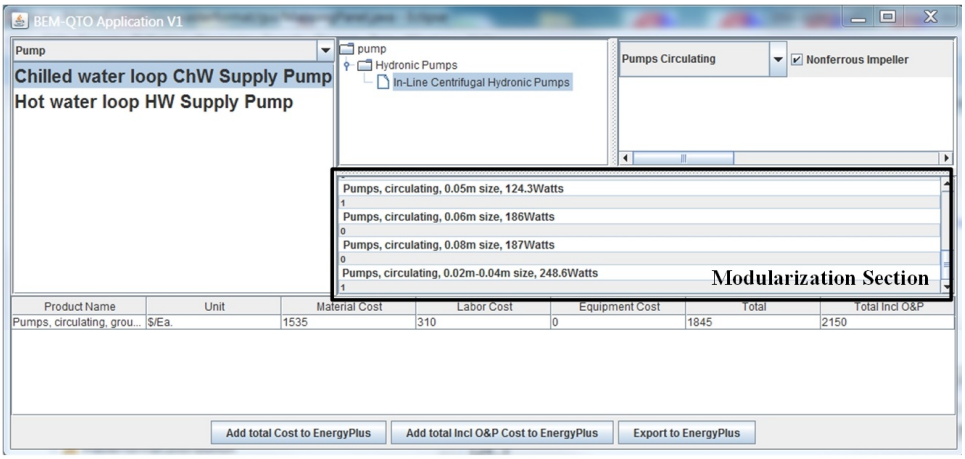

Figure A.3: GUI for HVAC and electrical systems

cost with the building system by exporting this cost to the EnergyPlus economic module.

The interface of electrical and HVAC systems is slightly different compared to the interface for construction system cost estimation. In Figure A.3, the most significant change of these two system's cost estimation interfaces is the modularization section. This section shows all available systems and indicates the quantity of each system needed to satisfy the requirements on the selected EnergyPlus object.

A.3 EplusQTO maintenance and replacement data

As illustrated in the Figure 2.2, the cost database in EplusQTO contains both capital and operation, maintenance and replacement cost data. The capital cost data in the database is collected from RSMeans construction data book (RSMeans, 2015). The operation costs are provided from various sources. Table A.1 lists all the collected OMR tasks and their cost information.

Table A.1: Building operation, maintenance and replacement database (dated on 05/10/2017)

OMR Task	Category	Year	Cost	Sources
Concrete patching	Maintenance	25	\$48/m^2	(RSMeans, 2015)
Masonry cleaning	Maintenance	50	\$82/m^2	
Metal cleaning	Maintenance	25	\$16/m^2	
Carpet cleaning	Maintenance	1	\$2.3/m^2	
Economizer	Maintenance	1	\$10/Ea.	(RSMeans, 2015; ASHRAE, 2015)
Terminal Unit	Maintenance	1	\$40/Ea.	
Air filters	Replacement	1	\$35/Ea.	
Fan motors	Replacement	10	\$416/Ea.	
Terminal Unit	Repair	10	\$15/Ea.	
Refrigerant	Replacement	10	\$81/Ea.	
Fan coil filters	Replacement	0.5	\$5/Ea.	
Fan coil	Maintenance	1	\$10/Ea.	
Fan coil motor	Replacement	10	\$140/Ea.	
Fluorescent	Replace T5	2.25	\$81/Ea.	(Scholand and Dillon, 2012)
Fluorescent	Replace T8	2.25	\$67/Ea.	
LED	Replacement	7	\$450/Ea.	

Appendix B

Building system database sources

The building system database is developed to carry the properties of various building systems for creating EnergyPlus energy models. Currently, the database has six types of passive building systems, three types of active building systems and one energy renewable system.

Table B.1: Building system database design variable list (dated on 05/10/2017)

Design Variables	Properties	Resources
Wall, roof, floor	Density (kg/m^3), Thickness (m), Conductivity (W/mK), Specific Heat (J/kgK)	(ASHRAE, 2010, 2016a; DOE, 2017)
Window	U-value (W/m^2K), SHGC and Vt	(LBNL, 2017)
Daylight shelf	Project length,	(Meresi, 2016; LBNL, 2016)
Lights	LPD (W/m^2)	(ASHRAE, 2016a; GE, 2016)
Daylight control	reference point illuminance setpoint	(LBNL, 2016)
HVAC	system type equipment properties	(ASHRAE, 2016a, 2010) and (Toshiba Carrier, 2016; Carrier, 2016)

Appendix C

ammNSGA-II algorithm performance validation and sensitivity analysis

C.1 Algorithm performance metrics

The performance of multi-objective optimization is measured by three attributes: (i) convergence, (ii) diversity preservation, and (iii) time. The first two attributes are assessed by comparing the optimal solution sets from an optimization study with a reference optimal set. A normalized convergence metric is used for evaluating the algorithm's convergence performance (Deb and Jain, 2002):

$$d_i = \min_{j=1}^{|P^*|} \sqrt{\sum_{k=1}^{M} \left(\frac{f_k(i) - f_k(j)}{f_k^{max} - f_k^{min}}\right)^2}. \qquad C(P^{(t)}) = \frac{\sum_{i=1}^{|F^t|} d_i}{|F^t|}. \tag{C.1}$$

In equation C.1, P^* is the reference optimal set and F is the generated optimal solution set, f_k^{max} and f_k^{min} are the maximum and the minimum function values of k^{th} objective function in P^* (Deb and Jain, 2002). $C(P^{(t)})$ is the convergence metric that averages the normalized distance d_i for all points in F^t. The normalized convergence metric is achieved in equation C.2:

$$\bar{C}(P^{(t)}) = \frac{C(P^{(t)})}{C(P^{(max)})} \tag{C.2}$$

This suggests that a smaller normalized convergence metric indicates a better convergence. Diversity preservation prevents the algorithm from having premature convergence as well as ensuring the diversity of design solutions in search spaces. The performance metric for evaluating the diversity of the optimal solution set is through a diversity metric Deb et al. (2002):

$$\Delta = \frac{d_f + d_l + \sum_{i=1}^{N-1} |d_i - \bar{d}|}{d_f + d_l + (N-1)\bar{d}} \tag{C.3}$$

In equation C.3, d_f and d_l are the euclidean distances between the extreme solutions and the boundary solutions of the obtained non-dominated set. $\bar{d}$ is the average of all distance $d_i = 1, 2...(N-1)$ Deb et al. (2002). A smaller diversity metric indicates a better diversity preservation.

Lastly, the speed performance is measured by the speed metric, which is the elapsed time for completing one optimization study.

C.1.1 Reference Pareto Front Curve

The P^* in Equation C.1 or the non-dominated set in Equation C.3 are both referring to the true global optimal solution set. However, the building system design problems are not only subject to the curse of dimensionality, but also slow to evaluate the fitness functions, it is impractical to generate a true global optimal solution set to validate the performance of proposed algorithm. However, as mentioned in Deb and Nain (2007), for multi-objective problems that are impractical to find the true global optimal solutions, a reference optimal curve can be extracted through repeat optimizations. In this thesis, in total 5 replicated optimizations are performed and a reference optimal curve, called reference Pareto Front, is defined according to the procedure described below:

1. Repeat the same optimization process for 5 times.
2. Combine the optimal solutions that are generated from the optimization processes.
3. Apply the NSGAII sorting algorithm to re-rank the optimal solutions
4. Extract the top design solutions to form the reference optimal curve.

C.2 Case study for demonstrating the algorithm performance

The performance of the ammNSGA-II has been demonstrated in a medium-size office building in Carnegie Mellon University campus, Pittsburgh, PA. It has four stories and a basement with more than 3700 m^2 of floor area. In total, 112 thermal zones were identified based on the location of air terminals in the provided computer-aided design (CAD) drawings. DesignBuilder v4.5 was used to create the building geometry. The geometry was then exported to EnergyPlus. Figure C.1 shows the actual building exterior view and its energy model in EnergyPlus. There

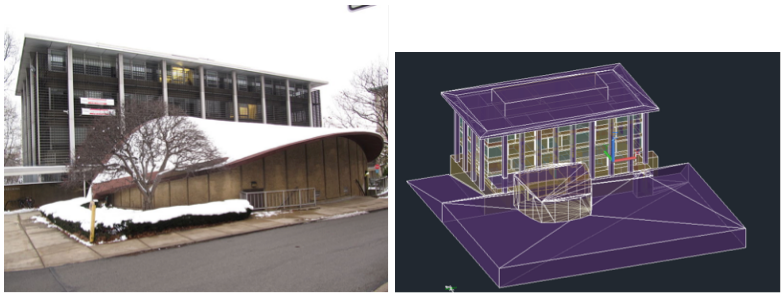

Figure C.1: Representation of Building in EnergyPlus

were six design parameters were selected, namely external wall, roof, window lighting fixture, daylight control and HVAC systems. In total, 71,820 possible design combinations and the task for ammNSGA-II was to found a group of optimal design solutions that minimize both capital cost and operation costs at the same time. A detail list of the design options under each design parameter can be found in (Xu et al., 2016a). Table C.1 shows the performance metrics comparison between the NSGA-II and ammNSGA-II. The results indicate that ammNSGA-II can achieve significant convergence improvement with 60% less time than NSGA-II algorithm. Although ammNSGA-II shows slight losses on solution diversity preservation, in the building system design field, design solutions' precision is more important than their diversity. This is because building owners could only view a limited number of design solutions instead of a whole range of solution set.

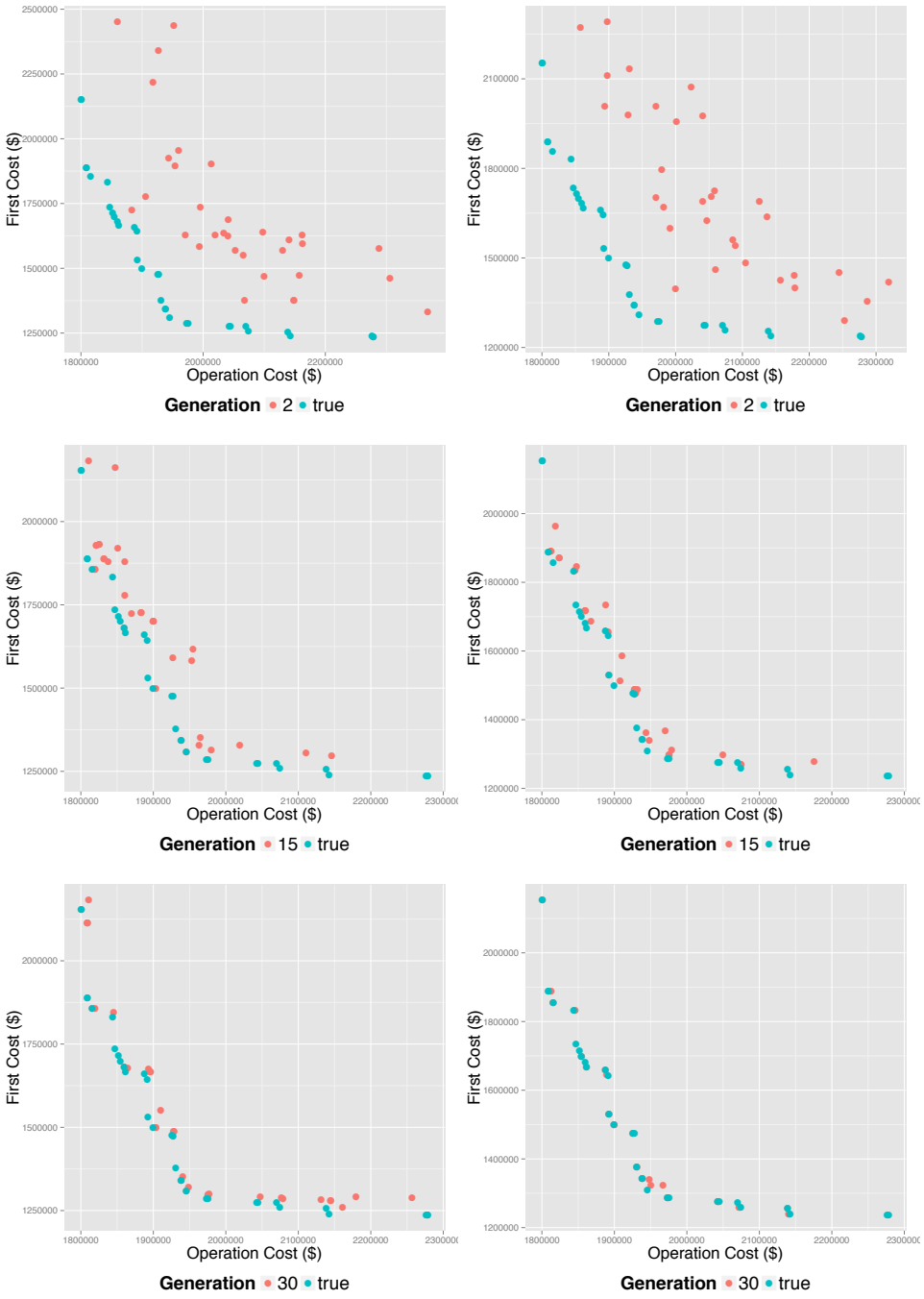

Figure C.2: Optimization comparison between NSGA-II and ammNSGA-II (left: NSGA-II; right: ammNSGA-II, adopted from (Xu et al., 2016a))

Table C.1: Performance comparison between NSGA-II and ammNSGA-II ((Xu et al., 2016a))

Model Name	Generation	Time (s)	Normalized Convergence Metric ($\bar{C}(P^{(t)})$)	Spread Metric (Δ)
NSGA-II	30	$82,924s$	0.025	0.410
ammNSGA-II	12	$32,070s$	0.001	1.022

Table C.2: Performance metrics comparison between the NSGA-II and different adaptive meta-model NSGA-II configurations

Model Name	Generation	Time (s)	Normalized Convergence Metric ($\bar{C}(P^{(t)})$)	Spread Metric (Δ)
NSGA-II	30	$82,924s$	0.025	0.410
B-3-20	12	$32,070s$	0.001	1.022
B-3-10	12	$32,008s$	0.019	1.158
B-4-20	16	$42,543s$	0.003	1.002
B-2-20	8	$20,432s$	0.099	0.810
I-3-20	12	$33,432s$	0.002	0.870

C.3 Hyper parameter sensitivity analysis

Figure 4.4 shows the overall procedure of adaptive meta-model evolutionary optimization. The critical parameters are n and Q which determine the size of the training dataset and the search power provided by the regression model. In integer type optimization, a small n may cause insufficient training data, which impacts the accuracy of the regression model. On the contrary, a large n will increase the time for optimization. Q affects the search power of the regression model because the proposed procedure expects regression models to improve their accuracy and precision after each cycle. A large Q will certainly mislead the search to an incorrect region, which could trap the optimal solutions in local optimal regions.

In (Xu et al., 2016a), 5 sets of n and Q were compared. The name of the tests was structured in a convention of "Type-n-G". Type included "I" and "B". "I" represented cumulative training data, where the database was built cumulatively after each cycle. "B" represented intermittent training data, where the database was rebuilt after each cycle. Each test performed three cycles in the optimization procedure. Table C.2 lists the performance metrics for these 5 tests. When comparing B-3-20, B-2-20 and B-4-20, it implies that a training dataset with less than 90

data points is insufficient for accurate prediction. B-2-20 has only 60 data points at each cycle, which means that it converges poorly at the third cycle. On the other hand, it can be concluded that $G = 20$ can provide enough search power to advance design solutions to the optimal region by comparing B-3-20 and B-3-10. I-3-20 indicates no obvious advantages on convergence performance; however, it can slightly improve the diversity of design solutions. All the test cases have similar spread metrics. The diversity preservation of these test cases is poorer than the conventional NSGA-II algorithm. This could be due to the regression model being confined to the search region at the later stage. Therefore, these results in a limited number of the available design solutions in the final optimal set. Thus, several duplicate design options appear in the optimal set, which increases the spread metric. Comparing the time, B-2-20 requires the least number of simulations; hence it performs the fastest. On the contrary, B-4-20 needs the most number of simulations, thus its demands twice as much as B-2-20. The other models have a similar time performance. However, I-3-20 shows a slightly higher time metric compared to the other two models. The observation suggests a longer time spent on training regression models with a cumulative database.

Appendix D

EBMA, a building energy baseline model automation system

D.1 System composition

The primary focus on designing a building energy baseline model automation (EBMA) system is to minimize user efforts in creating standard-compliant baseline models in design optimization problems. Since standards are being continuously updated to advance the architectural, engineering and construction (AEC) industry towards energy efficiency, the software architecture of EBMA is designed to be extensible and adaptable to various standards as well as future updates. The EBMA consists of four major components (Figure D.1):

- User input preparation module
- Standards building component database
- Energy model automation module
- Simulation outputs module

With these four modules, the EBMA could automatically generate baseline models, which comply with specified building standards, based on user's proposed energy model case.

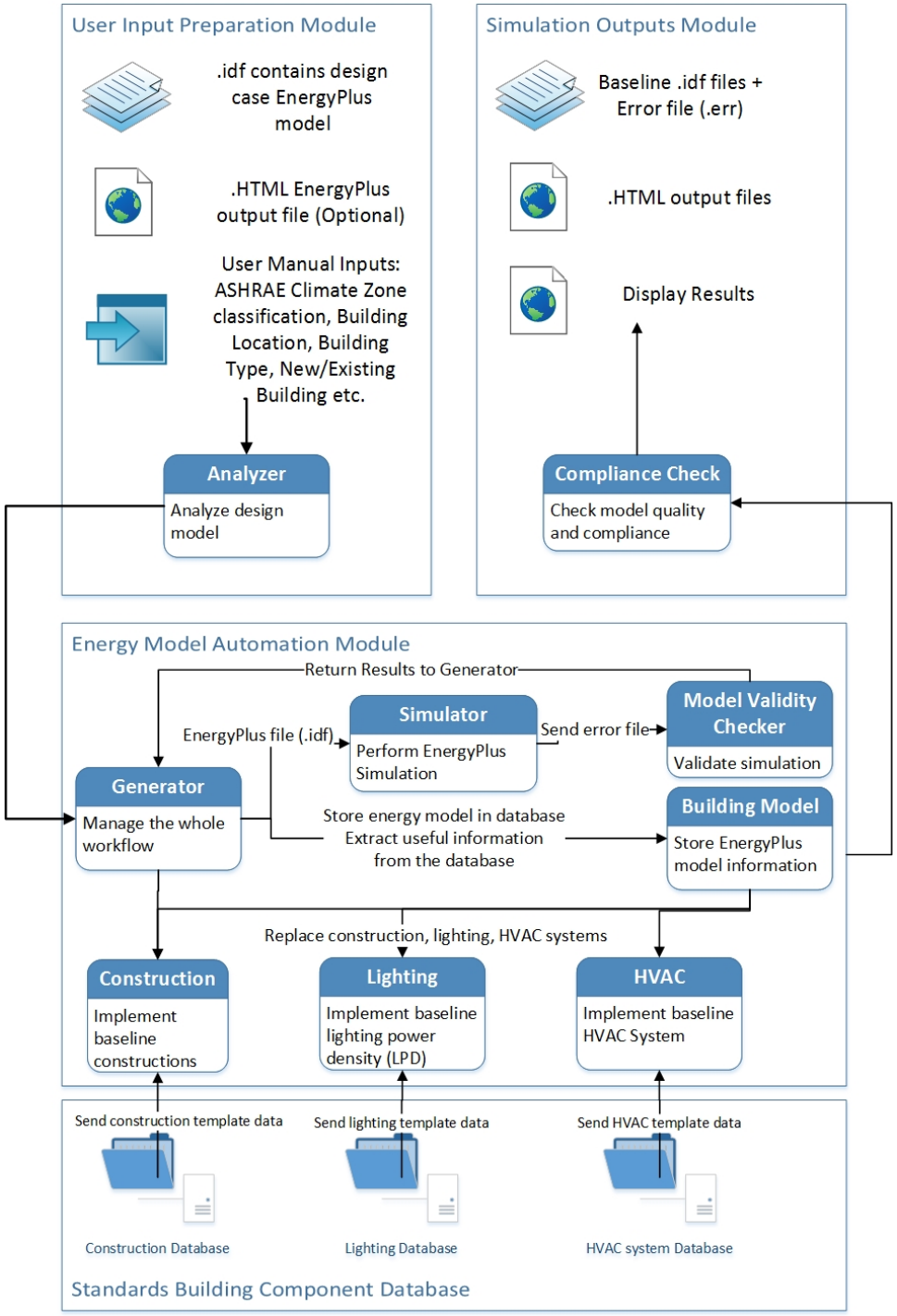

Figure D.1: EBMA System Components

D.2 User input preparation module

A critical goal of the EBMA is to reduce user modeling efforts by minimizing required inputs. One of the most crucial pieces of information is a structured building design energy model (i.e. the proposed design case model) in EnergyPlus format. The EBMA reads the layout of design energy model and extracts the building design information for baseline energy model generation. In addition to the baseline energy model, a simulation output file in HTML format is preferred but optional. Submitting the output file of design energy model can eliminate the necessity of design energy model evaluation, thus reducing the amount of execution time. In addition to the design energy model and its output file, the EBMA still requires users to specify a few more user manual input fields. Examples of such data include ASHRAE climate zone classification, building use type, lighting power density method and whether the building is a new or existing construction, etc. Although minimizing the number of input fields can reduce the amount of work, it is practically impossible to eliminate all the required information for generating baseline models. The is because some critical building information is missing in the design energy model as well as its result files.

Another important function of this module is to analyze and store building design information in an internal data structure through the "Analyzer" object (Figure D.1). The "Analyzer" object reads an EnergyPlus design energy model and then converts it into an internal data structure to facilitate search, sort, modification and export functions. Furthermore, based on the specifications in standard 90.1, this module will also check items that match any exceptions or rules set by standards. The results will be passed to the next module for baseline generation.

D.3 Standard 90.1 building component database

The Standard 90.1 building component database (hereinafter referred to as the component database) is created based on the specifications in Standard 90.1 in a specially designed extensive markup language (XML) schema. XML was originally developed by an XML Core Working Group with the goal of providing a human and machine readable format for easy and concise data

communication (Yergeau et al., 2004). Since the EBMA is built to couple with the EnergyPlus, which operates on text-based IO structure, XML becomes an ideal interoperable data format to consolidate the data linkage between the EBMA and EnergyPlus.

The component database is separated into construction, lighting, and HVAC system categories. Construction stores the complete building envelope assembly based on requirements and minimum performance in the Standard 90.1. Detailed information about construction assembly can be found in (ASHRAE, 2010) normative Appendix A and section 5. Lighting contains lighting power densities for both building types and space types. Depending on which lighting method is specified in the user input, EBMA extracts the corresponding information from this category. The HVAC system contains various system templates that match the Standard 90.1 requirements. However, creating an HVAC system involves not only generating system node linkage between the supply loop with hot water/chilled water/refrigerant side system, but also the node linkage inside the HVAC system as well as thermal zones. To overcome these challenges, the system data is stored in a format that is divided into an air supply loop, an air demand loop and a plant loop. The air supply and plant loop data can be used for internal connections. On the other hand, the air supply and air demand data can be used for loop-zone connections. The implementation of the connections will be further explained in section D.4.

All data are stored in this XML data schema, which is similar to that described in (Xu et al., 2016b). This XML data schema focuses on providing quick data conversion and manipulation from the construction, lighting, and HVAC performance data structure to the EnergyPlus .idf data structure. The quality attributes of the XML data schema include:

1. Adaptable to various systems' performance data
2. Extensible and easy to modify with EnergyPlus version upgrades.

The data schema can directly link to the EnergyPlus building system model based on two-layer logic processes. The first layer identifies building system category, building system and EnergyPlus version to extract the correspondent dataset in **dataset** element. The next step transfers data to correspondent EnergyPlus objects. The methods that are accessing, manipulating

and outputting XML in EBMA system is supported by JDOM 2.0.5 library (Hunter and Lear, 2015).

D.4 Energy modeling automation module

The energy modeling automation module focuses on envelope, lighting and HVAC system generation as well as analyzing and duplicating the equipment power load and operation schedules in the design energy model. In addition to the building systems, this module is also conducting EnergyPlus simulations. The two or three iterations that are required in this module depends on whether the user uploads the design model's output file in the user input preparation module. Besides the design energy model iteration, the other two are:

- HVAC system sizing (using design day data).
- Annual baseline model simulation (using annual hourly weather data).

In the baseline model sizing simulation, a baseline energy model is constructed with baseline envelope and lighting systems. Since the goal of this iteration is to determine HVAC system capacity, the ideal load system is built in the baseline model. After this iteration is complete, the baseline model's sizing results are passed to the next iteration for HVAC system generation. The second iteration performs after inserting constructed HVAC systems into the baseline model. A model validity checker checks whether the baseline model generation is successful based on the errors found in EnergyPlus error logs.

There are three engines are implemented in this module, namely the envelope engine, lighting engine and HVAC engine. The detail of these engines has been described in Chapter 5. One exception is the HVAC system for middle to high-rise residential building, which is not related to the thesis but included in the current release of EBMA.

D.5 Simulation outputs module

The simulation outputs in Figure D.1 consists of a compliance check process and three output data types. The compliance check process examines the baseline model's time-setpoint-not-

met during occupied hours based on Standard 90.1 requirements. If this value is higher than 300 hours for an annual simulation run (8760 total simulation hours), the baseline model would have to be re-tuned. The current retune techniques that are implemented in EBMA are increasing the sizing factor, the system capacity and minimum supply air flow rate of the problematic zones.

If the generated models pass the compliance check process, three types of outputs will be generated in the simulation outputs module.

- Baseline energy models in EnergyPlus data format and their error files.
- Design energy model simulation results in HTML format
- Generated baseline simulation results in JSON format for display on webpages.

The baseline energy models and results are useful for users to review the generated baseline model specifications and performance. These files can also be used in comparison with design cases for the LEED submission requirements for the points. The results sent in JSON format could be directly extracted from an EBMA API system. Therefore, application developers could request the information to acquire simulation results and display them in their application website.

D.6 System architecture

There are two major challenges in designing the EBMA system: (1) unpredictable data style of EnergyPlus files, and (2) the continuously Standard 90.1 update. The first challenge comes from the various EnergyPlus authoring tools. The EnergyPlus installation package includes the simulation engine and one authoring tool, called IDF Editor, which has limited functions. In the early 2000s, despite its advanced simulation concept and powerful algorithms, the software did not have a user-friendly interface, which restricted its application. In recent years, many EnergyPlus authoring tools have been developed to meet the industry needs. Tools such as DesignBuilder DesignBuilder (2016) and the asset score tool of Energy (2016) provide not only graphic drawing capability but also a user-friendly interface. However, different authoring tools

exports data in different styles. For example, DesignBuilder uses a colon (:) to separate block name from zone name while the asset score tool uses an underscore (_). It is impossible to have a generalized translator to accommodate every EnergyPlus authoring tool. Secondly, the Standard 90.1 is currently under a three-year update cycle. Additionally, different states may adopt a different version of the Standard 90.1. It implies that the EBMA system should generate baseline energy models according to a selected standard version. Therefore, the attributes of the EBMA system architecture are set to be adaptable and extensible.

Figure D.2 shows the object model of the EBMA system in unified modeling language (UML). A generator class is defined to control the workflow of the EBMA system. This class carries all the other classes including the EnergyPlusModel, which is the core data structure for the system, the RunSimulation that runs EnergyPlus simulations, version controller, construction, lighting and HVAC classes. The adaptable attribute is achieved through the thermal zone adaptor interface. This interface is designed to accommodate the dissimilar thermal zone conventions in the EnergyPlus authoring tools, where, different analysis strategies should be applied for data processing. The implementation of strategy is programmed in different classes that inherit this interface. This architecture proves that the EBMA system is adaptable to various EnergyPlus authoring tools.

Furthermore, EBMA should not only handle various EnergyPlus authoring tools, but also capable of future changes in EnergyPlus versions, HVAC specifications and exceptions in standards. Therefore, extensibility is a crucial attribute for the system. This attribute is achieved through both the version controller, the HVACSystem interface and exception observers. The version controller recorded both the standard version and EnergyPlus version, which extends the EBMA system baseline generation ability to multiple versions of the Standard 90.1. The HVAC system needs a special design architecture other than a simple version controller. Therefore, a HVACSystem interface is designed to accomplish this work. The core concept of HVAC system architecture is the use of a decorator pattern, where each additional feature, such as district heating system or return fan, are decorators to the original system. This process starts with

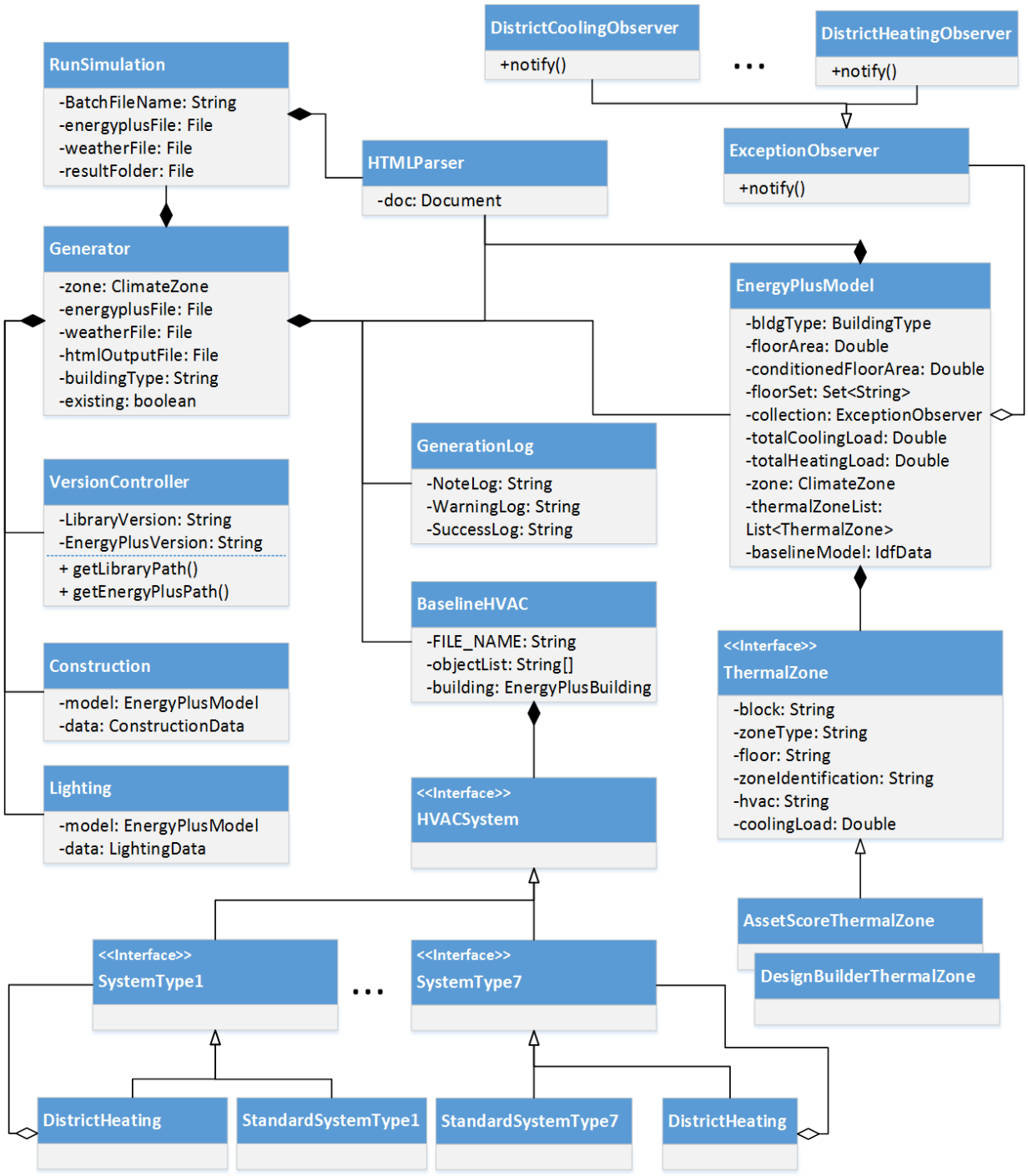

Figure D.2: EBMA system object model

a standard HVAC system. Afterwards, the EBMA fact checks the rules and exceptions based on the HVAC system in the design energy model. Any modifications will be added to the standard HVAC system as "decorators". One benefit of this system architecture is the extensibility. Additional features can be easily added anytime as new "decorators" without interrupting the integrity of the core engine. For changes in rules and exceptions from standards, an observer design pattern is implemented in Figure D.2. Exception observers can be registered in the initialization process. The registered observers (i.e. district cooling observer or district heating observer) listen to the data in the "EnergyPlusModel". Once the processed data match the exception criteria, the observers will notify the system and execute changes in the baseline model. With this software design, customized observers can be added in the future by inheriting the "ExceptionObserver" interface.

D.7 System deployment and test

The system is currently deployed on CMU server and is undergoing with private beta test. Figure D.3 shows the user interface of the system. Currently, there are only two inputs required from user: (1) EnergyPlus model, (2) ASHRAE climate zone. Once the user successfully uploaded their file, they can start the generation by click "Submit" button. Once the simulation is completed, the user can download the generated baseline models and view some of the outputs on the following table. This system can be accessed via the link: `http://128.2.108.198/Optimization/pages/baselineauto.html`.

D.8 EMBA application

This is an on-going work that focuses on developing a commercial ready energy model baseline automation (EMBA) system that can automatically generate a ASHRAE 90.1 compliant baseline energy model in EnergyPlus format. The system is detailed in Appendix D. The system is currently deployed in `http://128.2.108.198/Optimization/pages/baselineauto.html`.

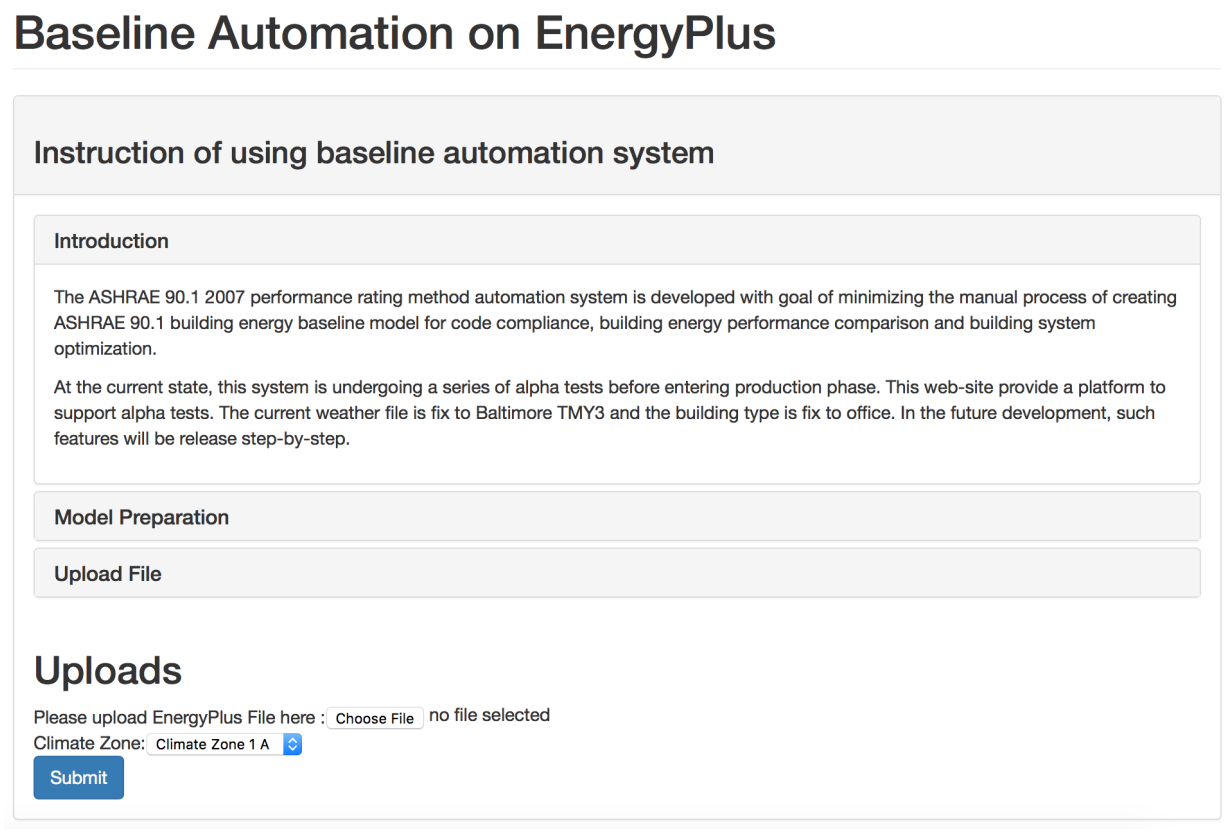

Figure D.3: Baseline automation system interface

Appendix E

CSL Case Study Results

E.1 Pareto Front curve

Table E.1, E.2, E.3 and E.4 list the optimization results generated from CSL case study.

Table E.1: List of the design solutions on the Pareto Front Curve (Part-1)

Solution Index	Insulation Level	WWR	HVAC	Lights	BiPV	LightShelf
1 Operation: $44.3k Capital: $1,991k PP: 75 year	Wall: R-6.5 Roof: R-5.3 Window: DTC	South: 80 North: 40 East: 70 West: 40	GEOPUMP	LED **Daylit Sensor:** On	South: Yes North: Yes East: Yes West: Yes	Inside: 0.86m Outside: N/A
2 Operation: $44.6k Capital: $1,845k PP: 65 year	Wall: R-3.8 Roof: R-5.3 Window: DTC	South: 40 North: 40 East: 40 West: 80	GEOPUMP	LED **Daylit Sensor:** On	South: Yes North: Yes East: Yes West: Yes	Inside: N/A Outside: 1.3m
3 Operation: $44.8k Capital: $1,624k PP: 51 year	Wall: R-6.5 Roof: R-5.3 Window: HRC	South: 40 North: 40 East: 70 West: 40	GEOPUMP	LED **Daylit Sensor:** On	South: Yes North: Yes East: Yes West: Yes	Inside: N/A Outside: N/A
4 Operation: $45.3k Capital: $1,590k PP: 49 year	Wall: R-6.5 Roof: R-4.9 Window: DTC	South: 40 North: 40 East: 50 West: 50	GEOPUMP	LED **Daylit Sensor:** On	South: Yes North: Yes East: Yes West: Yes	Inside: N/A Outside: N/A
5 Operation: $48.6k Capital: $1,544k PP: 46 year	Wall: R-2.1 Roof: R-5.3 Window: TG	South: 40 North: 40 East: 50 West: 60	GEOPUMP	LED **Daylit Sensor:** On	South: Yes North: Yes East: Yes West: Yes	Inside: N/A Outside: N/A

Table E.2: List of the design solutions on the Pareto Front Curve (Part-2)

Solution Index	Insulation Level	WWR	HVAC	Lights	BiPV	LightShelf
6	Wall: R-2.1	South: 40	GEOPUMP	LED	South: Yes	Inside:
Operation: $51.2k	Roof: R-3.1	North: 40		**Daylit Sensor:**	North: Yes	N/A
Capital: $1,493k	Window:	East: 40		On	East: Yes	Outside:
PP: 44 year	TG	West: 40			West: Yes	0.64m
7	Wall: R-6.5	South: 40	GEOPUMP	LED	South: Yes	Inside:
Operation: $63.9k	Roof: R-5.3	North: 60		**Daylit Sensor:**	North: No	0.88m
Capital: $1,429k	Window:	East: 70		On	East: Yes	Outside:
PP: 42 year	DTC	West: 40			West: Yes	N/A
8	Wall: R-2.1	South: 50	GEOPUMP	LED	South: Yes	Inside:
Operation: $66.4k	Roof: R-4.9	North: 40		**Daylit Sensor:**	North: No	N/A
Capital: $1,371k	Window:	East: 70		On	East: Yes	Outside:
PP: 39 year	DTC	West: 40			West: Yes	N/A
9	Wall: R-2.6	South: 40	GEOPUMP	LED	South: Yes	Inside:
Operation: $69.5k	Roof: R-3.1	North: 60		**Daylit Sensor:**	North: No	N/A
Capital: $1,365k	Window:	East: 40		On	East: Yes	Outside:
PP: 38 year	DTC	West: 50			West: Yes	N/A
10	Wall: R-2.1	South: 40	GEOPUMP	LED	South: Yes	Inside:
Operation: $69.8k	Roof: R-4.9	North: 40		**Daylit Sensor:**	North: No	N/A
Capital: $1,308k	Window:	East: 60		On	East: Yes	Outside:
PP: 34 year	TG	West: 40			West: Yes	0.64m
11	Wall: R-2.1	South: 40	GEOPUMP	LED	South: Yes	Inside:
Operation: $80.1k	Roof: R-4.9	North: 50		**Daylit Sensor:**	North: No	N/A
Capital: $1,257k	Window:	East: 40		On	East: No	Outside:
PP: 32 year	DTC	West: 50			West: Yes	N/A
12	Wall: R-2.1	South: 40	GEOPUMP	LED	South: Yes	Inside:
Operation: $86.3k	Roof: R-3.1	North: 40		**Daylit Sensor:**	North: No	N/A
Capital: $1,215k	Window:	East: 50		On	East: No	Outside:
PP: 30 year	TG	West: 40			West: Yes	1.5m
13	Wall: R-2.6	South: 40	GEOPUMP	LED	South: Yes	Inside:
Operation: $99.9k	Roof: R-3.1	North: 40		**Daylit Sensor:**	North: No	N/A
Capital: $1,177k	Window:	East: 50		On	East: No	Outside:
PP: 29 year	DTC	West: 40			West: No	N/A
14	Wall: R-2.1	South: 40	GEOPUMP	LED	South: Yes	Inside:
Operation: $103.0k	Roof: R-3.1	North: 60		**Daylit Sensor:**	North: No	N/A
Capital: $1,154k	Window:	East: 40		On	East: No	Outside:
PP: 28 year	TG	West: 80			West: No	N/A
15	Wall: R-2.1	South: 40	GEOPUMP	LED	South: Yes	Inside:
Operation: $103.6k	Roof: R-3.1	North: 40		**Daylit Sensor:**	North: No	N/A
Capital: $1,127k	Window:	East: 50		On	East: No	Outside:
PP: 25 year	TG	West: 40			West: No	1.5m

Table E.3: List of the design solutions on the Pareto Front Curve (Part-3)

Solution Index	Insulation Level	WWR	HVAC	Lights	BiPV	LightShelf
16	Wall: R-1.5	South: 40	GEOPUMP	LED	South: No	Inside:
Operation: $138.0k	Roof: R-2.2	North: 40		**Daylit Sensor:**	North: No	N/A
Capital: $1,064k	Window:	East: 50		On	East: Yes	Outside:
PP: 25 year	TG	West: 40			West: Yes	0.56m
17	Wall: R-2.6	South: 40	GEOPUMP	LED	South: No	Inside:
Operation: $146.4k	Roof: R-4.9	North: 40		**Daylit Sensor:**	North: No	N/A
Capital: $1,033k	Window:	East: 50		On	East: No	Outside:
PP: 23 year	DTC	West: 60			West: Yes	N/A
18	Wall: R-2.1	South: 40	GEOPUMP	LED	South: No	Inside:
Operation: $147.6k	Roof: R-4.9	North: 40		**Daylit Sensor:**	North: No	N/A
Capital: $960.7k	Window:	East: 50		On	East: No	Outside:
PP: 15 year	TG	West: 40			West: Yes	1.5m
19	Wall: R-2.1	South: 50	GEOPUMP	LED	South: No	Inside:
Operation: $164.3k	Roof: R-5.3	North: 40		**Daylit Sensor:**	North: No	N/A
Capital: $916.3k	Window:	East: 50		On	East: No	Outside:
PP: 11 year	TG	West: 40			West: No	1.45m
20	Wall: R-2.1	South: 40	GEOPUMP	T5	South: No	Inside:
Operation: $177.3k	Roof: R-4.9	North: 50		**Daylit Sensor:**	North: No	N/A
Capital: $882.6k	Window:	East: 40		On	East: No	Outside:
PP: 8.4 year	TG	West: 80			West: No	N/A
21	Wall: R-2.1	South: 40	GEOPUMP	T5	South: No	Inside:
Operation: $178.0k	Roof: R-3.1	North: 60		**Daylit Sensor:**	North: No	N/A
Capital: $869.5k	Window:	East: 40		On	East: No	Outside:
PP: 6.6 year	TG	West: 40			West: No	1.46m
22	Wall: R-2.1	South: 50	DOASVRF	LED	South: No	Inside:
Operation: $209.5k	Roof: R-5.3	North: 40		**Daylit Sensor:**	North: No	0.80m
Capital: $868.6k	Window:	East: 50		On	East: Yes	Outside:
PP: 9.1 year	TG	West: 40			West: Yes	0.61m
23	Wall: R-2.6	South: 80	DOASVRF	LED	South: No	Inside:
Operation: $213.6k	Roof: R-5.3	North: 60		**Daylit Sensor:**	North: No	0.98m
Capital: $856.0k	Window:	East: 40		On	East: No	Outside:
PP: 6.9 year	DTC	West: 40			West: Yes	N/A
24	Wall: R-2.1	South: 40	DOASVRF	LED	South: No	Inside:
Operation: $216.6k	Roof: R-2.2	North: 40		**Daylit Sensor:**	North: No	N/A
Capital: $854.7k	Window:	East: 50		On	East: Yes	Outside:
PP: 6.9 year	DTC	West: 50			West: Yes	1.40m
25	Wall: R-2.6	South: 40	DOASVRF	LED	South: No	Inside:
Operation: $217.1k	Roof: R-4.9	North: 40		**Daylit Sensor:**	North: No	N/A
Capital: $780.0k	Window:	East: 60		On	East: No	Outside:
PP: N/A	DTC	West: 40			West: Yes	N/A

Table E.4: List of the design solutions on the Pareto Front Curve (Part-4)

Solution Index	Insulation Level	WWR	HVAC	Lights	BiPV	LightShelf
26	Wall: R-2.1	South: 40	DOASVRF	LED	South: No	Inside:
Operation: $226.4k	Roof: R-3.1	North: 40		**Daylit Sensor:**	North: No	0.5m
Capital: $730.6k	Window:	East: 50		On	East: No	Outside:
PP: N/A	DTC	West: 40			West: Yes	0.5m
27	Wall: R-2.1	South: 50	DOASVRF	LED	South: No	Inside:
Operation: $234.4k	Roof: R-4.9	North: 40		**Daylit Sensor:**	North: No	N/A
Capital: $679.7k	Window:	East: 50		On	East: No	Outside:
PP: N/A	TG	West: 40			West: No	1.5m
28	Wall: R-2.6	South: 40	DOASVRF	LED	South: No	Inside:
Operation: $241.4k	Roof: R-4.9	North: 40		**Daylit Sensor:**	North: No	N/A
Capital: $657.2k	Window:	East: 40		On	East: No	Outside:
PP: N/A	TG	West: 40			West: No	N/A
29	Wall: R-2.1	South: 40	DOASVRF	LED	South: No	Inside:
Operation: $245.3k	Roof: R-3.1	North: 50		**Daylit Sensor:**	North: No	N/A
Capital: $640.5k	Window:	East: 40		On	East: Yes	Outside:
PP: N/A	TG	West: 40			West: No	N/A
30	Wall: R-1.5	South: 40	DOASVRF	T8	South: No	Inside:
Operation: $270.3k	Roof: R-3.1	North: 40		**Daylit Sensor:**	North: No	N/A
Capital: $627.2k	Window:	East: 40		On	East: No	Outside:
PP: N/A	TG	West: 60			West: No	0.56m

"PP" represents the payback period. It is calculated using Equation E.1. The $I_i - I_b$ indicates the additional capital cost over the baseline design and the $O_b - O_i$ calculates the annual operation cost savings generated with the proposed design. A design solution with N/A of "PP" represents it has lower operation costs and capital cost. This implies that the design have an instant payback compare to the ASHRAE baseline design.

$$PP = \frac{I_i - I_b}{O_b - O_i} \tag{E.1}$$

Where,

I_i is the capital cost of a design solution,

I_b is the capital cost of the ASHRAE baseline design,

O_b is the operation cost of the ASHRAE baseline design,

O_i is the operation cost of the design solution.

E.2 LCC model sensitivity analysis results

Table E.5: Net present value of total life cycle cost for time period of 25 years ($1k)

Solution Index	R=1%	R=3%	R=5%	R=7%	R=9%	R=11%	R=13%	R=15%	R=17%
1	2047.27	2035.6	2027.1	2020.9	2016.3	2012.7	2009.9	2007.7	2005.9
2	1901.6	1889.8	1881.3	1875.0	1870.3	1866.7	1863.9	1861.7	1859.9
3	1681.0	1669.1	1660.6	1654.3	1649.6	1643.209	1640.9	1639.2	1637.7
4	1607.1	1595.1	1586.4	1580.1	1575.3	1571.7	1568.8	1566.6	1564.8
5	1605.2	1592.3	1576.2	1571.1	1567.2	1564.2	1561.7	1559.8	1558.2
6	1557.5	1544.0	1534.2	1527.0	1521.6	1517.5	1514.3	1511.8	1509.7
7	1510.0	1493.1	1480.9	1471.9	1465.3	1460.1	1456.1	1452.9	1450.4
8	1455.2	1437.6	1424.9	1415.7	1408.7	1403.3	1399.2	1395.9	1393.2
9	1453.3	1434.9	1421.6	1411.9	1404.6	1399.0	1394.6	1391.2	1388.4
10	1396.1	1377.6	1364.3	1354.5	1347.2	1341.5	1337.2	1333.7	1330.9
11	1358.2	1337.0	1321.8	1310.5	1302.1	1295.7	1290.6	1286.7	1283.5
12	1324.2	1301.4	1285.0	1272.9	1263.8	1256.8	1290.6	1286.7	1243.7
13	1303.0	1276.5	1257.5	1243.5	1233.0	1224.9	1218.7	1213.7	1209.7
14	1284.3	1257.1	1237.4	1223.0	1212.2	1204.0	1197.5	1192.4	1188.3
15	1257.6	1230.2	1210.4	1195.9	1185.0	1176.7	1170.2	1165.0	1160.9
16	1238.3	1201.8	1175.5	1156.2	1141.7	1130.6	1121.9	1115.1	1109.5
17	1218.5	1179.7	1151.9	1131.4	1116.0	1104.2	1095.0	1087.7	1081.9
18	1147.5	1108.4	1080.2	1059.6	1044.0	1032.1	1022.9	1015.6	1009.6
19	1124.1	1080.6	1049.3	1026.3	1009.0	995.8	985.5	977.3	970.7
20	1106.8	1059.9	1026.1	1001.2	982.6	968.3	957.2	948.4	941.3
21	1094.6	1047.5	1013.6	988.6	969.9	955.6	944.4	935.6	928.4
22	1133.6	1078.1	1038.2	1008.8	986.8	969.9	956.8	946.4	938.0
23	1126.1	1069.6	1028.8	998.9	976.4	959.3	945.9	935.3	926.7
24	1128.6	1071.3	1029.9	999.6	976.9	959.4	945.8	935.1	926.4
25	1054.6	997.1	955.7	925.3	902.4	884.9	871.3	860.5	851.8
26	1016.9	957.0	913.9	882.2	858.4	840.1	825.9	814.6	805.6
27	976.1	914.1	869.4	836.5	811.9	793.0	778.3	766.7	757.3
28	962.4	898.5	852.5	818.6	793.3	773.9	758.7	746.8	737.1
29	950.8	885.8	839.0	804.6	778.9	759.1	743.7	731.5	721.7
30	969.1	897.5	846.0	808.1	779.7	757.9	741.0	727.6	716.7

Appendix F

One Montgomery Plaza Case Study Results

F.1 Pareto Front curve

Table F.1, F.2 and F.3 list the optimization results generated from One Montgomery Plaza case study.

Table F.1: List of the design solutions on the Pareto Front Curve (Part-1)

Solution Index	Insulation Level	Window	Lights	Heat	Cool	PV
1 Operation: $7.50M Capital: $4.24M	Wall: R-5.3 Window:Q	LED **Daylit Sensor:** On	New	New	South:Yes East: Yes West: No	39 year
2 Operation: $7.51M Capital: $3.35M	Wall: R-5.3 Window:Q	LED **Daylit Sensor:** On	New	New	South: Yes East: No West: No	30 year
3 Operation: $7.53M Capital: $3.15M	Wall: R-5.3 Window:TG	LED **Daylit Sensor:** On	New	New	South:No East: Yes West: No	29 year
4 Operation: $7.53M Capital: $3.17M	Wall: R-5.3 Window:TG	LED **Daylit Sensor:** On	New	New	South:No East: No West: Yes	20 year
5 Operation: $7.53M Capital: $2.25M	Wall: R-5.3 Window:TG	LED **Daylit Sensor:** On	New	New	South:No East: No West: No	20 year

Table F.2: List of the design solutions on the Pareto Front Curve (Part-2)

Solution Index	Insulation Level	Lights	Heat	Cool	PV	PP
6	Wall: R-5.3	LED	New	New	South:No	20 year
Operation: $7.59M	Window:TG	**Daylit Sensor:**			East: No	
Capital: $2.18M		Off			West: No	
7	Wall: R-3.3	LED	New	New	South:No	20 year
Operation: $7.60M	Window:TG	**Daylit Sensor:**			East: No	
Capital: $2.17M		Off			West: No	
8	Wall: R-5.3	LED	New	New	South:No	18 year
Operation: $7.67M	Window:DTC	**Daylit Sensor:**			East: No	
Capital: $1.90M		On			West: Yes	
9	Wall: R-3.3	LED	New	New	South:No	18 year
Operation: $7.69M	Window:DTC	**Daylit Sensor:**			East: No	
Capital: $1.89M		On			West: No	
10	Wall: R-5.3	LED	New	New	South:No	18 year
Operation: $7.72M	Window:DTC	**Daylit Sensor:**			East: No	
Capital: $1.83M		Off			West: Yes	
11	Wall: R-3.3	LED	New	New	South:No	18 year
Operation: $7.74M	Window:DTC	**Daylit Sensor:**			East: No	
Capital: $1.82M		Off			West: Yes	
12	Wall: R-5.3	T5	New	New	South:No	16 year
Operation: $7.89M	Window:DTC	**Daylit Sensor:**			East: No	
Capital: $1.52M		On			West: No	
13	Wall: R-3.3	No	New	New	South: No	16 year
Operation: $7.92M	Window:DTC	**Daylit Sensor:**			East: No	
Capital: $1.49M		On			West: No	
14	Wall: R-5.3	LED	New	New	South: No	7.7 year
Operation: $7.92M	Window:No	**Daylit Sensor:**			East: No	
Capital: $0.87M		On			West: No	
15	Wall: R-3.3	LED	New	New	South:No	6.9 year
Operation: $7.98M	Window:No	**Daylit Sensor:**			East: No	
Capital: $0.80M		Off			West: No	
16	Wall: R-5.3	T5	New	New	South:No	3.0 year
Operation: $8.15M	Window:No	**Daylit Sensor:**			East: No	
Capital: $0.50M		On			West: No	
17	Wall: R-3.3	No	New	New	South:No	1.4 year
Operation: $8.24M	Window:No	**Daylit Sensor:**			East: No	
Capital: $0.40M		On			West: No	
18	Wall: R-5.3	T5	No	New	South:No	1.1 year
Operation: $8.42M	Window:No	**Daylit Sensor:**			East: No	
Capital: $0.37M		On			West: No	
19	Wall: R-3.3	T5	No	New	South:No	N/A
Operation: $8.50M	Window:No	**Daylit Sensor:**			East: No	
Capital: $0.30M		Off			West: No	

Table F.3: List of the design solutions on the Pareto Front Curve (Part-3)

Solution Index	Insulation Level	Window	Lights	Heat	Cool	PV
20 Operation: $8.52M Capital: $0.27M	Wall: R-3.3 Window:No	No **Daylit Sensor:** Off	No	New	South:No East: No West: Yes	N/A
21 Operation: $8.76M Capital: $0.25M	Wall:No Window:No	No **Daylit Sensor:** Off	No	New	South:No East: No West: No	N/A
22 Operation: $8.86M Capital: $0.23M	Wall: R-5.3 Window:No	No **Daylit Sensor:** On	New	No	South:No East: No West: Yes	N/A
23 Operation: $8.94M Capital: $0.15M	Wall: R-3.3 Window:No	No **Daylit Sensor:** Off	New	No	South:No East: No West: Yes	N/A
24 Operation: $9.12M Capital: $0.12M	Wall: R-5.3 Window:No	T5 **Daylit Sensor:** On	No	No	South:No East: No West: No	Not Applicable
25 Operation: $9.21M Capital: $0.02M	Wall: R-3.3 Window:No	No **Daylit Sensor:** Off	No	No	South:No East: No West: Yes	Not Applicable
26 Operation: $9.48M Capital: $0.00M	Wall:No Window:No	No **Daylit Sensor:** Off	No	No	South:No East: No West: No	Not Applicable

The "PP" in Table F.1, F.2 and F.3 represents payback period. It is calculated in Equation E.1. Similarly, the "N/A" of "PP" implies that the design solution has a lower capital cost and operation costs. In addition, Table F.3 also has "Not Applicable". This value indicates that a design solution requires less capital cost than the ASHRAE baseline design. However, it generates higher annual operation costs. Therefore, there is no savings in the operation phase.

F.2 LCC model sensitivity analysis results

Table F.4: Net present value of total life cycle cost for time period of 25 years ($1 million)

Solution Index	R=1%	R=3%	R=5%	R=7%	R=9%	R=11%	R=13%	R=15%	R=17%
1	13.74	11.75	10.32	9.27	8.48	7.88	7.41	7.03	6.73
2	12.86	10.87	9.43	8.38	7.59	6.98	6.51	6.14	5.84
3	12.68	10.69	9.25	8.20	7.40	6.80	6.32	5.95	5.65
4	12.70	10.70	9.27	8.21	7.42	6.82	6.34	5.97	5.67
5	11.78	9.79	8.35	7.29	6.50	5.90	5.42	5.05	4.75
6	11.79	9.78	8.33	7.27	6.47	5.86	5.38	5.01	4.70
7	11.80	9.78	8.33	7.27	6.47	5.86	5.38	5.00	4.70
8	11.60	9.57	8.11	7.03	6.23	5.61	5.13	4.75	4.44
9	11.62	9.58	8.11	7.04	6.23	5.61	5.13	4.75	4.44
10	11.60	9.56	8.09	7.00	6.19	5.57	5.09	4.70	4.40
11	11.62	9.57	8.09	7.01	6.19	5.57	5.08	4.70	4.39
12	11.50	9.41	7.91	6.80	5.98	5.34	4.85	4.45	4.14
13	11.51	9.42	7.91	6.79	5.96	5.32	4.83	4.43	4.11
14	10.90	8.80	7.29	6.18	5.35	4.71	4.21	3.82	3.50
15	10.89	8.78	7.26	6.14	5.30	4.66	4.16	3.76	3.44
16	10.80	8.65	7.10	5.95	5.10	4.44	3.93	3.53	3.20
17	10.82	8.64	7.07	5.92	5.05	4.39	3.87	3.46	3.13
18	11.03	8.80	7.19	6.01	5.12	4.45	3.92	3.50	3.16
19	11.04	8.80	7.17	5.98	5.09	4.40	3.87	3.45	3.11
20	11.04	8.79	7.16	5.97	5.07	4.39	3.86	3.43	3.09
21	11.32	9.01	7.34	6.11	5.19	4.48	3.94	3.50	3.15
22	11.43	9.09	7.40	6.16	5.22	4.51	3.96	3.52	3.16
23	11.46	9.09	7.39	6.14	5.20	4.48	3.92	3.47	3.11
24	11.66	9.25	7.51	6.23	5.27	4.54	3.96	3.51	3.14
25	11.68	9.24	7.48	6.19	5.22	4.48	3.90	3.44	3.07
26	11.99	9.48	7.67	6.35	5.35	4.59	3.99	3.52	3.14

Appendix G

Step-by-step instruction

G.1 Required third-party applications

In order to use the platform, user need to download a few essential tools.

- DesignBuilder version 4.7 and above. This software is recommended for creating an EnergyPlus model. It can be downloaded in `https://www.designbuilder.co.uk/download/software/release-software`. However, this software has only 30 days free trial.
- An alternative to DesignBuilder v4.7 is the OpenStudio and SketchUp. OpenStudio is a free EnergyPlus model design tool, and SketchUp is free for education and research usage. OpenStudio can be downloaded in: `https://www.openstudio.net/downloads` and SketchUp is available in `https://www.sketchup.com`.
- EnergyPlus version 8.0 and above, this software can be downloaded in `https://energyplus.net`. It is free, and there are a lot supporting documents and forums on their website.
- MySQL Community package. This package is commonly used for running SQL server in the local or distributed systems. It is open source and can be downloaded in `https://dev.mysql.com/downloads/`. It is recommended to include MySQL Workbench in the installation.

- JAVA8, JAVA is the programming language used to build the optimization platform. The user must download and install the JAVA SE Development version via this link `http://www.oracle.com/technetwork/java/javase/downloads/jdk8-downloads-21331 html`.
- Eclipse is an open source development platform. It offers strong supports on JAVA and web development. This software can be downloaded through `https://www.eclipse.org/downloads/`.

G.2 System setup

G.2.1 Database setup

First, install all the downloaded software tools and correctly configure them according to the documentations. A recommended installation order is: (1) EnergyPlus, (2) JAVA, (3) DesignBuilder v4.7 or OpenStudio and SketchUp, (4) MySQL community package and last, the Eclipse software.

All data required in this platform is exported and packaged in a single file "migrate.sql". The user should first launch the MySQL Workbench to import this file. The detail importing process is described in the list below.

- Select a server instance you want to import to under the **Server Adminstration**.
- Click on **Manage Import/Export** button
- Click on **Data Import/Restore** on the left side of the screen
- Select **Import from Self-Contained File** radio button
- Select the file path of the "migrate.sql" file.
- Click **Start Import** button

Once the import is completed, MySQL Workbench will automatically list the SQL schema of the cost database and building system database. Figure G.1 shows the interface of the MySQL Workbench after the data is successfully imported. The "energyplusconstruction" schema con-

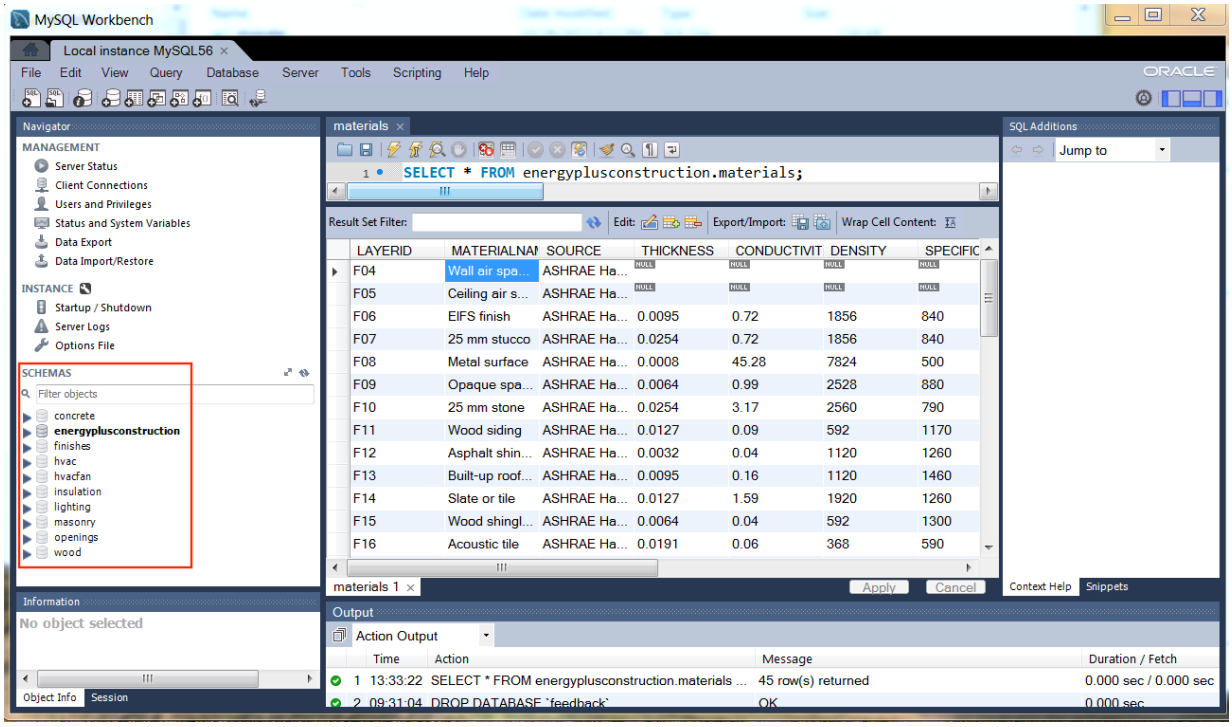

Figure G.1: mySQL WorkBench interface with data successfully imported

tains the building system database. All the rest schemas are the cost database.

Import data is a major step. However, the user should also make sure the SQL server is running on the local machine. The user can use the window command line tool to check the status. Click “Start” button on Windows, and enter ”CMD” in the “Search programs and files” option to initiate a new window command line tool session. Then, follow the instruction in Figure G.2. If the connection is successful, the SQL server will request the password to connect.

G.2.2 JAVA project setup

In this part, there are four JAVA projects to import, and a few configurations need to be done. The first JAVA project that should be imported is the customized JMetal project. This JAVA project can be downloaded or cloned from `https://github.com/weilixu/CustomJMetal`. The major difference between this customized JMetal project and the JMetal project in `https://github/com/jMetal/jMetal` is the adaptive meta-model algorithm called pNSGAII-IAdaptive under “metaheuristics.nsgaII package”. Other customized functions include mixed-

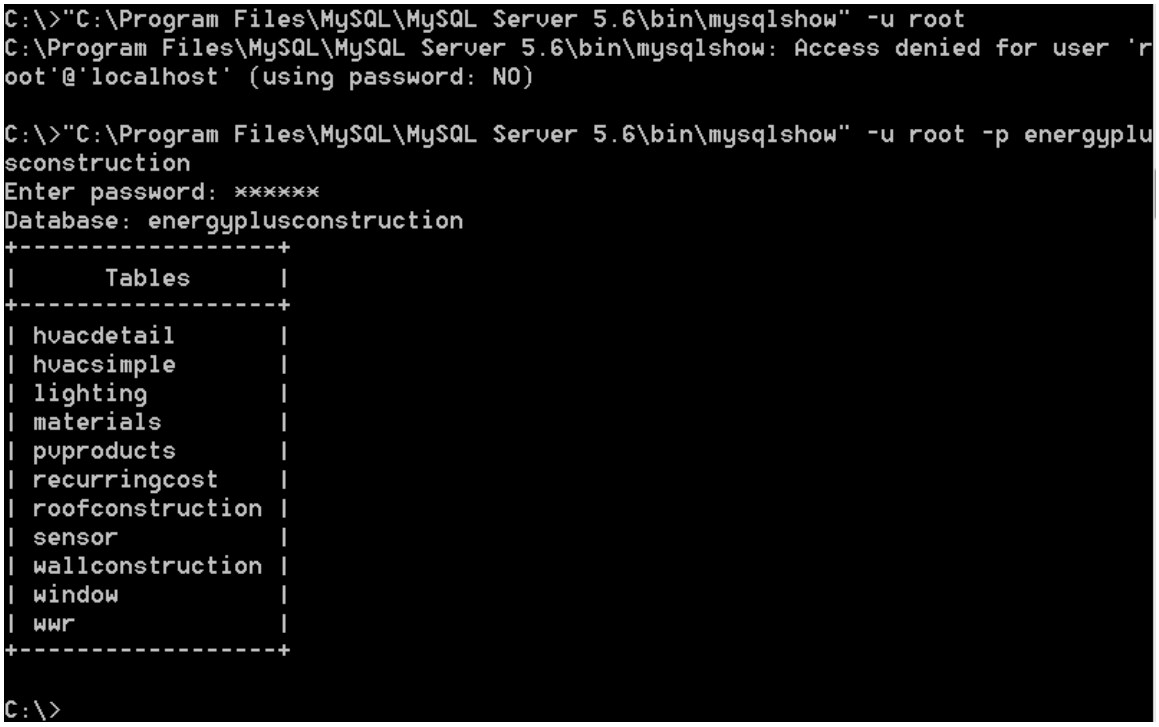

Figure G.2: Success SQL access using window command line tool

type data encoding function, crossover function (MixedSBXSinglePointCrossover) and mutation function (MixedBitFlipPolynomialMutation).

The second JAVA project required is the baseline automation project located in `https://github.com/weilixu/baseline` and the last JAVA project can be found in `https://github.com/weilixu/CostStandard`.

Import these three projects into Eclipse. The main executable is in the CostStandard project (Also, in the Eclipse, the name is changed to MasterFormat project). Therefore, configure the build path of this project by going to the “Project Properties”. Select the “JAVA Build Path” option in the prompt window, and select “Projects”. Click “Add” button to add the customized JMetal project and baseline automation project to the build path of the CostStandard project. Once the user completed these steps, the project setup is completed.

G.2.3 System configurations

The system can be started using the MappingPanel.java file under masterformat.gui. The file directory string in line number 5 in the createAndShowGUI() method should be modified to the local .idf file directory.

```
1  private static void createAndShowGUI() throws Exception{
     //create and setup the window
3    JFrame frame = new JFrame("EnergyPlus-Optimization Application V1");
     frame.setDefaultCloseOperation(JFrame.EXIT_ON_CLOSE);
5    File file = new File("E://User//Research//1MP//imp.idf");//change this
      line to the your .idf directory
     EnergyPlusModel model = new EnergyPlusModel(file);
7    //Add content to the window
     frame.add(new MappingPanel(model));
9
     //Display the window
11   frame.pack();
     frame.setVisible(true);
13 }
```

The hyper-parameters for the ammNSGAII algorithm can be configured in the EnergyPlus-Model.java file (under eplus package). A method called BudgetEUIOptimization() holds all the parameters that required.

The parameters are separated into three categories, namely the global parameters, operator parameters, and simulation parameters. The global parameters include the number of iterations running on actual EnergyPlus simulation (realSimuN), the number of iterations to complete one optimization cycle (circleDivider), the number of population generated in one iteration (pop) and the maximum evaluations (ammMaxEvaluation).

The operator parameters include the types of crossover, mutation and selection operators, the probabilities of executing these operators, and their distribution index if there are any numeric

values involved in the optimization.

Lastly, the simulation parameters needed in this function is the number of parallel simulations (thread).

```
public void budgetEUIOptimization() throws JMException,
    ClassNotFoundException{
  //algorithm global parameter setup
  int realSimuN = 3; //the actual No. of simulation
  int circleDivider = 20; //No. of iteration for one cycle
  int pop = 30; // number of population
  int ammMaxEvaluation = 2870; // stop criterion
  Problem problem = new OPT4(building, idfDomain, parentFolder);

  //operator parameter-setup
  String crossoverType = "MixedSBXSinglePointCrossover";
  String mutationType = "MixedBitFlipPolynomialMutation"
  String selectionType = "BinaryTournament2";
  double crossoverProbability = 0.9;
  double crossoverDistributionIndex = 20.0;
  double mutationProbability = 0.5;
  double mutationDistributionIndex = 20.0;

  //parallel simulation parameters
  int thread = 6; //number of concurrent simulations
  IParallelEvaluation paralleEval = new MultithreadedEvaluator(thread);

  //execute optimization
  ...
}
```

G.2.4 Configure optimization output file directory

Another important step in the system configuration is to configure the directory for optimization output files. First, there are two output files, “FUN” and “VAR” will be generated under the program directory. The “FUN” contains the value of each objective for every optimal design solution. Similarly, “VAR” contains the variables or design parameters selected for the optimal design solutions. The directory of these two files can not be changed. Besides these two, the directories that needs to be manually changed are the outputs of all the generated design solutions (“output.txt”) and the output of the prediction errors (“prediction.csv”).

To change the output files directory, the user needs to visit the “EnergyPlusBuildingForHVACSystems.java” and find the “writeOutResults” function.

```
public void writeOutResults() {
  int row = optResults.getResultSet().size();
  try{
    //change the directory here!!
    FileWriter writer = new FileWriter("E:\\02_Weili\\02_Research\\OneMP\\
   output.txt");
    for (int i=0; i<row; i++){
    ...
    }
    writer.flush();
    writer.close();
  }catch(IOException e){
    e.printStackTrace();
  }
}
```

To change the prediction error files directory, the user needs to visit one of the “OPT” file, for example, the “OPT5”, and locate the function “dataForplot()”. The number of the prediction error files depends on the number of optimization cycle the user specify. For instance, if the

number of cycle is calculated to be 5, then the optimization will generates 5 prediction error files.

```
public void dataForplot() {
  trainNumber ++;
  StringBuffer sb = new StringBuffer();
  ...
  try{
    //change the directory here!!
    File file = new File("E:\\02_Weili\\02_Research\\OneMP\\\predict" +
   trainNumber + ".csv");
    if (!file.exists()){
      file.createNewFile();
    }
    FileWriter fw = new FileWriter(file.getAbsoluteFile());
    BufferedWriter bw = new BufferedWriter(fw);
    bw.write(sb.toString());
    bw.close();
  }catch(IOException e){
    e.printStackTrace();
  }
}
```

G.3 Prepare EnergyPlus model

The EnergyPlus model can be prepared in DesignBuilder Version 4.7. There are a few limitations on the structure of energy model in order to successfully generate a qualified energy model for the study.

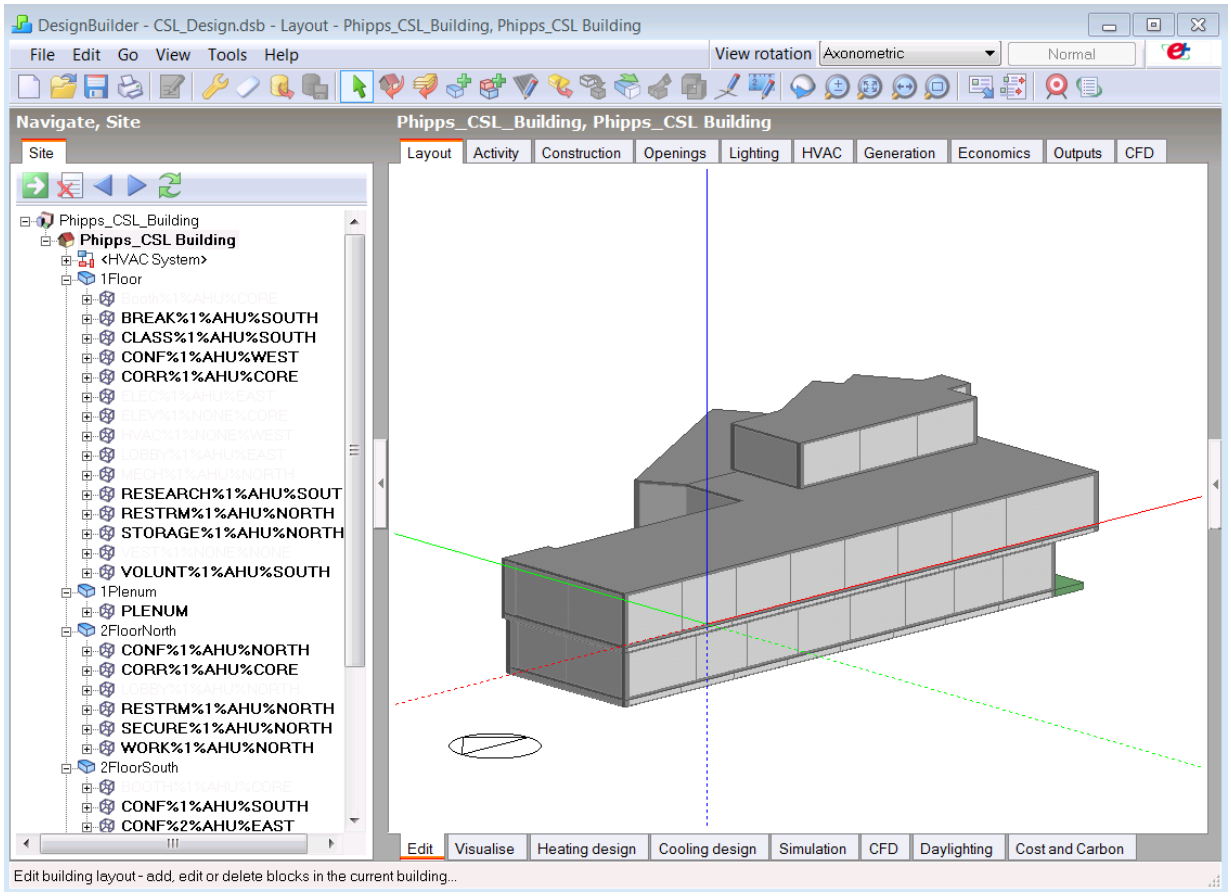

Figure G.3: CSL model in DesignBuilder editing interface

G.3.1 Zone naming

As described previous, the current HVAC system automation system does not equip with intelligence that can automatically configure the thermal zone groups. Therefore, manual thermal zone grouping is required, and the user should give the thermal zone a name format that follows $Block\%Function\%Identification\%Ventilation\%Thermal$. Figure G.3 shows the CSL energy model in DesignBuilder version 4.7. On the left side of the DesignBuilder interface is the thermal zone browser. It can be observed that the zone names are following the proposed format closely. The block name can be mapped to $Block$. The zone name consists of a zone's function (e.g. Break), identification (e.g. 1), ventilation system group (e.g. AHU) and thermal system group (e.g. South).

G.3.2 Window to wall ratio

Additionally, in Figure G.3, the window to wall ratio of the building is set to 90%. This is because the current algorithm can only shrink the window size on its host surface. The expansion function is implemented; however, it still requires comprehensive tests. The biggest challenges for developing a window expansion function in EnergyPlus can be summarized into two points.

- The expansion may require relocating the center of the window surface to prevent the over-expand issue, which the window dimensions exceed its host surface's boundary.
- The fenestration surface object in EnergyPlus only allows 3 or 4 coordinates to identify windows. The expansion could cause "too many coordinates" sever error, which will halt the simulation. This error is often seen when the host surface of the window is not in a regular shape.

These two points have made the development of expansion function significantly more challenging than the shrinking function. Therefore, as an alternative, the energy model should be built with 90% window to wall ratio to include this design parameter in the optimization process.

G.3.3 Daylighting position

The daylighting sensors should be predefined in the DesignBuilder. Figure G.4 shows the DesignBuilder daylighting sensor editing interface. On the tab "Lighting Control", the user should check on and configure the performance of daylighting sensors that should be performed in the optimization. This is because the current daylighting module does not equip with sensor location generator, which could generate coordinates that the sensor should be placed in a room. Therefore, rather than develop the entire daylighting sensors, a lighting sensor switch is adopted in the current version of the optimization system. Based on the selection of daylighting sensors (Yes/No) in the optimization process, the system will keep or delete these daylight sensors.

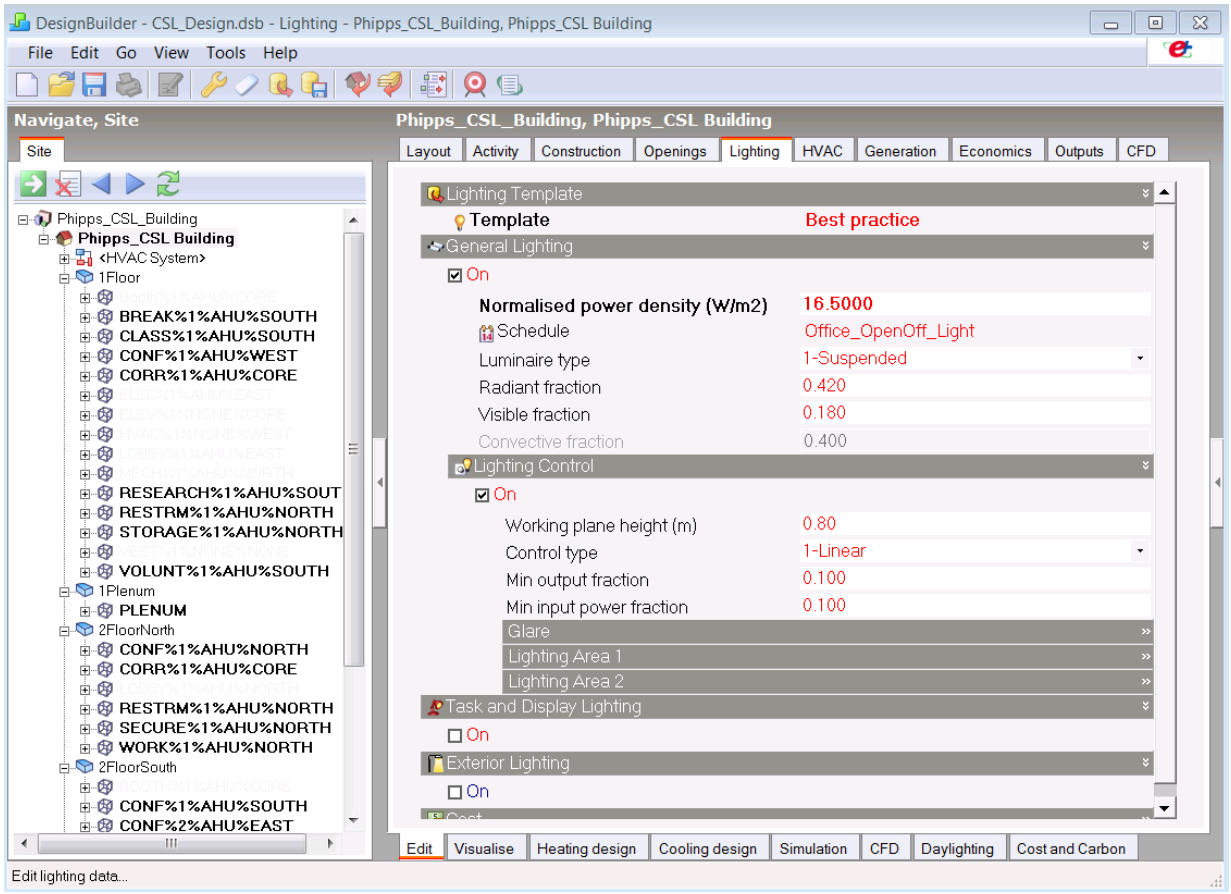

Figure G.4: CSL model in DesignBuilder editing daylighting sensor

G.4 Select design parameters

Once configured the platform directory and the EnergyPlus model, the user can start the program by clicking the “Run” button on “MappingPanel.java” (Figure G.5). The program will start loading the EnergyPlus model. Once it finished loading, the BEM-QTO application interface will be prompted as shown in Figure G.6.

Click the highlighted button, “Optimization”, to switch to the optimization interface. Figure G.7 shows the optimization interface. The red block highlights the optimization algorithm selection. In total there are three optimization algorithms available for the version 1. They are the conventional NSGA-II, adaptive meta-model NSGA-II and Particle Swarm algorithms. The green block illustrates the hyper-parameters for these algorithms. However, in this version,

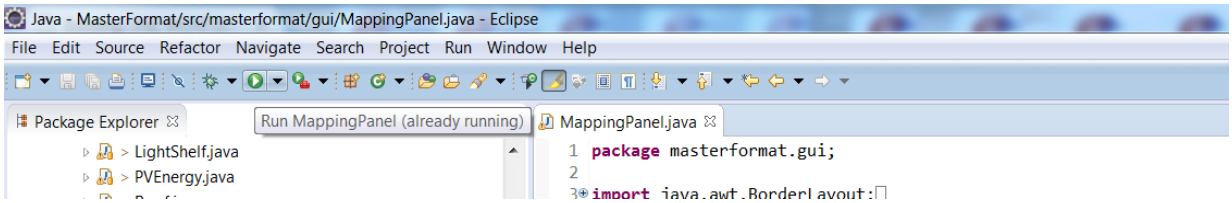

Figure G.5: Start the program on Eclipse

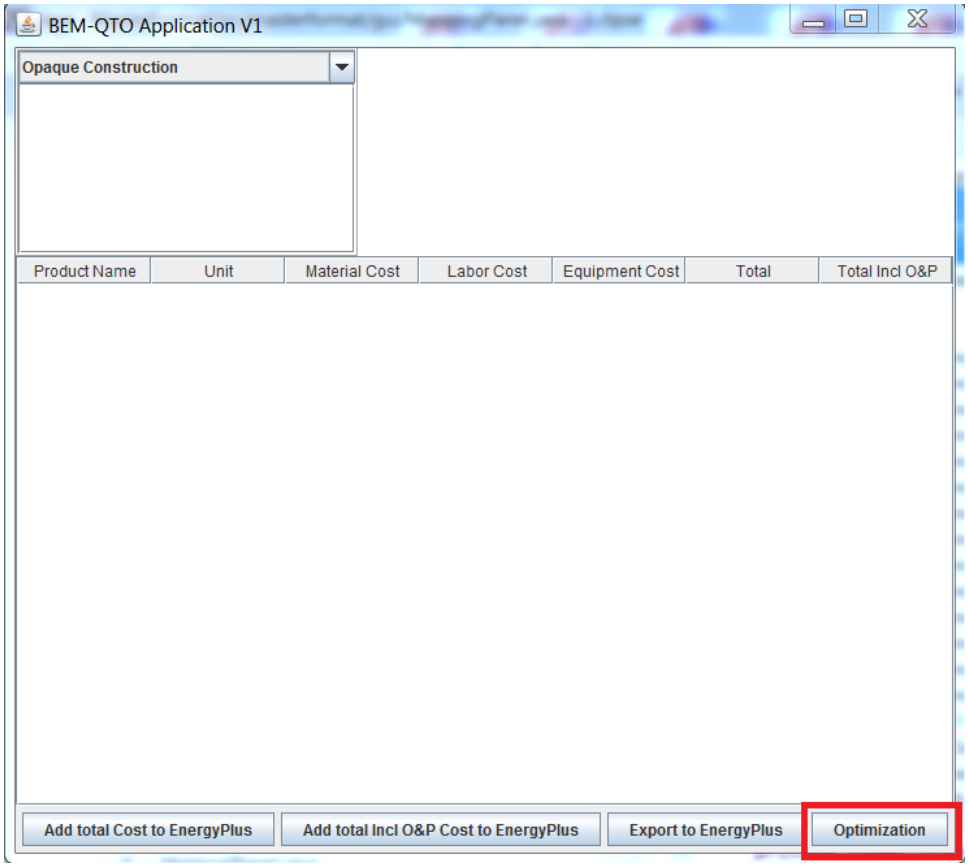

Figure G.6: BEM-QTO interface

the parameters are not fully connect to the optimization engine. User is still recommended to change these hyper-parameters by following the instruction in Section G.2.3. Furthermore, the blue blocks show the optimization type. In current version, user can switch between the new construction and the retrofit project. The change of optimization type will affects the available design parameters which are highlighted by a yellow block.

Within the yellow block, user can select the range of design options under each design param-

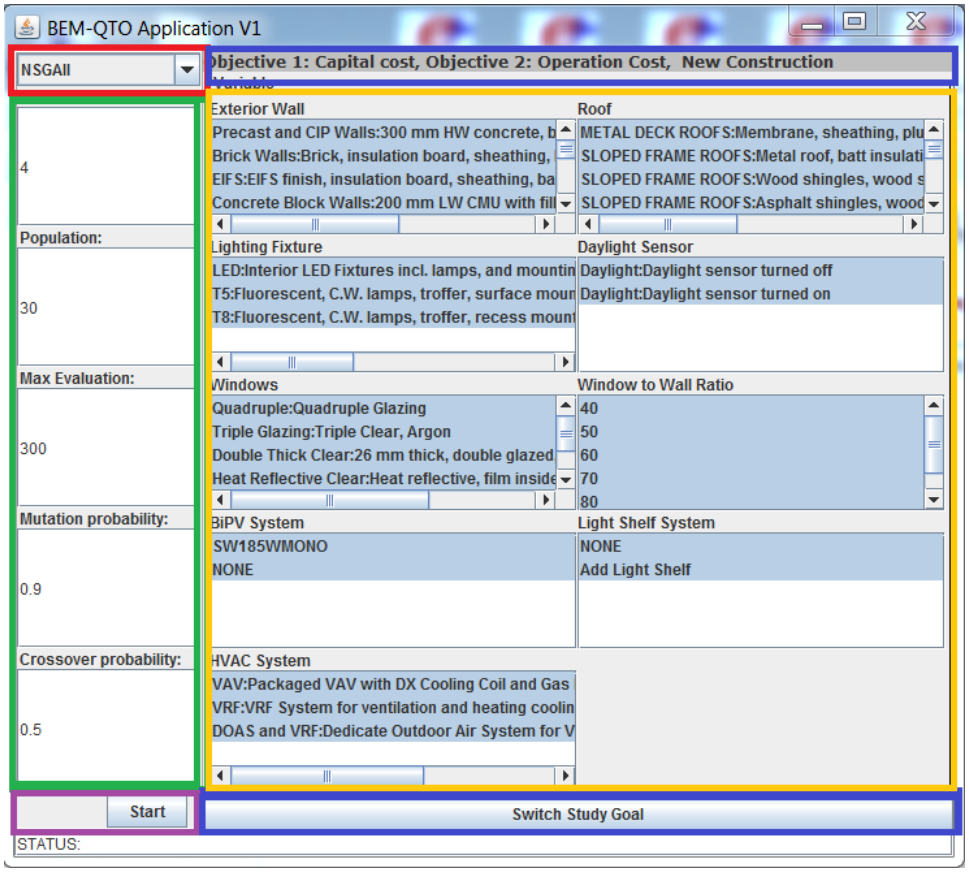

Figure G.7: Optimization interface

eters. Once the range is set, the optimization can be initialized by click the "Start" button. The program will not response to any further actions until severe errors detected or the optimization is completed.

G.5 Result analysis

Once the optimization is completed, the program will resume and the output files will be generated at the directory where the user have specified. Since both "output.txt" and "prediction.csv" follows the comma-separate values (CSV) format, it is recommended to analyze the data in R. In this instruction, a decision tree style results analysis is introduced for comparing the base case with all the generated design solutions. Figure G.8 shows the example from the new construction case study.

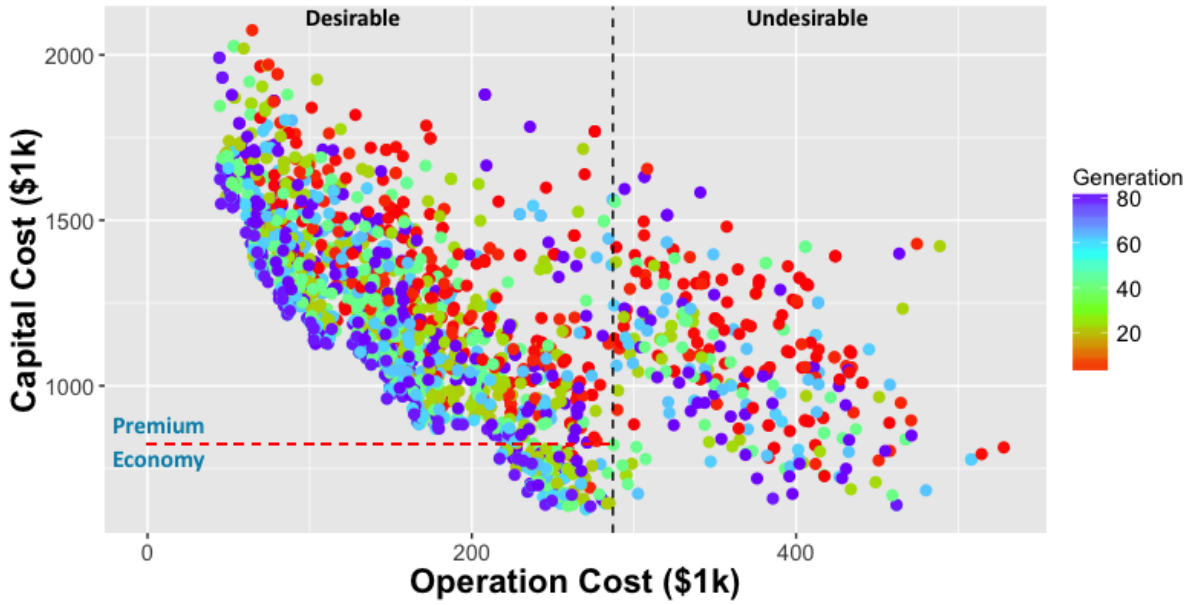

Figure G.8: Result analysis - decision tree style

The black dashed line indicates the operation costs of the base case and the red dashed line shows the capital cost of the base case. Based on the black dashed line, the entire design solutions can be separated into “Desirable” and “Undesirable”. The reason for this labeling is because the undesirable design solutions have higher operation costs than base case. If the base case is ASHRAE 90.1 2010 performance rating method, the undesirable design solutions will failed to meet building code and green building certifications such as LEED.

In addition, the “Desirable” design solutions can be further divided into “Premium” and “Economy”. The desirable economy solutions reduce both the capital cost and operation costs compare to base case. On the contrary, the desirable premium solutions increase the capital cost compare to the base case, but they save more energy cost than base case and desirable economy solutions.

Bibliography

Aibinu, A. and Venkatesh, S. (2013). Status of bim adoption and the bim experience of cost consultants in australia. *Journal of Professional Issues in Engineering Education and Practice*, 140(3):04013021. 1.3.2

Ascione, F., Bianco, N., De Stasio, C., Mauro, G. M., and Vanoli, G. P. (2015). A new methodology for cost-optimal analysis by means of the multi-objective optimization of building energy performance. *Energy and Buildings*, 88:78–90. 1.1.2, 1.2

ASHRAE (2002). Guideline 14-2002, measurement of energy and demand savings. *American Society of Heating, Ventilating, and Air Conditioning Engineers, Atlanta, Georgia*. 7.3

ASHRAE (2009). Ashrae handbook–fundamentals. *Atlanta, GA*. 3.2, 3.2.1, 6.4

ASHRAE (2010). Ashrae standard 90.1-2010 energy standard for building except low-rise residential buildings (si edition). Technical report, American Society of Heating, Refrigerating and Air-Conditioning Engineers, Inc 2010. 3.2, 3.2.1, 3.2.2, 5.2.1, 6.4, B.1, D.3

ASHRAE (2015). Ashrae owning and operating cost database. `http://xp20.ashrae.org/publicdatabase/default.asp`. 2.2, A.1

ASHRAE (2016a). Advanced energy design guides. `https://www.ashrae.org/standards-research--technology/advanced-energy-design-guides`. 3.2.1, 3.2.2, 3.2.2, 6.4, B.1

ASHRAE (2016b). Ashrae lowdown showdown modeling challenge teams recognized. `https://www.ashrae.org/news/2016/`. 1.2

Autodesk (2007). Bim and cost estimation. http://images.autodesk.com/apac_grtrchina_main/files/aec_customer_story_en_v9.pdf. 1.3.2, 1.5

Barg, S., Flager, F., and Fischer, M. (2015). Decomposition strategies for building envelope design optimization problems. In *Symposium on Simulation for Architecture & Urban Design*, pages 95–102. 1.2, 1.1.2

Bazjanac, V. (2005). Model based cost and energy performance estimation during schematic design. In *22nd Conference on Information Technology in Construction*, pages 677–688. 2.2

Blumenfeld, A. and Thumm, W. T. (2014). Passive building system vs active building system and the return on investment. 3.2.1, 3.2.2

Braun, M., Altan, H., and Beck, S. (2014). Using regression analysis to predict the future energy consumption of a supermarket in the uk. *Applied Energy*, 130:305–313. 4.4.5

Brownlee, A. E. and Wright, J. A. (2015). Constrained, mixed-integer and multi-objective optimisation of building designs by nsga-ii with fitness approximation. *Applied Soft Computing*, 33:114–126. 4.1

Building Technologies Office (2014). Building energy modeling (bem) overview - 2014 building technology office peer review. https://energy.gov/sites/prod/files/2014/05/f15/Building_Energy_Modeling_Overview_Roth_042214_and_042314.pdf. 6.7.2

Carrier (2016). Air cooled chillers and water cooled chillers. https://www.carrier.com/commercial/en/us/products/chillers-components/chillers/. 3.2.2, B.1

CBECCCOM (2016). Cbecc-com user manual 2016. Technical report, Archenergy. 1.6, 1.3.3

Chan, F. T., Jha, A., and Tiwari, M. K. (2016). Bi-objective optimization of three echelon supply chain involving truck selection and loading using nsga-ii with heuristics algorithm. *Applied Soft Computing*, 38:978–987. 4.3

Chang, C.-C. and Lin, C.-J. (2011). Libsvm: a library for support vector machines. *ACM Trans-*

actions on Intelligent Systems and Technology (TIST), 2(3):27. 4.4.5

Chen, X., Yang, H., and Lu, L. (2015). A comprehensive review on passive design approaches in green building rating tools. *Renewable and Sustainable Energy Reviews*, 50:1425–1436. 3.2.1, 3.2.2

Cheung, F. K., Rihan, J., Tah, J., Duce, D., and Kurul, E. (2012). Early stage multi-level cost estimation for schematic bim models. *Automation in Construction*, 27:67–77. 1.3.2, 1.5

Cho, N., Wang, W., Makhmalbaf, A., Yun, K., Glazer, J., Scheier, L., Srivastava, V., and Gowri, K. (2011). Extend energyplus to support evaluation, design, and operation of low energy buildings. Technical report, PNNL. 3.4.1

Choi, J., Kim, H., and Kim, I. (2015). Open bim-based quantity take-off system for schematic estimation of building frame in early design stage. *Journal of Computational Design and Engineering*, 2(1):16–25. 1.3.2

Chong, A., Xu, W., and Lam, K. P. (2015). Uncertainty analysis in building energy simulation: A practical approach. In *14th Conference of International Building Performance Simulation Association*, pages 2796–2803. 3.3, 7.3

CSI (2005). Masterformat tm 2004 edition numbers & titles. Technical report, Construction Specifications Institute. 2.2

Deb, K. (2011). Multi-objective optimisation using evolutionary algorithms: an introduction. In *Multi-objective evolutionary optimisation for product design and manufacturing*, pages 3–34. Springer. 1.1.3

Deb, K. and Agrawal, S. (1999). A niched-penalty approach for constraint handling in genetic algorithms. In *Artificial Neural Nets and Genetic Algorithms*, pages 235–243. Springer. 2

Deb, K. and Deb, D. (2014). Analysing mutation schemes for real-parameter genetic algorithms. *International Journal of Artificial Intelligence and Soft Computing*, 4(1):1–28. 4.4.4

Deb, K. and Goyal, M. (1996). A combined genetic adaptive search (geneas) for engineering design. *Computer Science and Informatics*, 26:30–45. 4.4.2

Deb, K., Gupta, S., Daum, D., Branke, J., Mall, A. K., and Padmanabhan, D. (2009). Reliability-based optimization using evolutionary algorithms. *IEEE Transactions on Evolutionary Computation*, 13(5):1054–1074. 8.3

Deb, K. and Jain, S. (2002). Running performance metrics for evolutionary multi-objective optimization. *Citeseer*. C.1, C.1

Deb, K. and Kumar, A. (1995). Real-coded genetic algorithms with simulated binary crossover: studies on multimodal and multiobjective problems. *Complex Systems*, 9(6):431–454. 4.4.3

Deb, K. and Nain, P. K. (2007). An evolutionary multi-objective adaptive meta-modeling procedure using artificial neural networks. In *Evolutionary Computation in Dynamic and Uncertain Environments*, pages 297–322. Springer. 4.4, 6.7.8, 7.6.6, C.1.1

Deb, K., Pratap, A., Agarwal, S., and Meyarivan, T. (2002). A fast and elitist multiobjective genetic algorithm: Nsga-ii. *Evolutionary Computation, IEEE Transactions on*, 6(2):182–197. 4.3, C.1, C.1

DesignBuilder (2016). Designbuilder, simulation made easy. `https://www.designbuilder.co.uk`. 1.6, 1.3.3, 6.4, D.6

DOE (2017). Commercial reference buildings. `https://energy.gov/eere/buildings/commercial-reference-buildings/`. 3.2, 3.2.1, 3.2.2, B.1

Dong, B., Cao, C., and Lee, S. E. (2005). Applying support vector machines to predict building energy consumption in tropical region. *Energy and Buildings*, 37(5):545–553. 4.4.5

Duquesne Light Co. (2016). Schedule of rates: For electric service in allegheny and beaver counties. `https://www.duquesnelight.com/docs/default-source/default-document-library/tariff-no-24-(150)---effective-2017-03-01-(rider-no-8---dss-medium-c-i-update)-clean-final-as-filed.pdf?sfvrsn=24`. 6.2

Eastman, C., Teicholz, p., Rafael, S., and Liston, K. (2011). *A BIM Application Areas For Owners*. John Wiley & Sons Inc, Hoboken, New Jersey. 1.3.2

Eberhart, R. and Kennedy, J. (1995). Particle swarm optimization, proceeding of ieee international conference on neural network. *Perth, Australia*, pages 1942–1948. 4.2

EcoGlobe (2016). Case studies. http://www.ecoglobe.de/case-studies/. 1.2

EIA (2016). Average price of electricity to ultimate customers by end-use sector. https://www.eia.gov/electricity/monthly/epm_table_grapher.cfm?t=epmt_5_6_a. 3.3

Eichholtz, P., Kok, N., and Yonder, E. (2012). Portfolio greenness and the financial performance of reits. *Journal of International Money and Finance*, 31(7):1911–1929. 1

Eisenhower, B., ONeill, Z., Narayanan, S., Fonoberov, V. A., and Mezić, I. (2012). A methodology for meta-model based optimization in building energy models. *Energy and Buildings*, 47:292–301. 1.4, 1.3.1

Emmerich, M. and Naujoks, B. (2004). Metamodel assisted multiobjective optimisation strategies and their application in airfoil design. In *Adaptive computing in design and manufacture VI*, pages 249–260. Springer. 4.1

Enkvist, P., Nauclér, T., and Rosander, J. (2007). A cost curve for greenhouse gas reduction. *McKinsey Quarterly*, 1:34. 1

Esfe, M. H., Hajmohammad, H., Moradi, R., and Arani, A. A. A. (2017). Multi-objective optimization of cost and thermal performance of double walled carbon nanotubes/water nanofluids by nsga-ii using response surface method. *Applied Thermal Engineering*, 112:1648–1657. 4.3

Euroglas (2016). Coated glass, silverstar series. http://www.euroglas.com/en/products/glass-type/coated-glass.html. 6.4

Evins, R. (2013). A review of computational optimisation methods applied to sustainable building design. *Renewable and Sustainable Energy Review*, 22:230–245. 1.1.1, 1.1.2, 4.3

Evins, R., Pointer, P., and Burgess, S. (2012). Multi-objective optimisation of a modular building for different climate types. In *First building simulation and optimization Conference*.

1.1.1, 1.1, 1.1.2, 1.3, 1.1.3

Flager, F., Basbagill, J., Lepechand, M., and Fischer, M. (2012). Multi-objective building envelope optimization for life-cycle cost and global warming potential. *eWork and eBusiness in Architecture, Engineering and Construction: ECPPM 2012*, pages 193–200. 1.1.1, 1.1, 1.3, 1.1.3

Fthenakis, V., Frischknecht, R., Raugei, M., Kim, H. C., Alsema, E., Held, M., and de Wild-Scholten, M. (2011). Methodology guidelines on life cycle assessment of photovoltaic electricity. *IEA PVPS Task*, 12. 3.2.3

Fuller, S. K. and Petersen, S. R. (1995). *NIST Handbook 135: Life-Cycle Costing Manual for the Federal Energy Management Program.* National Institute of Standards and Technology, Gaithersburgh, MD. 3.4, 3.2, 3.4.1, 3.4.1

GE (2016). Ge energy-efficient lighting systems. `http://www.gelighting.com/LightingWeb/na/images/60654-GE-LFL-T5-Brochure_tcm201-34678.pdf`. 3.2.2, 6.4, B.1

Giannakoglou, K. (2002). Design of optimal aerodynamic shapes using stochastic optimization methods and computational intelligence. *Progress in Aerospace Sciences*, 38(1):43–76. 4.1

Gilan, S. S. and Dilkina, B. (2015). Sustainable building design: A challenge at the intersection of machine learning and design optimization. In *Workshops at the Twenty-Ninth AAAI Conference on Artificial Intelligence*. 4.1

Glover, F. (1986). Future paths for integer programming and links to artificial intelligence. *Computers & operations research*, 13(5):533–549. 4.2

Glover, F. and Laguna, M. (2013). *Tabu Search*. Springer. 4.2

Glover, F. and Sörensen, K. (2015). Metaheuristics. *Scholarpedia*, 10(4):6532. 1.1.1

Glover, F. W. and Kochenberger, G. A. (2006). *Handbook of metaheuristics*, volume 57. Springer Science & Business Media. 4.2

Goldberg, D. E. and Holland, J. H. (1988). Genetic algorithms and machine learning. *Machine learning*, 3(2):95–99. 4.2, 4.4.3

Greiner, D., Galván, B., Periaux, J., Gauger, N., Giannakoglou, K., and Winter, G. (2015). *Advances in Evolutionary and Deterministic Methods for Design, Optimization and Control in Engineering and Sciences*. Springer. 1.3.1

Gulledge, E. C., Beougher, L. J., King, M. J., Dean, R. P., Hall, D. J., Giglio, N. M., Bevier, G. W., and Steinberg, P. (2007). Masterformat 2004 edition 2007 implementation assessment. Technical report, Construction Specifications Institute and Construction Specifications Canada. 2.2

Hall, M., Frank, E., Holmes, G., Pfahringer, B., Reutemann, P., and Witten, I. H. (2009). The weka data mining software: an update. *ACM SIGKDD explorations newsletter*, 11(1):10–18. 4.4.5

Hamdy, M., Hasan, A., and Siren, K. (2011). Applying a multi-objective optimization approach for design of low-emission cost-effective dwellings. *Building and environment*, 46(1):109–123. 1.1.2, 1.4, 1.3.1

Hardin, B. and McCool, D. (2015). *BIM and construction management: proven tools, methods, and workflows*. John Wiley & Sons. 1.3.2, 1.5

Holland, J. H. (1992). Genetic algorithms. *Scientific american*, 267(1):66–72. 4.2

HomeAdvisor (2017). Guide to gas boiler prices & costs. `http://www.homeadvisor.com/cost/heating-and-cooling/gas-boiler-prices/`. 7.6.2

Hunter, J. and Lear, R. (2015). Jdom. D.3

IRS (2016). Publication 946: How to depreciate property. Technical report, Department of the Treasury, Internal Revenue Service. 3.2, 8.3

Juan, Y.-K., Gao, P., and Wang, J. (2010). A hybrid decision support system for sustainable office building renovation and energy performance improvement. *Energy and buildings*, 42(3):290–297. 1.3.1

Karaguzel, O., Zhang, R., and Lam, K. P. (2014). Coupling of whole-building energy simulation and multi-dimensional numerical optimization for minimizing the life cycle costs of office buildings. *Building Simulation*, 7(2):111–121. 1.1.1, 1.1, 1.1.2, 1.1.3

Kirkpatrick, S., Gelatt, C. D., Vecchi, M. P., et al. (1983). Optimization by simulated annealing. *science*, 220(4598):671–680. 4.2

Kuhn, M. (2008). Caret package. *Journal of Statistical Software*, 28(5):1–26. 4.4.6

Lam, K. P., Zhao, J., Ydstie, B. E., Wirick, J., Qi, M., and Park, J. (2014). An energyplus whole building energy model calibration method for office buildings using occupant behavior data mining and empirical data. *CMU*. 6.3

LBNL (2016). Input output reference: The encyclopedic reference to energyplus input and output. Technical report, Lawrence Berkeley National Laboratory. 2.3.1, 2.3.2, 3.2.1, 3.2.2, 3.2.3, 3.3, 5.2.1, B.1

LBNL (2017). The international glazing database. `http://windowoptics.lbl.gov/data/igdb`. 3.2.1, B.1

Lovins, A. (2007). Tunneling through the cost barrier. In *Natural capitalism*, chapter 6, pages 111–124. Little, Brown. 8.2

Marenjak, S. and Krstic, H. (2010). Sensitivity analysis of facilities life cycle costs. *Tehnicki Vjesnik*, 17(4):481–487. 6.7.7

Meresi, A. (2016). Evaluating daylight performance of light shelves combined with external blinds in south-facing classrooms in athens, greece. *Energy and Buildings*, 116:190–205. 3.2.1, 6.4, B.1

Monteiro, A. and Martins, J. P. (2013). A survey on modeling guidelines for quantity takeoff-oriented bim-based design. *Automation in Construction*, 35:238–253. 1.3.2

National Research Council (2013). *Energy-Efficiency Standards and Green Building Certification Systems Used by the Department of Defense for Military Construction and Major Renovations*. National Academies Press. 1

Ng, P. K. and Mithraratne, N. (2014). Lifetime performance of semi-transparent building-integrated photovoltaic (bipv) glazing systems in the tropics. *Renewable and Sustainable Energy Reviews*, 31:736–745. 3.2.3

Nguyen, A.-T., Reiter, S., and Rigo, P. (2014). A review on simulation-based optimization methods applied to building performance analysis. *Applied Energy*, 113:1043–1058. 1.1.1

NIST (2016). Building life cycle cost programs. `https://energy.gov/eere/femp/building-life-cycle-cost-programs`. 3.4.1

of Energy, U. D. (2016). Asset score user guide. `https://help.buildingenergyscore.com/support/solutions`. D.6

Oracle (2015). Database jdbc developer's guide and reference. 2.2

PECO (2016). Current electric rate information. `https://www.peco.com/MyAccount/MyBillUsage/Pages/CurrentElectric.aspx`. 7.5

PECO Energy Co. (2016a). Electric service tariff. `https://www.peco.com/SiteCollectionDocuments/current%20electric%20tariff%20eff%20March%201%202017.pdf`. 7.2

PECO Energy Co. (2016b). Gase service tariff. `https://www.peco.com/SiteCollectionDocuments/current%20gas%20tariff%20eff%20March%201%202017.pdf`. 7.2

People Natural Gas (2016). Rates and rules for gas service in city of pittsburgh and territory adjacent thereto. `https://www.peoples-gas.com/my-account/files/Peoples_Equitable_Tariff.pdf`. 6.2

Pountney, C. (2012). Better carbon saving: using a genetic algorithm to optimize building carbon reductions. In *First building simulation and optimization Conference, Loughborough*, pages 165–172. 1.1.1, 1.1, 1.1.2

Roberti, F., Oberegger, U. F., Lucchi, E., and Troi, A. (2017). Energy retrofit and conservation of a historic building using multi-objective optimization and an analytic hierarchy process.

Energy and Buildings, 138:1–10. 4.3

Roth, A. (2016). New openstudio standards gem delivers one two punch. https://energy.gov/eere/buildings/articles/new-openstudio-standards-gem-delivers-one-two-punch. 1.6, 1.3.3

RSMeans (2015). *Building Construction Cost Data*. Construction Publishers & Consultants, Norwell, MA. 2.2, 3.2.1, 6.4, 8.2, 8.3, A.3, A.1

Rushing, A. S., Kneifel, J. D., and Lavappa, P. (2016). Energy price indices and discount factors for life cycle cost analysis 2015. Technical report, National Institute of Standards and Technology. 3.2, 6.2, 6.6, 7.5

Rysanek, A. and Choudhary, R. (2013). Optimum building energy retrofits under technical and economic uncertainty. *Energy and Buildings*, 57:324–337. 1.3.1

Sattineni, A. and Bradford, R. H. (2011). Estimating with bim: A survey of us construction companies. In *ISARC Conference, Seoul, Korea*. 1.3.2

Scholand, M. and Dillon, H. E. (2012). Life-cycle assessment of energy and environmental impacts of led lighting products part 2: Led manufacturing and performance. Technical report, Pacific Northwest National Laboratory (PNNL), Richland, WA (US). 2.2, A.1

ScienceDirect (2016). Energy and buildings. http://www.sciencedirect.com/science/journal/03787788. 1.2

Shi, X., Tian, Z., Chen, W., Si, B., and Jin, X. (2016). A review on building energy efficient design optimization rom the perspective of architects. *Renewable and Sustainable Energy Reviews*, 65:872–884. 1.1.1

SolarWorld (2016). Sunmodule solarworld module sw 185 mono. http://pdf.wholesalesolar.com/module20pdf20folder/SW165175185.pdf. 3.2.3, 6.4

Stocker, E., Tschurtschenthaler, M., and Schrott, L. (2015). Cost-optimal renovation and energy

performance: Evidence from existing school buildings in the alps. *Energy and Buildings*, 100:20–26. 1.1.2

Tiwari, S., Odelson, J., Watt, A., and Khanzode, A. (2009). Model based estimating to inform target value design. *AECBytes" Building the Future*. 1.3.2

Toshiba Carrier (2016). Toshiba carrier variable refrigerant systems. `http://www.carrier.com/commercial/en/us/products/variable-refrigerant-flow/toshiba-carrier-vrf-products/`. 3.2.2, B.1

Trane (2016). Trace700. `http://www.trane.com/commercial/north-america/us/en/products-systems/design-and-analysis-tools/analysis-tools/trace-700.html`. 1.6, 1.3.3

UIUC and LBNL (2016). Energyplus engineering reference: the reference to energyplus calculations. *US Department of Energy*. 3.2.1, 6.4, 6.7.6

Wang, N., Goel, S., Srivastava, V., and Makhmalbaf, A. (2015). Building energy asset score program overview and technical protocol (version 1.2). *PNNL-22045. Richland, WA, USA: Pacific Northwest National Laboratory. Google Scholar*. 7.4, 8.2

Wetter, M. (2004). *Simulation-based building energy optimization*. PhD thesis, UNIVERSITY OF CALIFORNIA, BERKELEY. 4.2

WGBC (2013). The business case for green building: A review of the costs and benefits for developers, investors and occupants. Technical report, World Green Building Council. 1

Wu, S., Wood, G., Ginige, K., and Jong, S. (2014). A technical review of bim based cost estimating in uk quantity surveying practice, standards and tools. *Journal of Information Technology in Construction (ITCon)*, 19:534–562. 1.3.2, 2.2, A.1

Xu, W., Chong, A., Karaguzel, O. T., and Lam, K. P. (2016a). Improving evolutionary algorithm performance for integer type multi-objective building system design optimization. *Energy and Buildings*, 127:714–729. (document), 3.3, 4.2, 4.4, C.2, C.2, C.1, C.3

Xu, W., Lam, K. P., Chong, A., and Karaguzel, O. T. (2016b). Multi-objective optimization of building envelope, lighting and hvac systems designs. In *ASHRAE-IBPSA Simbuild 2016*. 3.2.2, D.3

Yang, X.-S. (2011). Metaheuristic optimization. *Scholarpedia*, 6(8):11472. 4.2

Yergeau, F., Bray, T., Paoli, J., Sperberg-McQueen, C. M., and Maler, E. (2004). Extensible markup language (xml) 1.0. *W3C Recommendation, third edition, February*. D.3

Zhao, H.-x. and Magoulès, F. (2012). A review on the prediction of building energy consumption. *Renewable and Sustainable Energy Reviews*, 16(6):3586–3592. 4.4.5

Zhao, J. (2015). Design-build-operate energy information modeling for occupant-oriented predictive building control. 6.3